Evaluation of gauge-based, satellite, and reanalysis rainfall datasets in capturing extreme rainfall and precipitation concentration index over India.

By

Suman Bhattacharyya

Dissertation submitted in partial fulfillment of the requirements

for the degree of

Master in Philosophy in Geography

JNU

Centre for the Study of Regional Development
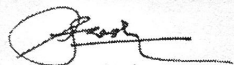
Jawaharlal Nehru University

2020

RECOMMENDATION FORM FOR EVALUATION BY THE EXAMINER/S

CERTIFICATE

This is to certify that the dissertation/thesis titled "**Evaluation of gauge-based, satellite, and reanalysis rainfall datasets in capturing extreme rainfall and precipitation concentration index over India** "submitted by Mr. .....SUMAN BHATTACHARYYA....in partial fulfillment of the requirements for award of degree of M.Phil. of Jawaharlal Nehru University, New Delhi, has not been previously submitted in part or in full for any other degree of this university or any other university/institution.
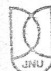
We recommend this thesis/dissertation be placed before the examiners for evaluation for the award of the degree of M.Phil.
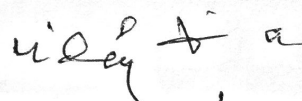

S Sreekesh

Signature of Supervisor

Date: 11.02.2021

Centre for the Study of Reg Dev.
School of Social Sciences
Jawaharlal Nehru University
New Delhi - 110067

Signature of Dean/Chairperson

Date: 16.2.21

Chairperson
Centre for the Study of Reg. Dev.
School of Social Sciences
Jawaharlal Nehru University
New Delhi - 110067

Preface

Precipitation process is time concentric in nature and with recent anthropogenic warming, the spatial and temporal distribution of precipitation is changing over the Earth mainly with an increase in extreme climatic events. Understanding the occurrences of extreme climatic events and their changes is crucial for reducing the risk associated with extreme events, especially under recent warming. For conducting such studies related to the analysis and changes in precipitation and more importantly the extreme precipitation, researchers and practitioners need reliable precipitation dataset. So far various attempts have been made in understanding the relative strength and weakness of different gridded rainfall datasets, mainly focusing on how well these gauge based, satellite-derived and reanalysis datasets can represent the seasonal and monthly precipitation amount over India. However, little is known about their performance in capturing different characteristics of extreme rainfall and precipitation concentration over India. Therefore, through this work, one has attempted to comprehensively evaluate eleven different gridded rainfall datasets in representing different characteristics of extreme rainfall, Precipitation Concentration Index (PCI) and their trends over India during the study period of 1986 to 2015.

These eleven selected datasets fall into three categories: gauge-based (APHRODITE, CPC, GPCC), satellite-derived (CHIRPS, PERSIANN-CDR) and reanalysis (ERA-5, ERA-Interim, MERRA2, NCEP2, PGF and JRA-55) rainfall data are used for studying various characteristics of annual and extreme rainfall indices as well as PCI over India. For comparison, a purely gauge-based, high resolution (0.25° × 0.25°) daily gridded rainfall dataset, obtained from the India Meteorological Department (IMD) is used as the reference dataset. Thirteen extreme climate indices, defined by the World Meteorological Organization's Expert Team on Climate Change Detection and Indices (ETCCDI) and the IMD are used to capture the magnitude, frequency, and duration of extreme rainfall events over India. Analysis of precipitation concentration is done using the PCI. All these rainfall indices including the PCI is calculated over grid-cell for each rainfall datasets over 30 years and compared with the IMD dataset using various evaluation metrics. Consequently, this study conjectures that the gauge-based GPCC data showed the greatest agreement with the reference data (IMD) in representing extreme rainfall over India. The CHIRPS and ERA-5 performed well in the satellite and reanalysis rainfall datasets group, respectively. Notably,

all of these selected datasets consistently underestimated extreme rainfall events over the northern Himalayan region. Results of PCI analysis suggest that the annual PCI is irregularly distributed over most parts of India, influenced by geographical factors such as latitude, longitude, and altitude. Significant increasing and decreasing trends in annual PCI can be observed over the North-Eastern and Western coasts of India, respectively. The gridded data inter-comparison results suggest that the gauge based APHRODITE and GPCC, satellite-derived CHIRPS, and the reanalysis dataset ERA5 better perform in capturing the temporal and spatial variation in PCI over India as compared to the IMD gridded dataset.

Declaration

I confirm that this is my own work and the use of all material from other sources has been properly and fully acknowledged.

Suman Bhattacharyya

30.12.2020

Dedication

dedicated to my parents

and dadu thamma (grandparents)

Acknowledgements

I owe thanks to many people than I could list here. I would like to extend my gratitude to all those who helped me or influenced my work in some the way.

Firstly, I would like to express my sincere gratitude to my supervisor Dr. S. Sreekesh for his guidance, suggestions and support throughout my M.Phil. study. I could not have imagined having a better supervisor and mentor for my M.Phil. dissertation. He always encouraged me to explore new avenues and gave me the freedom to develop new collaborations.

My sincere thanks and deepest sense of appreciation also goes to Dr. Andrew King, The University of Melbourne, for providing his valuable suggestions and generosity in reviewing this work.

I am greatly indebted to Prof. Subimal Ghosh, IIT Bombay for providing the IMD gridded rainfall data at the initial stage of this work. Without his contribution, it would not have been possible for me to pursue this topic and finish my work.

I would also like to acknowledge the finical help received from the University Grant Commission, under the Junior Research Fellowship scheme.

There are too many friends to thank and name individually but I would definitely like to mention my hostel mates, especially the whole team of *Chandrabucks*. They incessantly made all possible efforts to cheer me up and helped me to keep up my mental health during the pandemic. From trying out new cuisines to endless talks of high and low, you guys were so supportive and fun. Without you five, it might not have been possible for me to continue my work during this pandemic.

Finally, I would like to thank my family; I couldn't have done this without you. I look forward to spend more time with you all. I also want to thank my sister for always giving me positivity, support and love. I am so grateful to my father for his constant support and encouragement. I owe him everything that I have achieved in so far. Things would have been so difficult without his enthusiasm. Thank you for thrusting me back into the real world!

Table of Contents

List of Tables

List of Figures

Abbreviation

APCI Annual precipitation concentration index

APHRODITE Asian Precipitation Highly-Resolved Observational Data Integration Towards Evaluation of water resources

CPC Climate Prediction Center

CFSR Climate Forecast System Reanalysis

CHIRPS Climate Hazards Group InfraRed Precipitation with Station data

ECMWF European Centre for Medium-Range Weather Forecasts

ERA-Interim European Centre for Medium-Range Weather Forecasts reanalysis systems

ERA-5 European Centre for Medium-Range Weather Forecasts reanalysis systems

ETCCDI Expert Team on Climate Change Detection and Indices

GPCC Global Precipitation Climatology Centre

IMD India Meteorological Department

MERRA Modern-Era Retrospective Analysis for Research and Application system

NCEP National Centers for Environmental Prediction

PERSIAN Precipitation Estimation from Remotely Sensed Information using Artificial Neural Networks

PCI Precipitation concentration index

PGF Princeton Global Forcing

PDF Probability density function

SPCI Seasonal precipitation concentration index

TRMM Tropical Rainfall Measuring Mission

TMPA TRMM Multi-satellite Precipitation Analysis

Chapter 1

Introduction

Precipitation is a key hydrological variable, associated with the circulation of moisture and heat over the Earth. Amount of precipitation, its spatio-temporal variability and seasonality have great influences in determining regional or global climate (Falkenmark and Rockström, 2006). Also, accurate measurement of precipitation over an extended period is a prerequisite factor for detecting trends in regional precipitation and to trace its possible linkages to global climate change (Faiz et al., 2018). Measurement of precipitation is not only necessary for understanding regional precipitation process but also crucial in designing engineering structures for managing water resources and to better combat frequent natural disasters i.e. floods and droughts. Besides, precipitation data arguably is also the most important meteorological input necessary to force and calibrate any climate and eco-hydrological models (Fallah and Orth. 2020; Pang et al., 2020)

Extreme hydro-climatic events play a key role in shaping the natural environment around the world and sometimes pose significant risks to the inhabitants of that place. There is a growing interest among climate scientists on how anthropogenic climate change is affecting the risks associated with climate extreme and how they may change under non-stationary climate (Emori and Brown, 2005; Thornton et al., 2014; Forestieri et al., 2018). This concern is driven by the growing impacts of recent extreme weather and climate events on the ecosystem, economy and infrastructure around the world (Madsen et al., 2014; Ummenhofer and Meehl., 2017). Extreme precipitation events are associated with an array of atmospheric processes, such as strong vertical convection, presence of atmospheric rivers, monsoon, tropical and extratropical cyclones (Kunkel et al., 2013). Despite mounting shreds of evidence of an increase in the frequency and magnitude of extreme events and their associated impacts around the world, studies on extreme climate events often acknowledge the fact that a proper universal definition of an extreme climate event is lacking in the literature (Bailey and van de Pol, 2016). Therefore, various attempts have been made to define the 'extreme climate events', mostly in a synthesized way (Van de Pol et al., 2017; Pendergrass, 2018; Dey et al., 2020). Existing definitions mainly tried to define 'extreme climate events' either from a purely *climatological* perspective or related to the *impacts* of any particular climate event (Van de Pol et al., 2017). In general, the term *extreme* is used

to characterize a *rare* event of a certain magnitude or the impacts associated with it. In case of a climatic variable (e.g. precipitation, temperature), extreme can be defined by only considering the values which are located at the far ends of a variable's distribution that doesn't occur frequently. While considering impacts, defining extreme associated with a particular climate event becomes trickier as there is no unique way to assess the impacts quantitatively (Van de Pol et al., 2017). The Intergovernmental Panel on Climate Change (IPCC) defines extreme climate events based on *rarity* that is how uncommon an event is in a particular place and time (IPCC, 2014). The IPCC redefined this definition, stating that "the occurrence of a value of a weather or climate variable above (or below) a threshold value near the upper (or lower) ends of the range of observed values of the variable" (IPCC, 2014). These events include a range of weather or climate events including, for example, heatwaves, cold waves, heavy rainfall, episodes of floods and drought and severe storms. The India Meteorological Department (IMD) uses an explicit method for defining extreme weather and climate events in India based on some fixed threshold values of the concerned climate variable (i.e. temperature, precipitation, wind speed, etc.).

Extreme precipitation event is defined as one in which accumulated rainfall amount over a specific period exceeds a particular threshold, either at a recording place or on average over a spatial domain. In practice, definition and identification of extreme precipitation events vary from place to place. The period considered for calculating accumulated precipitation varies from hour to days and the choice of threshold is also quite variable and needs expert judgments. Some studies use a percentile-based threshold, derived from the probability distribution of precipitation of selected period to consider the regional variation of precipitation characteristic. Choice of a fixed threshold is also popular due to its simplicity. For example, the IMD follows a nine-fold intensity-based rainfall classification scheme to identify extreme rainfall events (e.g. rainfall above 64.5mm/day as heavy rain) at any place over India. However, in practice, choice of fixed threshold-based event identification can be misleading especially when a single threshold value is applied over a large geographic region (Dey et al., 2020). This is even for pertinent in India since annual rainfall distribution varies from 300 mm to 10,000 mm in different parts of India. Depending on the location of the threshold value near the upper or lower tails of the probability density function (PDF), an extreme precipitation event can be identified as higher (located near the right tail of the PDF) or lower (located near the left tail of the PDF) extremes. For example,

identifying the number of consecutive rainfall days below 1mm threshold can be used to identify the maximum or average length of dry days over a region during a season, which can be used while assessing drought conditions and climate change related studies. Similarly, maximum 1day rainfall amount or rainfall amount above 99th percentile is higher extreme precipitation indices which can be used to study the contribution of extreme to total rainfall or the changes in rainfall amount associated with climate change over a region. Indices developed by the Expert Team on Climate Change Detection and Indices (ETCCDI) provides a list of extreme precipitation indices considering both of the (absolute and percentile) rainfall threshold which is very popular in climate change studies around the world (Panda et al., 2016. Hong and Ying et al., 2018). Also, ETCCDI recommended indices consider higher as well as lower precipitation thresholds for identifying extremes precipitation over a region. Therefore, there is a need to consider an array of extreme rainfall indices while carrying out analysis related to extreme rainfall or especially when assessing climate change-induced extreme rainfall change studies.

Extreme precipitation is often associated with an array of natural disasters i.e. floods, landslides, etc. damaging agricultural crops and infrastructure around the world. Analysis of extreme precipitation events is therefore necessary for understanding the nature of precipitation extreme over a region as well as to build preparedness to manage these natural disasters. Extreme precipitation event is a key controlling variable of soil erosion, thus, controlling the fluvial sediment system. Study of extreme precipitation also helps in designing engineering structures i.e. dams, urban drainage system to better manage regional water resource. Given the recent changes in the frequency, magnitude and duration of extreme precipitation events, are also changing globally. In India, more than 80% of the total annual precipitation comes from monsoon precipitation of which about 44% is associated with heavy rainfall events (Pattanaik and Rajeevan, 2010). Heavy rainfall and devastating floods are recurring hydro-climatic events in India, especially during the monsoon and post-monsoon seasons. According to the Central Water Commission (CWC, 2018), heavy rainfall and floods alone caused an average economic damage equivalent to $7.6 billion per year to the Indian economy between 1953 and 2016. Therefore, there is a need for a detailed investigation to better characterize rainfall, focusing on extreme rainfall, in India.

In contrast to this, the low-intensity daily precipitation also has implication for water availability and occurrence of drought in a region. Occurrences of daily precipitation are discrete (rain or no rain) in nature and can be well represented by a negatively skewed exponential distribution (Brooks and Carruthers, 1953). The negative exponent implies that there are too many wet days with light rainfall and very few days with heavy rainfall. This time-compressed nature of precipitation event is common in many climatic regions around the world and explains the need for studying precipitation concentration (Martin-Vide, 2004; Cortesi et al., 2011). The low rainfall amounts are characteristics of arid and semi-arid regions and often it leads to drought condition. It occurs even in regions of moderate to heavy rainfalls and thus results in droughts there too. Besides, the annual precipitation distribution also shows varying degrees of monthly and seasonal concentration in different parts of the World. For this purpose, various indices such as Precipitation Concentration Index (PCI)(Oliver, 1980), Seasonality Index (Walsh and Lawer, 1981), and Concentration Index (CI) (Martin-Vide, 2004) have been developed to study the time-concentric nature of precipitation events around the world. CI provides information about the contribution of heavy precipitation events to total precipitation where the seasonal or annual PCI can be used for understanding the long-term variability of total precipitation received on annual and seasonal scale. PCI can also be used indirectly to understand variation in precipitation in a place. A large number of recent studies have used the PCI to understand the regional variation in precipitation concentration in different parts of the world. For example in Bangladesh (Mondol et al., 2018), Nepal (Shrestha et al., 2019), China (Deng et al., 2018; Faiz et al., 2018b; Zhang et al., 2019; Lu et al., 2019), Italy (Bartolini et al., 2018), Sardinia (Caloiero et al., 2019) and in Greece (Tolika, 2019).

Understanding the changes in extreme precipitation and precipitation concentration over a region is vital for understanding the impacts of climate change in regional precipitation. Such kind of analysis is not only helpful to answer recent questions regarding changes in precipitation associated with the rising concentration greenhouse gases in the atmosphere but also can help inform policymakers, planners, and to build awareness for managing recurring natural disaster i.g floods which are very common in India.

1.1 Extreme precipitation and climate change

According to the IPCC, the global mean surface temperature has increased by 0.89°C between 1901 and 2012 with significant regional differences, which mainly attributed to

anthropogenic warming (IPCC, 2013). Climate change has direct impacts on regional precipitation pattern, mainly through changes in precipitation amount, intensity and frequency of heavy rainfall events leading to catastrophic floods and droughts (Roxy et al., 2017; Mal et al., 2018). Therefore, understanding the spatial and temporal distribution of precipitation is necessary for managing regional water resources, reliable hydrological predictions and building disaster preparedness, especially under a non-stationary climate (Wang et al., 2016; Marengo and Espinoza, 2016). The nature of extreme climatic events, such as extreme precipitation, drought, and heatwaves, is also changing in response to recent human-induced warming (Matthews et al., 2019; Perkins-Kirkpatrick and Lewis 2020; Fischer and Knutti et al., 2015). Precipitation extremes have great socio-economic impacts as these extreme events often translate into devastating floods and landslides, which disrupt transportation networks, hinder agricultural production and result in human casualties.

Seasonality of precipitation event is another key determinant in controlling freshwater flux over land surfaces. With an increase in global mean temperature, extreme precipitation events are expected to intensify over most parts of the globe (Kharin et al., 2013, Fischer and Knutti et al., 2015). This means, the amount of precipitation associated with a certain 'return period', such as once in 50 years event or once in 20 years event, is expected to increase (Tandon et al., 2018). The reason for the increasing and future expected increase in rainfall can be explained using Clausius-Clapyeron equation, which states that if the global surface temperature increases the saturation vapour pressure of the atmosphere will also increase, with a rate of 7% per degree of warming (Trenberth et al., 2011; Trenberth et al., 2003). As a result, the moisture-holding capacity of the atmosphere increases, which brings more rain during an extreme rainfall event. Due to energy constraints, global mean precipitation increases at a slower rate, by 1 - 3% per degree of warming (Allen and Ingram, 2002). Studies based on observational precipitation record also indicate an increase in one day maximum rainfall by 6-10% per degree of warming over the land areas (Asadieh and Krakauer 2015; Westra et al., 2013). This mechanism is presented in weather and climate models to predict the changes in rainfall in future under different emission scenarios.

1.2 Precipitation data sources

Point-based measurements of precipitation are highly accurate, however, they are limited over much of the globe owing to the sparse distribution of gauge networks (Kidd et al.,

2017) and can suffer from data quality issues (Viney and Bates 2004). The gridded and satellite-based data sets, which are continuous in space-time domains, could overcome the limitation poised by the point data. Various gridded precipitation datasets are now available with global or near-global coverage but the relative performance of this datasets varies with geographical space and time (Sun et al., 2018). Despite several limitations, gridded datasets are widely used in climate science for studying global/regional rainfall characteristics (Masunaga et al., 2020; Satgé et al., 2020), in climate change detection and attribution studies (Paik et al. 2020), event attribution studies (e.g. Wiel et al., 2017), and they are commonly used for climate model evaluation. Satellite-based rainfall retrieval is now providing ~40-year long records of precipitation over the globe making these datasets potentially suitable for climate change studies (Nguyen et al., 2018). Another popular choice is to use the reanalysis rainfall datasets as they provide a dynamically consistent record of several atmospheric variables around the globe. Reanalysis use models that simulate thermodynamic and dynamic processes to produce synthesized outputs by integrating irregular observations into the model domain (Sun et al., 2018).

Precipitation is a key variable of the global hydrological cycle as it distributes mass and energy over the land surfaces and has a direct influence in controlling the subaerial processes. However, precipitation varies greatly over space, which poses a key challenge in measuring it satisfactorily over a large spatial domain. Based on measurement techniques and estimation methods, precipitation data sets are mainly grouped into three different categories i.e. gauge-based, satellite rainfall and reanalysis (Sun et al., 2018). At Earth's surface, precipitation is commonly measured using rain gauges (Tapiador et al., 2012). There are several types of rain gauges available, such as accumulation gauges, weighing gauges, tipping bucket gauges and optical gauges (Tapiador et al., 2012). Owing to the sparse distribution of rain gauges, it is necessary to assemble all gauge-based observations of precipitation to national and subsequently into one integrated global data set for large scale climatic study or related application.

1.2.1 Gauge- based gridded data

In-situ precipitation observations are often combined into gridded precipitation dataset using a suitable interpolation algorithm for better understanding of regional precipitation process (Pai et al., 2014). Several gridded precipitation datasets have been developed with different spatial and temporal coverage by using in-situ precipitation measurements

around the world. For example, the Climate Prediction Center (CPC), Global Precipitation Climatology Centre (GPCC), Climatic Research Unit (CRU), and the Asian Precipitation Highly Resolved Observational Data Integration Towards Evaluation of Water Resources (APHRODITE) gridded precipitation datasets are available at daily, and monthly temporal scale with a spatial resolution ranging from 0.25° to 1°. However, gauge based precipitation datasets have several drawbacks, such as too many missing data, incomplete spatial coverage and inadequacy over rugged terrain and ocean surfaces (Kidd et al., 2017). Gauge-based gridded datasets aim to provide rainfall record over spatially homogeneous grid-cells by interpolating point-based rainfall measurements over a region.

1.2.2 Satellite-based estimation

Satellite has become an indispensable tool for monitoring the Earth's surface resources as well as atmospheric variables at regular interval from space. After the launch of first Television and IR Observation Satellite (TIROS) in April 1960, a growing interest in satellite meteorology enriched our understanding of atmospheric phenomena through imaging (Kidd, 2001). In the early stage of its development, images of clouds obtained from this satellite manually interpreted by comparing them with in-situ meteorological observations (Kidd, 2001). Since then, the number of satellites for observing Erath's atmospheric processes has increased and subsequently advanced our understanding of satellite meteorology. Based on sensor characteristics these satellites are classified into three categories (Michaelides et al., 2009; Prigent, 2010); Visible/IR (VIS/IR) sensors on low Earth orbit (LEO) and on geostationary (GEO) satellites, passive microwave (PMW) and active microwave sensors on LEO satellites.

Bright and cold clouds are subjected to greater vertical convection. Using this principle, the cloud top temperature measured by IR sensors of VIS/IR satellite is used to estimate precipitation process. Probability and intensity of precipitation at ground level are then estimated applying different algorithm such as Griffth-Woodley algorithm (Griffith et al., 1978). VIS/IR sensors have an advantage in measuring rainfall at a high spatial resolution over tropical areas with adequate temporal resolution. However, it should be noted not all cold and bright cloud form precipitation and the relation between cloud top temperature and precipitation is indirect. Unlike, VIS/IR sensors PMW sensor is sensitive to the droplet size of precipitation and can sense through cloud thus provides a unique opportunity to measure precipitation from space. Since the launch of Special Sensor Microwave/Imager

(SSM/I) in 1987 by NASA's WetNet project, precipitation retrieval based PMW sensors advanced significantly. Launch of PMW TRMM MW Imager in 1997, made great progress in depicting and analyzing rainfall patterns over tropical areas. After that, NOAA's advanced MW sounding unit (launched in July 1998) and the development of Advanced MW Scanning Radiometer for the Earth Observing System (AMSR-E) in 2002 with multichannel PMW radiometer to measure water-related geophysical parameters. PMW sensors are currently placed at LEO, therefore, have a poor temporal resolution (3h or less) compared to the rapid temporal sampling (30minuites or less) of the GEO based IR instruments. At the early phase of its development, precipitation is estimated by using simple regression-based methods between surface precipitation rate and estimated or measured brightness temperature by the PMW sensors. After that, however, other approaches, such as physical algorithm, probabilistic and iterative retrieval algorithm have been developed which improved the accuracy PMW estimates. To improve accuracy, data collected through VIS/IR and PMW sensors are often merged together to improve resolution, accuracy and coverage of precipitation products (Tapiador et al. 2004, Sorooshian et al. 2002). In 1997, precipitation measurement with active MW sensors started with the launch of TRMM. It is the first spaceborne precipitation radar which has improved the understanding of three-dimensional structures of precipitation events and its measurement accuracy over tropical regions.

With the recent advancements in infrared (IR) and microwave (MW) sensors, and retrieval algorithms, satellite-based precipitation products fill the deficiencies associated with gauge based measurements by providing spatially homogeneous and temporally continuous records with near-global coverage of precipitation processes (Kidd and Levizzani, 2011; Sun et al., 2018). Satellite-based measurements are often merged with gauge based products to improve the accuracy of measured climatic variables and to maximize the benefits for climatological applications (Sun et al., 2018). Although, the performance of satellite estimates found to vary over geographical space and significant differences exists between different satellite rainfall products.

1.2.3. Reanalysis

Climate variables (i.e. precipitation, temperature, wind speed etc.) are also available from retrospective-analysis or *reanalysis*. Reanalysis products provide synthesized estimates of atmospheric variables by combining observation with model data over regular grid surface

and provide climate variables as multidimensional hierarchical outputs, with spatial homogeneity and continuous temporal coverage (Sun et al., 2018). In a reanalysis system, advance data assimilation algorithm is used to assimilate irregular observations into numerical weather forecast model that encompasses a range of physical and dynamical processes (Bosilovich et al., 2008; Saha et al., 2010). Thus, the quality of synthesized climatic variables from reanalysis systems depends on the complex interaction between observational input, chosen model and the parameterization scheme used. With improved understanding of the dynamical process of climate and increase in computational power of modern computers, reanalysis products are continuously being updated with improved modelling scheme (representing physical processes), new observational data sets from various sources to improve the quality of these forecasts (Sun et al., 2018; Hersbach et al., 2020). Reanalysis products are being extensively used in climate research and other allied disciplines, primarily as a substitute of gauge based observations. Most commonly used reanalysis products are distributed by the National Centers for Environmental Prediction (NCEP) and the National Center for Atmospheric Research (NCEP-NCAR), European Centre for Medium-Range Weather Forecasts (ECMWF), National Aeronautics and Space Administration (NASA) and Japan Meteorological Association (JMA). These reanalysis systems use different sources of observational data, assimilation methods, models, and parameterization scheme and spatial resolution which affect their performance in reproducing the mean state of weather across different regions. These inter-differences among the reanalysis products provide a unique opportunity to assess their reliability in reproducing different climatic events across various spatial domain.

1.3 Literature Review

Studies focusing on extreme precipitation are essential as these events have large socio-economic impacts. However, the analysis of extreme precipitation has remained sensitive to the choice of definitions of extreme precipitation. In most cases, absolute and percentile based thresholds of extreme rainfall events are used to study extreme precipitation. The IMD uses a six-tier intensity-based rainfall classification scheme for classifying daily rainfall events over India. Pattanaik and Rajeevan (2010) used this scheme for studying extreme rainfall over India during the monsoon season. Rajeevan et al., (2008) studied the changes in moderate (5 – 100mm/day), heavy (100 - 150mm/day) and very heavy (>150mm/day) rainfall events over India following the classification of Goswami et al.,

(2006) and reported significant increases in the frequency of extreme rainfall events over India, associated with increasing sea surface temperature. However, a single absolute threshold of rainfall for identifying extreme events may not be useful to the whole of India, considering the significant variations in rainfall patterns and the differing levels of resilience and adaptation across the country. Percentile based identification of extreme precipitation event is more suitable in accounting for the spatial variability of extreme precipitation events, especially while conducting studies in regions with diverse climate regimes, like India. Another common choice is to use the ETCCDI recommended extreme precipitation indices, which have been developed with global and regional analyses in mind. The majority of extreme precipitation studies have used these ETCCDI indices for studying observed and future changes in extreme rainfall over India (Dash and Maity, 2019; Pradhan et al., 2019; Rai et al., 2020; Gupta and Jain, 2020; Sharma and Goyal, 2020).

Studying the strength and weakness of different precipitation datasets for hydro-climatological applications is interesting and at the same time essential in finding suitable datasets for large scale climate studies, especially when the study region is poorly monitored. Various attempts have been made on global as well as regional scale in finding suitable precipitation datasets for hydro-climatological studies. Some recent works are reviewed and cited in the following section.

Li et al., (2018) assessed the performance of four precipitation datasets over western Himalaya and found that the APHRODITE and WRF simulated precipitation better matches with rain-gauge (Bhuntar gauge) data and performed well compared to ERA-Interim and the coarser resolution gridded data from the IMD. Awange et al., (2016) evaluated six satellite precipitation products against GPCC dataset and found that the PERSIANN product is most suitable in capturing precipitation distribution over Africa. Paredes-Trejo et al., (2017) reported that satellite-derived CHIRPS estimates well correlate with observation over the North-Eastern parts of Brazil and better performs during we season. They also commented that the same data overestimated lower rainfall and underestimated higher rainfall (100mm/month) over the study area. Iqbal and Athar (2018) evaluated TRMM-TMPA satellite data over Pakistan and found that satellite-derived precipitation data overestimated precipitation compared to gauge-based data during the pre-monsoon and monsoon season, where it underestimated precipitation during post-

monsoon and winter season. The study also found that the performance of TMPA data better performed over plain and medium elevation zones than higher-elevation areas. Also, higher agreement is observed areas on annual and monthly precipitation than estimating daily precipitation. Alexander et al. (2020) compared 22 daily precipitation products over global land areas by calculating 10 annual rainfall and extreme precipitation indices and reported that in-situ precipitation products are similar to each other where the reanalysis showed the largest variation. However, over the extra-tropical areas, the reanalysis precipitation products performed better than satellite datasets. Chen et al (2020) compared six precipitation products over global and regional scale using two extreme rainfall indices i.e maximum one day rainfall and annual rainfall above 95th percentile for the period of 1979 – 2017. They found that the satellite-based PERSIANN-CDR performs better than reanalysis and merged datasets in capturing the temporal variability of the intensity and amount of precipitation extremes. However, the reanalysis and merged products underestimate the intensity of precipitation extremes over most areas and performed differently in various regions depending on the season. Kim et al (2019) compared seven gridded precipitation datasets over the Asian domain to assess their performance in capturing extreme precipitation in the summer monsoon season and found larger discrepancies over South East Asia including the maritime islands where smaller differences are observed over South Asia and East Asia. Besides, higher similarities among the precipitation datasets are observed over East Asia.

There are also several gridded precipitation data comparison studies are available over India. For example, Rana et al (2015) analyzed seven gridded precipitation datasets obtained from three different sources (gauge-based, satellite and reanalysis) in capturing seasonal precipitation climatology over India. They reported that for the monsoon season (JJAS), the gauge-only (CPC) and satellite-derived precipitation products (GPCP, 3B42-V6, and 3B42-V7) capture the JJAS rainfall variability better than the reanalysis (CFSR and ERA-Interim) when compared to the APHRODITE where the performance of other six gridded datasets were less agreeable with respect to APHRODITE during the winter (DJF). Sunilkumar et al., (2015) compared five multi-satellite precipitation datasets for two contrasting monsoon season (southwest and northeast) over India with a coarse resolution (1°×1°) gridded rainfall datasets from the IMD and reported that overestimation of rainfall over the dry regions (northwest and southeast India) and underestimation over

mountainous regions (west coast and northeast India) was a general feature of the multi-satellite precipitation products, whereas the bias was relatively small over the core monsoon zone. However, they found near similar values of the evaluation metrics for two contrasting monsoon season, implying that the performance of these datasets does not change with the season. Mondal et al., (2018) compared four multi-satellite precipitation estimates with a high resolution (0.25°×0.25°) gridded rainfall datasets obtained from the IMD to analyze their ability in representing monthly precipitation over 25 river basin of India for 1998 to 2015 and found that the TMPA precipitation product (in terms of accuracy) and PERSIANN (in terms of annual and monsoon trend) show a better agreement with IMD. All the datasets showed a higher variation of rainfall for the river basin located above 2000m in the northern parts of India. They also found that the trend patterns in annual and monsoon rainfall for TMPA, CMORPH, PERSIANN, and MSWEP matched with IMD data for some river basins located in the north, northwest, and central part of India. Ghodichore et al., (2018) compared six reanalysis datasets with the IMD gridded data to analyse the spatio-temporal variability of precipitation and temperature over India for 34 years and found that the MERRA-Land reanalysis has the best performance for precipitation over India where the ERA-interim and JRA-55 better performed for temperature than other reanalysis datasets. Chaudhary et al (2017) compared the gauge-based CPC and APHRODITE datasets with the high-resolution IMD gridded dataset in accounting dry and wet spell characteristics over India. The study found that the CPC better resembles with the IMD in replicating spell characteristics while the APHRODITE significantly deviates with over-estimation of wet days and under-estimation of dry days over India due to the increase of rainfall intensity during dry periods. However, the datasets showed major differences over the Northern Himalayan parts (Jammu and Kashmir) in representing the spell characteristics. They also found that the trend patterns in dry and wet spells over different parts of India are also not consistent between these three datasets. Recently Mahato and Mishra (2019) showed that the recent generation ERA-5 reanalysis data from the ECMWF outperforms the other five reanalysis datasets (i.e. NCEP-CFSR, MERRA-2, ERA-Interim and JRA-55) for the monsoon season precipitation, Tmax, evapotranspiration, and soil moisture over India when forced into a hydrological model.

Previous gridded data evaluation studies over India agree on the fact that the gauge-based, satellite and reanalysis datasets poorly performs over the Northern Himalayan. In a recent work, Jena et al., (2020) explored the ability of high-resolution IMD data and seven other satellite precipitation datasets in detecting cloudburst event over the northwestern parts of Himalaya. They found six out of eighteen cloudburst events are present in the IMD dataset over the Northwestern parts of Himalaya. The CHIRPS is found to give best rainfall estimate over the study region in monitoring cloudburst events than other satellite estimates when compared to the IMD datasets with an improved probability of detection values ranging from 60.5% to 78.6%. Gridded data comparison studies focusing on extreme precipitation over India is limited and well explored by considering a large subset of gauge, satellite, and reanalysis datasets. For example, Gupta et al., 2019 studied the ability of three satellite rainfall products (i.e. CHIRPS, Satellite Soil Moisture to Rain - SM2RAINASCAT and TRMM) in capturing extreme rainfall events over India. They reported that the TRMM and CHIRPS data well performed in representing extreme rainfall over various parts of India and with closer match with the IMD gridded data than SM2RAIN-ASCAT satellite-precipitations.

Studying the concentration of precipitation over a region using the PCI to characterize the regional climate and to explore the role of teleconnection and climate change is also another popular choice. For example, Skander et al., 2014 used the PCI to study precipitation characteristics over Bangladesh during 1971 – 2010 and reported that a strong irregularity of precipitation concentration over the south-eastern region where PCI in the rest of the country is mostly irregularly distributed which is line with the findings of Mondol et al., (2018). Raziai (2014) using the GPCC dataset, studied the PCI over Iran during 1951 – 2009 and reported irregular distribution of precipitation in the northern parts of Iran during all seasons. Khalili et al. (2016) noted that PCI on annual scale and during the rainy season (winter) over Iran is increasing in response to the decrease in precipitation over most parts of Iran. Shrestha et al., 2019 studied PCI in two river basins (Koshi and Kaligandaki) in Nepal and reported that substantial differences in monthly precipitation distribution in this two river basin and the PCI values showed irregular distribution at stations located in the southwestern region of Kaligandaki and the western region in Koshi basin, and concentrated within a few months, only during the monsoon where the uniform distribution of precipitation is found for the stations located in the central region. PCI on

annual and seasonal scale is extensively studied over China (Deng et al., 2018; Faiz et al., 2018b; Huang et al., 2019; Zhang et al., 2019; Lu et al., 2019) some studies also explored the role of large scale teleconnection on PCI over China. Jiang et al., 2016 reported that PCI has a positive significant correlation with urbanization over China especially over the eastern parts where the population density is very high, signifying that anthropogenic activity has a role in modifying regional precipitation regime. Guo et al., 2020 reported a positive correlation of PCI with drought indices over china indicating that the usability of PCI as an auxiliary index for drought assessment studies. Bartolini et al., 2018 investigated the trends in PCI over Tuscany (central Italy) between 1955 and 2013 and found positive significant trend at some stations on spring and summer seasons where no significant trends are detected for the studied 35 stations on annual basis and during the winter season. Caloiero et al., 2019 studied the long-term behaviour of rainfall and PCI changes over the Sardinia, the second-largest island in the Mediterranean sea and found that the decreasing trend in annual rainfall over the island especially in the western dry areas during winter months resulting annual PCI to be decreased and shifted towards uniform PCI distribution. Tolika, 2019 investigated annual and seasonal distribution of PCI over Greece and reported moderate precipitation concentration with an increase in PCI values while moving to its southern parts. On seasonal scale, the author argued that the increase in PCI in winter is mainly due to the increasing trends of the December precipitation, contributing to the seasonal totals. Few studies are carried out in India focusing on the long-term variability of PCI despite the need for managing recurring climatic hazards like floods and droughts, especially under a changing climate. After analyzing 141 years (1871 to 2012) of rainfall records Thomas and Prasannakumar (2016) reported that annual precipitation concentration is irregularly distributed over the Indian state of Kerala and is decreasing over time. Chatterjee et al., (2016) found that the PCI during the monsoon season is uniformly distributed over the Indian state of West Bengal throughout 1901 - 2002. Nandargi and Aman (2017) studied annual and monsoon PCI over 34 meteorological subdivision of India and found no sub-division has a uniform distribution of PCI over India on annual scale. However, PCI during monsoon is uniformly distributed over NE and EC parts India. Besides, Zamani et al (2018) found an irregular distribution in annual and seasonal PCI over the Jharkhand state in India except for the summer monsoon season, which is similar to the findings of Valli et al 2014 for the same region. However, a comprehensive analysis of different characteristics of annual and seasonal PCI over India is

lacking. Also, the ability of various gridded rainfall datasets in capturing the spatio-temporal variability PCI and its changes over India is never been explored. These are particularly important as recent changes in climate are affecting the regional distribution precipitation in various parts of the world.

1.4 Research gaps

Global or regional scale gridded precipitation datasets are not consistent with each other, primarily due to the differences in the number of observations used during preparation, resolution mismatch and interpolation algorithm applied to assimilate them. Hence, assessing the reliability of different precipitation products is imperative before using for any regional or global hydro-climatic applications. Previous gridded data inter-comparison studies mainly focused on the mean state of climate while assessing their reliability for climatological application (Rana et al. 2015; Fallah et al. 2019). Gridded datasets have also been compared for drought characterization (Zhan et al. 2016; Golian et al. 2019; Chen et al. 2019) and hydrological modelling (Bhattacharyya and Sanyal 2019; Kolluru et al. 2020) in different parts of the world. As extreme rainfall events are particularly important to erosional process, in triggering natural hazards and for designing hydrological structures, data inter-comparison studies should emphasize their ability in reproducing different characteristics of extreme precipitation events. Some recent analyses have assessed the reliability of these gridded datasets in capturing extreme precipitation characteristics on global (Alexander et al. 2020; Bador et al. 2020) and regional scale (Kim et al. 2019; Timmermans et al. 2019; Cavalcante et al., 2020). However, these studies are limited to the analysis of a small subset of available gridded datasets or have given lesser emphasis to extreme precipitation characteristics especially over India (Singh et al. 2019; Prakash 2019; Gupta et al., 2019). For example, Chaudhary et al. 2017 compared CPC and APHRODITE data over India and found that CPC better matches with the IMD gridded data in capturing dry and wet spell characteristics. Gupta et al., (2019) found that the TRMM and CHIRPS datasets performed well in capturing the intensity of extreme precipitation across most regions in India.

India, the second-most populous country in the world is frequently affected by floods, which are mainly associated with extreme rainfall events i.e. the Mumbai flood in 2013, Chennai flood in 2015 and the recent devastating floods of Kerala that occurred in 2018 and 2019. About 44.2% of total monsoonal rainfall in India comes from heavy rainfall (above

35.5mm/day) events (Pattanaik and Rajeevan, 2010), mainly associated with the wet spells during monsoon, and modulated by Low-Pressure Systems (LPS) or monsoon depressions (Rajeevan et al. 2010; Hurley and Boos 2015). In data-sparse countries like India, few gridded data comparison studies have been carried out (Mondal et al 2018), and with a handful of studies emphasizing on extreme precipitation (Bharti et al. 2016; Gupta et al. 2019). Owing to the variability of Indian summer monsoon rainfall and recurring occurrences of hydro-climatic extremes, it is important to evaluate the performance of gridded rainfall datasets in reproducing extreme rainfall characteristics over India. Also, previous gridded precipitation data inter-comparison studies in India have mainly assessed the reliability of satellite and reanalysis rainfall products based on mean precipitation amount (Rana et al., 2015; Kishore et al., 2016; Mondal et al., 2018), dry and wet spell characteristics (Sushama et al., 2014; Chaudhary et al., 2017), aridity index (Ramarao et al., 2019), but their reliability in capturing the spatio-temporal dynamics of PCI has never been explored.

1.5 Research objectives

The core motivation for this study stems from the need to understand the ability of different gauges based, satellite and reanalysis rainfall products in capturing various characteristics of precipitation (i.e. *extreme rainfall* and *precipitation concentration*) over India. Given that floods and drought are recurring hydro-climatic events in India and cause huge damage to the country's economy, it is, therefore, necessary to focus our attention to understand the spatio-temporal occurrences of extreme hydro-climatic events for better monitoring and predicting these events and to reduce the socio-economic impacts. In addition to this, water management requires an understanding of existing tools and development of new data set and methodologies to detect extreme precipitation events, their characteristics (e.g. intensity, duration, spatial distribution and temporal changes) which better facilitate the nature of management strategies and disaster preparedness. In light of these factors, the primary objective of this study is *to comprehensively assess the reliability of eleven different gauge-based, satellite-derived and reanalysis rainfall datasets in capturing various characteristics of extreme precipitation and precipitation concentration over India.*

More specifically the objectives are to analyze:

(1) the ability of gridded rainfall datasets in reproducing different characteristics of extreme rainfall and its trends over India.

(2) the spatial and temporal variability of annual and seasonal PCI over India and explore the influence of geographical factors (i.e. latitude, longitude, and altitude) on the spatial distribution of PCI over India.

(3) the ability of the datasets to capture different characteristics of annual and seasonal PCI and its trends over India.

This is done by comparing the results obtained from the eleven datasets with a purely in-situ based gridded rainfall datasets obtained from the India Meteorological Department (IMD).

Chapter 2

Study area and datasets

2.1 Study area

In this study, we focus our attention to India, home to around 1.3 billion people where more than 55% of the total population is still dependent for their livelihood on the highly rainfall-sensitive agricultural sector. India's food security, inland water resources, and the overall economy have remained sensitive to monsoon rainfall variability throughout the past (Gilmont et al., 2018). To analyze extreme rainfall events over India, smaller homogenous regions are identified based on physiographic divisions and spatial rainfall patterns over India (Fig. 2). These regions are Thar Dessert (TD), Northern Himalaya (NH), Ganga plain (GP), North-East (NE), Central India (CI), Eastern Peninsula (EP), Southern Peninsula (SP), Western Ghat (WG), West Coast (WC) and East coast (EC). A strong latitudinal rainfall gradient is observed in the distribution of annual average rainfall over India, which extends from the NE parts covering Meghalaya plateau to the Thar Desert of WI (Fig. 1B). Annual average rainfall over India increases from <200mm (Thar Dessert) to >6000mm (NE India) following the east to west rainfall gradient. Due to the strong influence of monsoon circulation, monthly precipitation in most of these regions reaches its peak during JJAS months with the arrival of South-West monsoon winds. An exception to this is observed in parts of Southern EC and SP region, where rainfall mostly occurs during post-monsoon (SON) months with the reversal of the monsoon wind.
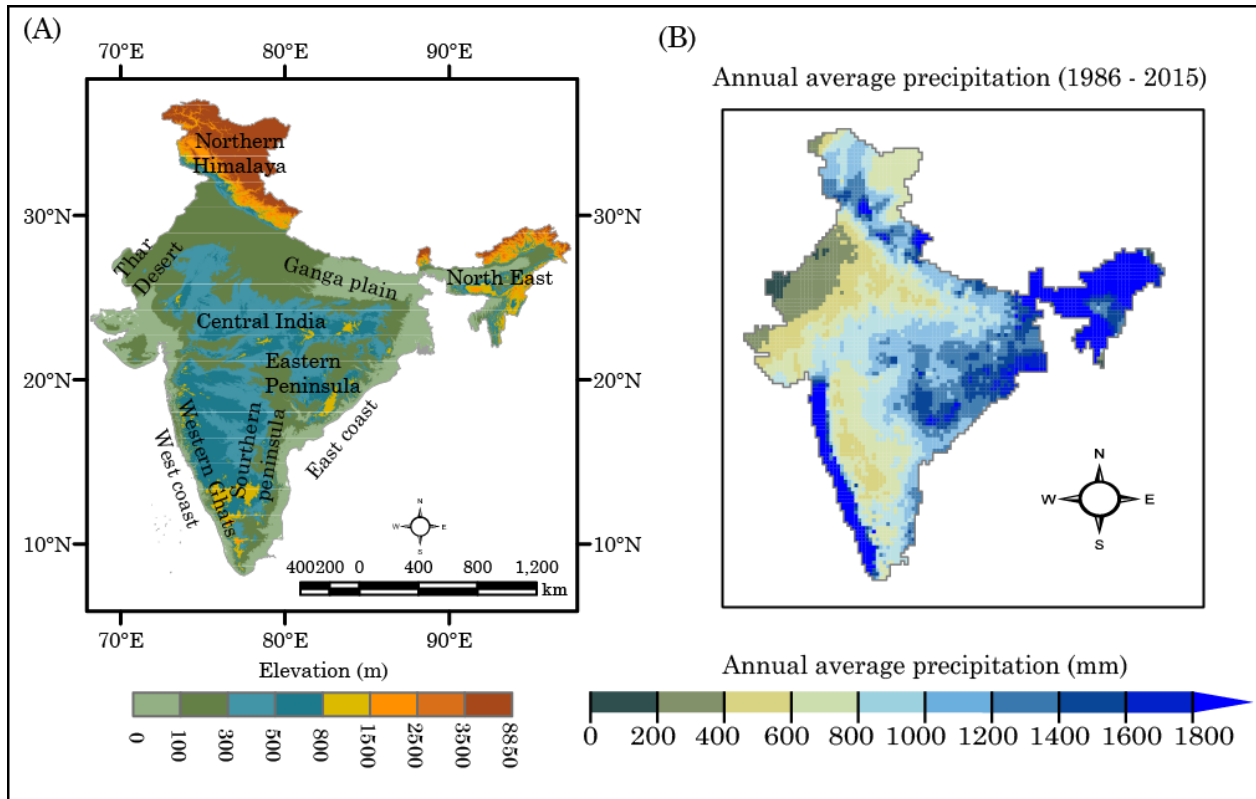
Fig. 2 (**A**) Elevation distribution along with major physiographic regions in India and (**B**) the right panel shows the distribution of annual average precipitation over India (derived from the IMD gridded dataset) during the study period (1986 – 2015).

In India, extreme rainfall events are mainly associated with the wet spells during monsoon and modulated by the Low-Pressure Systems (LPS) or monsoon depressions (Rajeevan et al. 2010; Hurley and Boos 2015). These LPS have an average frequency of 13-15 storms per season and an average lifespan of 3-6 days (Godbole, 1977; Hurley and Boos, 2015). Most of these LPS form in the Bay of Bengal (BOB) and propagates towards central India from southeast to northwest following the monsoon trough, and cause heavy rainfall across central India and Gangetic plain (Ajayamohan et al., 2010). Revadekar et al. (2016) found that frequency of cyclonic disturbances and extreme rainfall of different thresholds are positively correlated over India. However, the strength of correlation decreases as extreme rainfall threshold increases. The study also concludes that LPS and disturbances that form over BOB play a dominant role in determining the distribution and occurrence of extreme rainfall events over India. Monsoon lows and depressions after moving northwards towards the Himalayas interact with extra-tropical disturbances under a strong orographic forcing and cause extreme rainfall events in parts of Pakistan, Northern-India and Nepal (Vellore

et al., 2016; Bohlinger et al., 2017; Priya et al, 2017; Hunt et al., 2018). The axis of monsoon trough periodically oscillates in north-south direction over the Gangetic plain, resulting regionally concentrated heavy rainfall events during monsoon. Additionally, in long-term, LPS activities are influenced by global teleconnection patterns. For instance, during El-Niño conditions depressions are more likely to be formed and characterized with heavy rain events in the core-region compared to La Niña conditions (Hunt et al., 2016; Hunt et al., 2016).

Though there is no significant trend in average monsoon rainfall over India, a regionally significant trend exists especially in rainfall variability, spell characteristics and extreme precipitation events (Singh et al., 2019). With anthropogenic warming, sea surface temperature of the Indian Ocean (especially in the Western Equatorial part) has increased. This coupled with the slow northward propagation of monsoon intraseasonal oscillation (MISO) has diversely affected the regional precipitation pattern over India. For instance, daily rainfall variability over WI, CI and NE India has increased significantly (Sabeerali et al., 2014; Singh et al., 2019). In line with that, the frequency of short duration dry spell has increased in consistent with the slower progression of MISO towards the north (Singh, 2013b). Although, there are no significant changes in the frequency of wet spells but progressively warming and wetter atmosphere have increased the intensity of short duration (4 - 7 days) wet spells over India (Singh, 2013a; Singh, et al., 2014; Pai et al., 2016). This compensating effect may explain the phenomena of no detectable changes in mean annual precipitation over India. In response to climate change, occurrences of extreme rainfall events are increasing especially over central India and this increasing pattern is dominated by short-duration events (Dash et al., 2011; Vinnarasi & Dhanya, 2016). Sagar et al. (2017), found that large rainstorms (~50,000 km^2) lasting at least 2 days have doubled over past six decades over central India, where more intense but smaller rainstorms (>6250 km^2) have tripled over this time (Roxy et al. 2017). Further, extreme rainfall events (>95th percentile) are increasing in intensity and frequency in most part northwestern, west-central, north-eastern and peninsular India but decreasing over east-central and northern India (Krishnamurthy et al., 2009; Dash et al., 2011; Vittal et al., 2013; Malik et al., 2016; Bisht et al., 2018; Mukherjee et al., 2018).

2.2 Data sets

2.2.1 Gauge-based gridded data

In this study, four gauge-based (IMD, APHRODITE, CPC and GPCC), two satellite-derived (CHIRPS, PERSIAN-CDR) and six reanalysis datasets (ERA5, ERA-Interim, MERRA2, NCEP2, PGF and JRAA-55) are used for calculating different extreme rainfall indices over India. A brief description of these datasets is presented in Table 2.1 and detailed descriptions are given below.

Table 2.1 Description of gridded rainfall datasets used in this study.

Dataset	Period	Resolution	Data source	References
IMD	1901-2015	(0.25° × 0.25°)	Gauge-based	Pai et al. (2014)
APHRODITE	1951 – 2015	(0.25° × 0.25°)	Gauge-based	Yatagai et al. (2012)
CPC -Unified	1979 - Present	(0.5° × 0.5°)	Gauge-based	Xie et al. (2007)
GPCC_V2	1982 - 2016	(1° × 1°)	Gauge-based	Schamm et al. (2014)
CHIRPS	1981 - Present	(0.25° × 0.25°)	Satellite	Funk et al. (2015)
PERSIANN-CDR	1983 - Present	(0.25°× 0.25°)	Satellite	Ashouri et al. (2015)
PGF	1948 - 2016	(0.25° × 0.25°)	Reanalysis	Sheffield et al. (2006)
NCEP-2	1979 - Present	(1.875° × 1.875°)	Reanalysis	Kanamitsu et al. (2002)
ERA-Interim	1979–present	(0.75° × 0.75°	Reanalysis	Dee et al. (2011)
ERA-5	1979–present	(0.25°× 0.25°)	Reanalysis	Hersbach (2016)
MERRA-2	1980 - Present	(0.5° × 0.67°)	Reanalysis	Gelaro et al. (2017)
JRA-55	1958-Present	(0.5625° × 0.5625°)	Reanalysis	Kobayashi et al. (2015)

IMD Gridded data

To evaluate the reliability of different satellite, reanalysis and gauge based gridded rainfall product over India, we considered the latest generation gridded rainfall product, developed by the IMD, as a benchmark dataset for inter-comparison. The gridded rainfall product is produced using the Shepard interpolation scheme (Shepard, 1968) and has a spatial

resolution of 0.25°×0.25°. Daily rainfall records from 6329 hydro-meteorological stations, monitored by different agencies across India, are used for this purpose (Pai et al., 2014). However, the density of weather stations and their record lengths vary from time to time. This gridded rainfall product contains daily rainfall time series for a period of 115 years (1901 – 2015) covering whole India from 60° to 100°E and from 6° to 39°N. It is an improved version compared to the previous 1°×1° (Rajeevan et al., 2006) and 0.5°×0.5° (Rajeevan and Bhate, 2009) gridded rainfall products and well captures the orographic influence on precipitation (Pai et al., 2014). This data has been used in many previous studies for analyzing climatological extremes over India (Vinnarasi and Dhanya 2016; Deshpande et al., 2016). In this study, we used rainfall records of 30 years (1986 – 2015).

APHRODITE

The APHRODITE (Asian Precipitation-Highly Resolved Observational Data Integration Towards the Evaluation of the water resources) gridded precipitation product provides daily rainfall climatology over the monsoon dominated Asia at 0.25°×0.25° spatial resolution (Yatagai et al., 2012). Different versions of APHRODITE rainfall product are available with an updated time for different regions. The Shepard interpolation scheme (Shepard, 1968) and an angular based weighting function for elevation correction are used to produce this gridded rainfall product (Yatagai et al., 2012). It is purely a gauge based rainfall data set, developed by using observations from 5000 to 12000 rain gauges from different countries. The gridded data files are constructed by interpolating rain-gauge observations from different countries over the Asian domain (Yatagai et al., 2012). Here, the APHRODITE version V1101 (1986-1997) and the recently updated version of V1901 (1998 – 2015) from the APHRODITE-2 project are used to construct daily precipitation climatology over India for the study period 1986 – 2015. The APHRODITE is mainly limited to the Asian domain only. The quality of this data depends on the amount of gauge-data which varies over space and time. The distribution of rain-gauges in APHRODITE is quite uneven over India, especially over the EP and dry parts of WI.

CPC

The NOAA's (National Oceanic and Atmospheric Administration) Climate Prediction Centre (CPC) provides a unified gauge based gridded precipitation product at a resolution

of 0.5° × 0.5° (Chen et al., 2008). CPC data contains daily precipitation climatology over global land surface areas from 1979 to present. This gauge based data was constructed using around 2200 gauges observations spreading over East Asia (Xie et al., 2007). The Optimal Interpolation technique is used to represent the area-averaged daily precipitation field over each grid box considering the effects of topography (Xie et al., 2007). CPC is a land only product and its performance

GPCC

The GPCC provides gauged based gridded rainfall data set over the land surface based on data supplied from different institutions around the world. The product is derived using the block kriging interpolation method and provides daily precipitation from January 1982 to December 2018 at a spatial resolution of 1° × 1° (Schamm et al., 2015). Here the GPCC Full Data Daily (GPCC-FDD) product version (V2018) is used for this study. The GPCC-FDD product is particularly recommended for the analysis of daily extreme precipitation and related statistics than other categories of GPCC datasets (http://dx.doi.org/10.5676/DWD_GPCC/FD_D_V1_100).

2.2.2 Satellite rainfall estimates

PERSIANN-CDR

PERSIANN-CDR is a satellite-based gridded rainfall product, developed by the Center for Hydrometeorology and Remote Sensing (CHRS) at the University of California, Irvine (UCI) for the Climate Data Record (CDR) program of the National Oceanic and Atmospheric Administration (NOAA). Data from infrared (IR) and passive microwave measurement (PMW) from multiple Geostationary Earth Orbiting (GEO) and low Earth orbit satellites are combined using an Artificial Neural Network (ANN) to provide daily estimate of precipitation between the latitude band of 60°S to 60°N. PERSIANN-CDR provides a continuous estimate of daily precipitation from 1983 onwards with consistency to study the changes in global and regional precipitation patterns and water cycle under climate change (Ashouri et al., 2015; Liu et al., 2017). PERSIANN-CDR is developed especially to address hydrological and climate issues. It provides long term precipitation record (over 35 years) which is not so common for satellite-rainfall datasets. The main

datasets for the construction of PERSIANN-CDR product include the infrared GridSat-BI satellite data, National Centers for Environmental Prediction (NCEP) Stage IV radar data, and the GPCP monthly precipitation data at 2.58. The PERSIANN-CDR product is first generated from the PERSIANN algorithm using GridSat-BI IR data as the primary satellite input. Then, the NCEP stage IV radar data are used to train the ANN and to create the nonlinear regression parameters for the ANN model. The satellite-gauge merged product – the GPCP gridded monthly data is then used to adjust the biases of the estimated rain rate by the ANN model. Lastly, the 3-hourly adjusted PERSIANN precipitation data are accumulated to a daily scale to produce the PERSIANN-CDR product. More details about the PERSIANN-CDR data can be found in Ashouri et al. (2015). The main limitations associated with this data are that it heavily relies on IR measurements and conversion of IR requires complex algorithm. Also, the data is available for quasi-global coverage (60°S to 60°N).

CHIRPS

CHIRPS, developed by the Climate Hazards Group (CHG), is a satellite-based rainfall estimate providing long-term precipitation data at a spatial resolution of 0.05° between the latitude band of 50°S to 50°N from 1981 to present (Funk et al., 2015; 2014). CHIRP is firstly generated by merging the IR-derived precipitation with the Climate Hazards Group Precipitation Climatology (CHPclim) and is then blended with the ground station observations using a modified Inverse Distance Weighing (IDW) method (Funk et al., 2015) and called as CHIRPS (CHIRP with Stations). The updated CHIRPS version 2.0 is available on the CHG website (chg.geog.ucsb.edu/data/) from which daily precipitation data for 1986 – 2015 is obtained. The CHIRPS also provides quasi-global precipitation data and not a global product. In this study, the CHIRPS daily data at 0.25° spatial coverage is used between 1986 and 2015.

2.2.3 Reanalysis rainfall products
ERA-Interim

ERA-Interim is a third-generation global atmospheric reanalysis, a successor of ERA-40 product, with an improved atmospheric model and assimilation system, produced by the European Centre for Medium-range Weather Forecasts (ECMWF) providing data from 1979 to present (Dee et al., 2011). It is developed to address several difficulties associated with

the data assimilation during the production of ERA-40. The observational datasets that come before 2002 are from the ERA-40 The improved four-dimensional variational assimilation (4D-Var) system is used in ERA-Interim instead of 3D-Var that used in ERA-40 which improves its performance for hydro-meteorological applications including flood and drought monitoring and assessment (Misra et al., 2012; Seager & Henderson, 2013; Shah & Mishra, 2014). It has a spatial resolution of 0.75° × 0.75°

ERA-5

Era-5 is the most recent reanalysis product from the ECMWF, a successor of ERA-Interim and also provides data from January 1979 onwards. Compared to ERA-Interim, analysis based on 10-member ensemble 4D-Var, an upgraded radiative transfer model, improved bias correction method and observed sea surface temperature from second Hadley Centre sea surface temperature are included in ERA-5 (Urraca et al., 2018). This reanalysis product has a higher spatial resolution compared to ERA-Interim and used for various hydro-climatic researches (Albergel et al., 2018; Hwang et al., 2019; Mahto and Mishra 2019; Olauson, 2018). ERA5 provide multidimensional atmospheric variables at very high spatial (0.25°) and temporal (1hr) resolution and better able to resolve tropospheric circulation as well as complex atmospheric phenomena like a hurricane than previous generation reanalysis products.

MERRA2

The Modern-Era Retrospective Analysis for Research and Applications, version 2 (MERRA-2), atmospheric reanalysis product provides hourly precipitation estimates generated on a 0.5° × 0.625° latitude-longitude grid. MERRA2 is the newest reanalysis product by NASA's Global Modeling and Assimilation Office (GMAO) replacing the previous generation MERRA product. It uses the new version of the GEOS-5 atmospheric model and includes more observational data, recent satellite observations and an improved assimilation model (Molod et al. 2015) to produce various meteorological variables. In MERRA2, precipitation over polar oceans is thought to be overestimated and also higher overestimation over the orographic belts in tropical latitudes.

PGF

Princeton global forcing (PGF) is developed by the terrestrial hydrology research group at Princeton University by merging NCEP reanalysis data set with observational data from different sources, such as TRMM, CRU, GPCP and NASA SRB products (Sheffield et al. 2006). PGF provides daily precipitation rate over the entire globe at 0.25° spatial resolution from January 1948 to December 2016. The dataset is developed to provide various near-surface meteorological inputs require for driving land surface (and other terrestrial models) and also been utilized in various hydro-climatic studies around the world (El Kenawy and McCabe 2016; Sheffield et al. 2006).

NCEP2

The NCEP-2 of National Centers for Environmental Prediction (NCEP) is an updated and human-error-fixed version of NCEP-NCAR (R1), with similar input data and vertical resolutions (Kanamitsu et al. 2002, Chen et al. 2019). NCEP2 is based on a fully coupled ocean–land-atmosphere model and it uses numerical weather prediction techniques to assimilate and predict atmospheric states using a three-dimensional variational (3D-Var) assimilation scheme (Saha et al. 2010). The improvements in NCEP2 include an updated model with better physical parameterizations, assorted data assimilation errors were fixed and also additional data were included. However, the reanalysis is still first-generation and suffer from mainly quality issues like poor spatial and temporal resolution and relatively poor performance over the southern hemisphere.

JRA-55

JRA-55 is the second reanalysis product from the Japan Meteorological Agency (JMA) which is an improved version of the previous JRA-25 reanalysis. The JRA-55 has been extended to 55yeras to provide data from 1958 to present (Kobayashi et al., 2015). It uses a 4D-VAR approach for data assimilation compared to 3D-Var used in JRA-25 and uses variational bias correction technique that improves its performance than JRA-25 (Ebita et al., 2011).

Chapter 3

Methodology

3.1 Pre-processing of gridded datasets

The spatial resolution of these selected gridded rainfall datasets varies widely (from 0.25° to 1.875°) thus hindering direct comparison with the reference (IMD) dataset. Also, upscaling of fine resolution gridded data into relatively coarser spatial resolution reduces signal-to-noise ratio and introduce additional uncertainties by suppressing important climatological features (Yang et al., 2014). Therefore, all the datasets are re-gridded to a common (0.25° × 0.25°) grid using a bilinear interpolation technique (Chen et al., 2018), consistent with the IMD dataset for direct comparison. We acknowledge that this re-gridding process from lower to higher resolution can affect extreme rainfall values but we also want to clarify that doing the reverse, that is re-gridding into lower resolution by increasing grid-size (*through averaging*) may dilute the spatial heterogeneity of extreme rainfall. Given the higher spatial variability of extreme rainfall, re-gridding into lower resolution often significantly dampens localized maxima (Herold et al., 2017), especially frequency or intensity of extreme rainfall (Kursinski and Zeng, 2006), which may have implications for regional flood forecasting and preparedness. Here only wet day rainfall is considered for the analysis of extreme and PCI where a wet is defined as a day with rainfall $1\geq$ mm (Chaudhary et al., 2017; Sushma et al., 2014).

3.2 Extreme rainfall indices

Study of extreme rainfall is carried out in two ways, either by fitting parametric extreme value distribution to assess rare events or by using non-parametric methods of calculating indices for extreme rainfall events, solely based on empirical data analysis. Here we used the non-parametric approach by calculating thirteen extreme rainfall indices (Table 3.1) to encompass a wider range of the extreme and annual rainfall climatology over India, based on absolute and percentile based rainfall thresholds, to evaluate gridded rainfall datasets. Out of these thirteen indices, ten indices are selected from ETCCDI (for more details see http://etccdi.pacificclimate.org/indices_def.shtml) and have been widely used for detection, attribution and climate change projection studies around the world (Cavalcante et al., 2020; Dash and Maity, 2019; Kim et al., 2020; Schoof and Robeson, 2016; Srivastava et al., 2020). The other three indices, Heavy rain (HR) Very heavy rain (VHR) and extremely heavy rain

(EHR) are selected from the IMD rainfall intensity classes (http://img.indiaonline.in/weather/Weather-Glossary.pdf) and have direct linkages to floods and in triggering flash floods, landslides over India. Extreme indices; characterizing different magnitude (RX1day, RX5day, PRCPTOT, SDII, R95tp and R99tp), frequency (R10mm, R20mm, R64.5mm and R244.5mm) and duration (CDD, CWD) of annual extreme rainfall over India are calculated over each grid-cell for each gridded datasets, resulting in one value per year.

Table 3.1 Description of extreme rainfall indices used in this study.

Category	Index	Indicator Name	Description	Unit
Magnitude	PRCPTOT	Annual total wet day rainfall amount	Annual total rainfall in wet days (>1 mm/day)	mm
	SDII	Simple Daily Intensity Index	Annual total wet day rainfall divided by the number of wet days	mm/day
	RX1day	Maximum 1-day rainfall	Annual 1-day maximum rainfall	mm
	RX5day	Maximum 5-day rainfall	Annual 5-day maximum rainfall	mm
	R95tp	Very wet days	Annual rainfall above long-term 95th percentile	mm
	R99tp	Extremely wet days	Annual rainfall above long-term 99th percentile	mm
Frequency	R10mm	number of 10mm or more rainfall days	Annual count of days when daily rainfall ≥10mm	days
	R20mm	number of 20mm or more rainfall days	Annual count of days when daily rainfall ≥20mm	days
	R64.4mm*	Heavy Rain (HR)	number of days with rainfall above 64.4mm	days
	R124.4mm*	Very Heavy Rain(VHR)	number of days with rainfall above 124.4mm	
	R244.4mm*	Extremely Heavy Rain (EHR)	number of days with rainfall above 244.4mm	days
Duration	CDD	Maximum length of dry spell	Maximum number of consecutive days with daily rainfall ≤1mm	days
	CWD	Maximum length of wet spell	Maximum number of consecutive days with daily rainfall ≥1mm	days

* Indices as per IMD rainfall intensity classification.

3.3 Precipitation Concentration Index (PCI)

PCI is a useful index for accounting the heterogeneity of precipitation amount on annual scale and defined as the ratio between the sum of monthly squared precipitation to the square of annual precipitation. In this study, the PCI, proposed by Oliver (1980) and

further modified by De Luis et al., (1997), is used for the calculation of the annual PCI (APCI), as indicated in the equation (1)

$$APCI = \frac{\sum_{i=1}^{12} p_i^2}{\left(\sum_{i=1}^{12} p_i\right)^2} \times 100 \qquad \qquad \text{Equation (1)}$$

Where p_i represent the monthly precipitation in ith month. In addition, to account the seasonal variability of precipitation, the seasonal PCI (SPCI) for winter (JF), summer (MAM), monsoon (JJAS), and post-monsoon (OND) seasons were calculated using the equation (2).

$$SPCI = \frac{\sum_{i=1}^{n} p_i^2}{\left(\sum_{i=1}^{n} p_i\right)^2} \times C \qquad \qquad \text{Equation (2)}$$

We used C values of 16.667 for winter (January-February), 25 for summer (March-May), 33.333 for Monsoon (June – September) and 25 for post-monsoon (October - December) seasons respectively. Following Oliver (1980) and Zamani et al., (2018), PCI values are classified in different concentration classes to represent spatial heterogeneity of PCI qualitatively. PCI values less than 10 represent a uniform distribution of precipitation, values between 11 to 15 represents moderate precipitation distribution. PCI values from 16 to 20 irregular distribution and PCI values above 20 represent strong irregularity of precipitation distribution. In this study, only the rainy days (rainfall ≥ 1mm) are considered for the calculation of annual and seasonal PCI over India (Sushma et al., 2014; Chaudhary et al., 2017). The coefficient of variation (CV) of PCI is studied on an annual and seasonal scale. The relationship between PCI and average annual/seasonal precipitation is explored using Pearson's correlation coefficient (CC). Besides, the heterogeneity in the spatial distribution of average APCI values over India is investigated by calculating CC between the average APCI and geographical factors such as latitude, longitude and altitude.

3.4 Evaluation metrics for data inter-comparison
We aim to assess the performance of the gridded rainfall products with the IMD gridded data, using some basic model evaluation criterion to infer whether these datasets can reasonably reproduce the extreme rainfall climatology over India or not. Therefore, five model performance indices i.e. correlation coefficient (CC), index of agreement (d), present-BIAS (PBIAS), mean-absolute-error (MAE) and root-mean-square-error (RMSE) which are

frequently being used in hydro-climatic research (Moriasi et al., 2007) are calculated for each grid-cell between 1986 and 2015.

Willmott (1984) defined the index of agreement (d) as the ratio of the mean square error and the potential error (which is the maximum possible or potential error that can be found for any pair set of observations) multiplied by N (number of observations) and then subtracted from 1. It varies from 0 to 1; higher value 1 reveals high agreement of the model with observed, whereas 0 indicates no agreement. The index of agreement (d) is calculated as follows

$$d = 1 - \frac{\sum_{i=1}^{n}(R_{oi} - R_{si})^2}{\sum_{i=1}^{n}(|R_{si} - \bar{R}_o| + |R_{oi} - \bar{R}_o|)^2}$$ Equation (3)

MAE is an important error matric, used to quantify the average magnitude of error between observed data (IMD) and model data (other gridded datasets) and is calculated by summing the magnitude of errors by the total number of observation that is n.

$$MAE = \frac{1}{n} \sum_{i=1}^{n}|R_{si} - R_{oi}|$$ Equation (4)

PBIAS is used to measure the average tendency of model datasets to be larger or smaller than their observed counterpart (IMD), expressed in percentages. Positive PBIAS means overestimation where negative PBIAS means underestimation of rainfall by other gridded rainfall datasets, with a desirable value of 0, signifying perfect match between IMD and other gridded datasets.

$$PBIAS = \frac{\sum_{i=1}^{n}(R_{si} - R_{oi})}{\sum_{i=1}^{n}(R_{oi})} \times 100$$ Equation (5)

Where R_{oi} is the ith observation from IMD gridded data, R_{si} is the corresponding i^{th} rainfall from other gridded datasets considered in the present study, $\bar{R}_o$ is the observed mean of IMD data and n is the number of observations.

The CC ranges from -1 to 1 and the d ranges from 0 to 1. For both of these two dimensionless indices, a positive 1 means a perfect fit/agreement between observations (IMD) and other gridded datasets. Where, the error indices i.e. RMSE, PBIAS, and MAE have a desirable value of zero, representing a perfect match between observations (IMD) and other datasets. Here only the spatial distribution of PBIAS over India is presented. We

then computed the median value of all evaluation metrics for each rainfall indices over India to facilitate an easier comparison between datasets.

The relative performance of the gridded datasets in representing one particular extreme index over India is also evaluated by computing a Relative Skill Score (RSC) for each rainfall datasets. For this, the error indices (Eq. 6 to 8) are first normalized as they have different units and a wider theoretical range. Considering this, the error indices are normalized as follows;

$$PBIAS' = \frac{(|PBIAS_{median,i}| - |PBIAS_{median,min}|)}{(|PBIAS_{median,max}| - |-PBIAS_{median,min}|)}$$
$$\text{Equation (6)}$$

$$MAE' = \frac{(MAE_{median,i} - MAE_{median,min})}{(MAE_{median,max} - MAE_{median,min})}$$
$$\text{Equation (7)}$$

$$RMSE' = \frac{(RMSE_{median,i} - RMSE_{median,min})}{(RMSE_{median,max} - RMSE_{median,min})}$$
$$\text{Equation (8)}$$

Normalization thus would yield a value between zero and one, where zero means relatively better performance and a value of one represents poor performance among the selected datasets, for a particular extreme rainfall index. The results of these normalized error indices (RMSE, PBIAS, and MAE) and dimensionless indices (CC and d) are presented using 'portrait diagrams' (Gleckler et al., 2008). Portrait diagram is a two-dimensional plot used here used to represent of median values of evaluation indices for each extreme rainfall index (rows) and each dataset (columns). Different colours in portrait diagram represent relative magnitude of error indices and dimensionless indices in different dataset.

Finally, a relative skill score (RSC) is developed (Eq. 9) for each selected extreme rainfall indices using the dimensionless indices (i.e. CC and d) and the normalized values of error indices. We acknowledge that different approaches may be taken to combine error indices, or to present them separately. This RSC is defined as

$$RSC_{i=5} = [CC + d + (1 - PBIAS') + (1 - MAE') + (1 - RMSE')] \quad -1 \leq RSC \leq i \quad \text{Equation (9)}$$

Where i stands for the number of evaluation indices incorporated to calculate RSC. A value closer to -1 means poor or *unsatisfactory performance* and a value closer to i (here 5) means *very good performance*. The range of RSC depends on the number of indices selected for calculating it. Here, five indices are used; therefore, the RSC has a range of -1 to 5. The

RSC values are further used to rank these eleven datasets where a dataset with the highest RSC given a rank of 1 and the one with the lowest RSC got a rank value of 11, considering a particular extreme rainfall index.

Apart from this, the probability density functions (PDFs) of average extreme rainfall from eleven other datasets are compared to the PDF of IMD to explore how well these datasets resembles the average spatial distribution of different rainfall indices over India. For this, long-term average values of extreme rainfall indices from all the grid cells over India are considered. Here, the PDFs are estimated using a nonparametric smoothing technique, the Kernel Density Estimator (KDEs) to reduce the sampling error associated with the choice of distribution functions. A Gaussian kernel is used to develop KDEs (Teegavarapu et al., 2013). Also, the temporal variations in average extreme rainfall values over India in different datasets are compared using line graph.

3.5 Trend analysis of PCI and Extreme indices

Further, inter-comparison between different gridded rainfall datasets is made for analyzing its ability to capture the temporal variations in extreme rainfall and PCI over each grid cell. We estimated the trends in extreme rainfall indices using non-parametric Mann-Kendall (MK) test (Mann 1945; Kendall 1948), the widely used test to analyze trend (Kundu and Mondal 2019; Ji et al., 2019; Zhong et al 2017) Xu et al. (2005) commented that while analyzing the trend in hydro-climatic variables such as trends in long-term rainfall, MK-test performs better than parametric tests. MK test is a nonparametric test, checks the existence of any monotonically increasing/decreasing trend against the null hypothesis of no trend. The Mann-Kendall test statistics S is calculated as

$$S = \sum_{i=1}^{n-1} \sum_{j=i+1}^{n} sgn(x_i - x_j)$$

Where, x_j and x_i are the sequential data values at times j and i, respectively, $j > i$; n is the length of the time-series and:

$$sgn(x_i - x_j) = \begin{cases} +1, & if & x_i - x_j > 0 \\ 0, & if & x_i - x_j = 0 \\ -1, & if & x_i - x_j < 0 \end{cases}$$

The value of S indicates the direction of the trend. A positive S value indicates an increasing trend where the negative value indicates a decreasing trend. For independent and identically distributed random variables, when $n \geq 8$, the S statistic is nearly normally distributed, where the mean is zero and the Variance(S) is calculated as:

$$Var\ (S) = \frac{n(n-1)(2n+5)}{18}$$

The standardized test statistics Z is computed as follows.

$$Z = \begin{cases} \dfrac{S-1}{\sqrt{Var(S)}}, & if\ S > 0 \\ 0, & if\ S = 0 \\ \dfrac{S+1}{\sqrt{Var(S)}}, & if\ S < 0 \end{cases}$$

Positive or negative values of Z indicate increasing or decreasing trends, respectively. Computed Z statistic is tasted against a significant level α to check whether it is statistically significant or not. When, $|Z| > Z_{(α/2)}$ it signifies that the time series exhibit a significant trend. In this study, the significance level (α) of 0.05, corresponding to a $Z_{(α/2)}$ value of 1.96 is used.

The magnitude of trend (Q) of selected indices, over grid cells is calculated using the Theil-Sen's slope estimator (Sen, 1968) for N pairs of observations, using the following equation:

$$Q_i = \frac{(x_j - x_k)}{(j-k)}\ for\ i = 1 \dots\dots N$$

Where, x_j and x_k are data values at time j and k (j > k) respectively. Median of n values of Q_i is the estimated Sen's slope which is computed using the following equation

$$Q_{med} = \begin{cases} Q_{(N-1)/2} & if\ N\ is\ odd \\ \dfrac{Q_{(N/2)} + Q_{(N+2)/2}}{2} & if\ n\ is\ even \end{cases}$$

A positive (negative) value of slope indicates an upward (downward) trend, i.e. increasing (decreasing) values with time. One of the advantages of the Theil-Sen estimator is that it is not prone to the influence of extreme values. When a time series contains extreme values, linear regression methods are prone to their influences, resulting in overestimation or

underestimation of slope values. In contrast, as the Theil-Sen's estimator takes the median of a slope between two points in a time series as the true slope, thus unaffected by outliers.

Chapter 4

Characteristics of extreme rainfall in different gridded datasets over India

In this chapter, the analysis of extreme rainfall is presented. For more detail descriptions about the datasets and methodology please see chapter 2 and 3. First, all the gridded datasets are compared with the IMD dataset to see how well these datasets can capture the magnitude, frequency and duration based extreme rainfall indices over India. Subsequently, the overall performance of each gridded product in capturing extreme rainfall is explored using evaluation metrics and portrait plot. Finally, the results of trend analysis are presented and the results are discussed following this section.

4. Results

4.1 Extreme rainfall magnitude
PRCPTOT

According to the IMD data, annual average rainfall in wet days (PRCPTOT) over India ranges from 8599.5 mm (NE India) to 156 mm (WI) between 1986 and 2015, and have a median value of 968.6 mm over India. The spatial distribution of average PRCPTOT over India in the PERSIANN-CDR, JRA-55 and NCEP2 datasets is less comparable to the IMD (Fig. 4.1) than other datasets. The PRCPTOT over NH region is mostly underestimated by all the datasets. However, the JRA-55, ERA-Interim and ERA5 reanalysis product better capture the spatial distribution of PRCPTOT over NH. Notably, only the ERA-5 reanalysis data reproduces the areas of PRCPTOT above 1600 mm in parts of EP and EC region compared to other datasets. The ERA5 data overestimated PRCPTOT over the southwestern parts of NH. Satellite-derived PERSIANN-CDR overestimates PRCPTOT over the rain shadow zones of the WG, lower GP (West Bengal) and northern parts of the EC region compared to the IMD dataset. Positive PBIAS in PRCPTOT is observed in GPCC, PERSIANN-CDR, CHIRPS, ERA-Interim, ERA-5 and PGF datasets over WI, GP and parts of NE India and it is highest in the JRA-55 reanalysis data (Fig. 4.2). While the selected gridded datasets overestimate rainfall over the rain shadow zones of the WG and SP, the JRA-55 data underestimated rainfall over these areas. Also, the JRA55 data highly overestimated PRCPTOT over most parts of WI and GP. All the gridded datasets show

some degree of over/underestimation of PRCPTOT over different areas of India, while the gauge-based APHRODITE data mostly underestimated PRCPTOT amount over India with a highest negative median PBIAS value of -14.64% followed by NCEP2 (-10.62%), MERRA2 (-8.8%) and CPC (-8.1%). Highest positive PBIAS in PRCPTOT is noted for PERSIANN-CDR (13.16%) followed by the JRA-55 (12.89%) where the lowest PBIAS is noted for CHIRPS (0.26%), GPCC (-1.25%) and ERA5 (2.4%) datasets.
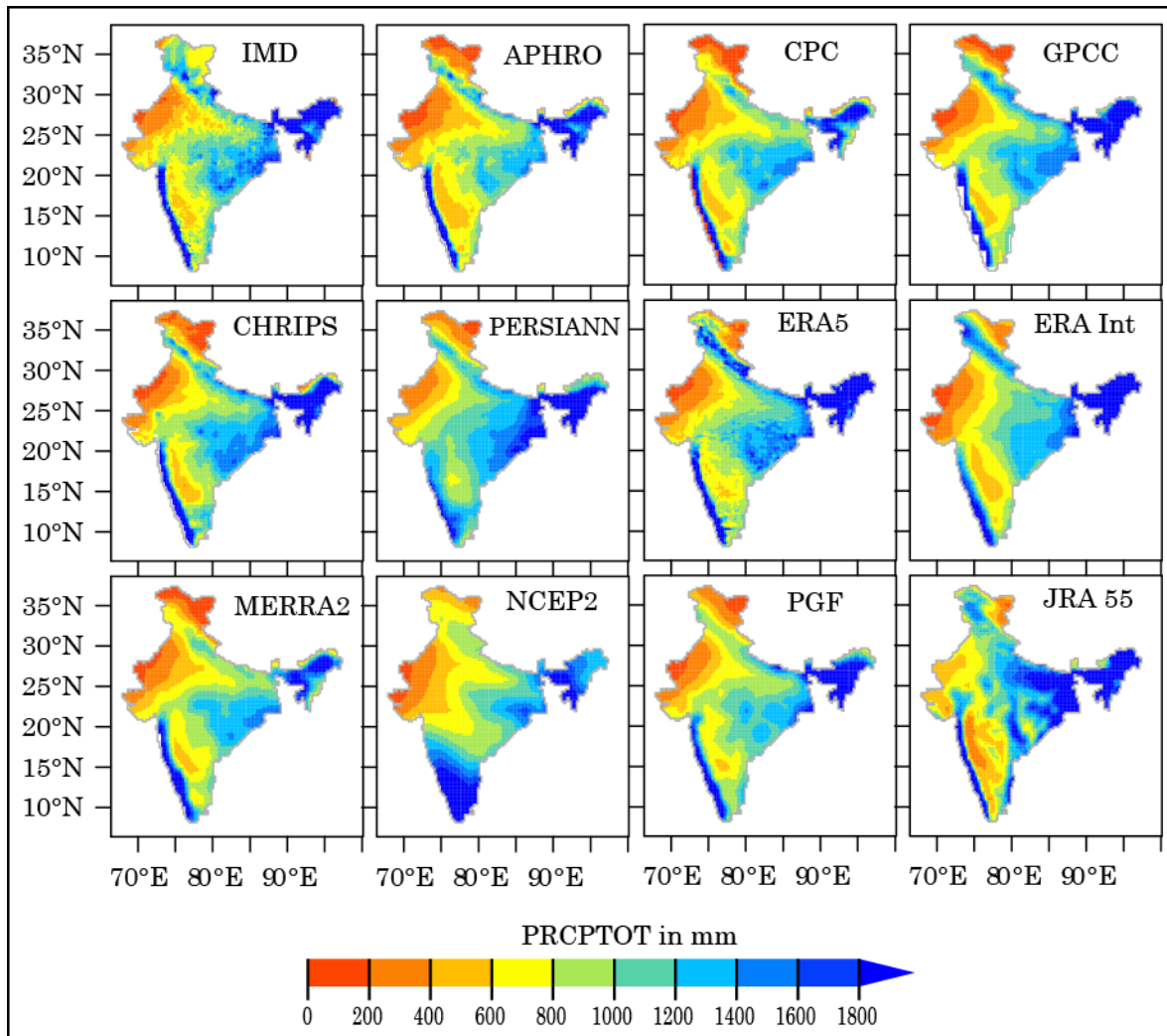
Fig. 4.1. Average annual rainfall in wet days (PRCPTOT) during 1986 – 2015.
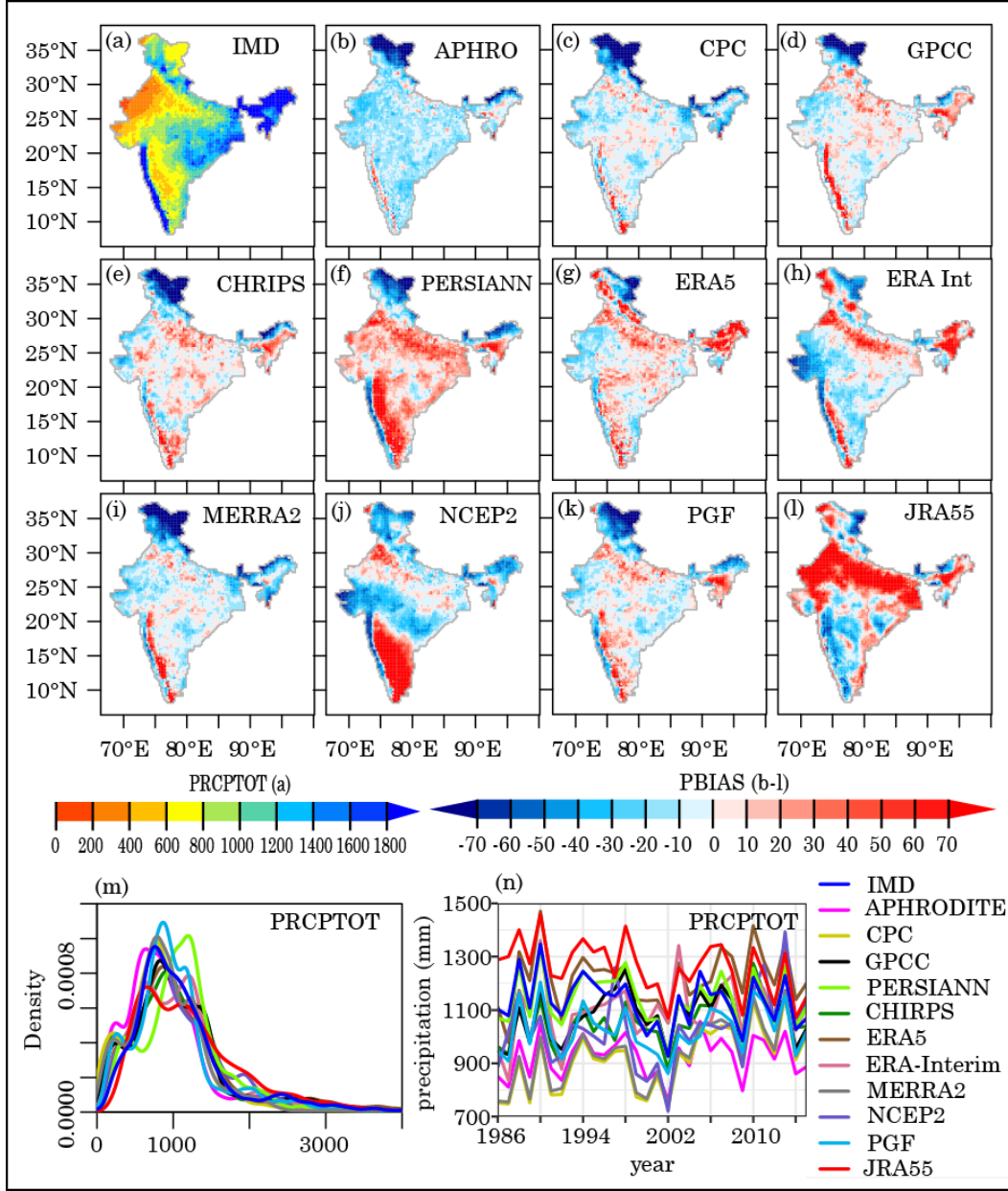
Fig. 4.2. Average PRCPTOT (mm) over India (**a**) during 1986 – 2015. Percentage BIAS in PRCPTOT in different gridded datasets (**b-l**) in comparison to IMD. The probability density function (**m**) estimated from annual average values over India and variation of PRCPTOT rainfall during the study period (**n**) are shown in the lower panel.
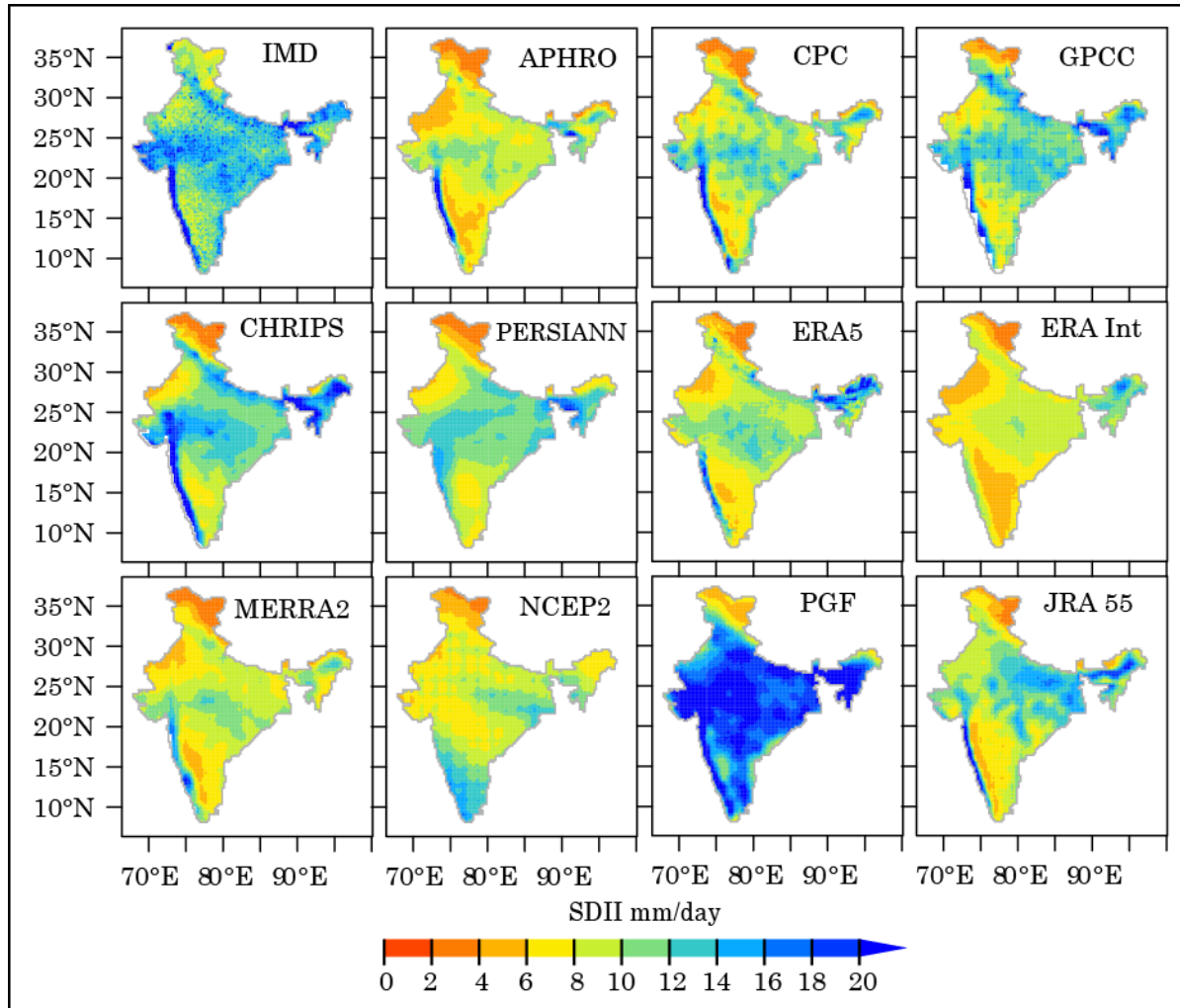
Fig. 4.3. Spatial distribution of average annual SDII during 1986 – 2015.

SDII

Average simple daily intensity index (SDII) over India varies from 48.56 mm/day to 6.79 mm/day with an all India median value of 13.11 mm/day (Fig. 4.3). Satellite-derived CHIRPS and gauge based GPCC data show relatively better agreement with the IMD in estimating mean daily rainfall intensity (SDII) over India (Fig. 4.4). The gauge based APHRODITE underestimated SDII values over most parts of India, mainly over the WI, CI, GP and parts of NE India compared to CPC and GPCC. PERSIANN-CDR, ERA-Interim, MERRA2 and NCEP2 highly deviated from the IMD data in representing the SDII over WG, CI, and WI and over the orographic belts of Himalaya.

Fig. 4.4. Average SDII (mm) over India (**a**) during 1986 – 2015. Percentage BIAS in SDII in different gridded datasets (**b-l**) compared to IMD. The probability density function (**m**) estimated from annual average values over India and variation of SDII rainfall during the study period (**n**) are shown in the lower panel.

Over most parts of India, the ERA-Interim estimated average SDII values are below 8 mm/day where the PGF reanalysis estimated average SDII values are well above 14 mm/day for most parts India. These two datasets highly deviated from the IMD data in representing the spatial distribution of SDII over India. The JRA-55 estimated SDII values

over GP and parts of central NE are well above the values that are obtained from the IMD. While all other gridded rainfall datasets mainly underestimating SDII values, the PGF reanalysis data show positive PBIAS over most parts of India with all India median PBIAS of 39.33% (Fig. 4.4). APHRODITE, ERA-Interim, MERRA2, NCEP2 and JRA-55 underestimated SDII with corresponding median PBIAS of -37.25%, -42.76%, -36.12%, -35.35% and -24.49% respectively. Lower PBIAS values are observed in the CHIRPS (-11.69%) and GPCC (-14.16%) datasets.

RX1day and RX5day

Spatial distribution of average annual RX1day and RX5day rainfall amount in different datasets over India are shown in Fig. 4.5 and Fig. 4.6 respectively. The higher average RX1day and RX5day rainfall are concentrated over the orographic rainfall zones of Himalaya, NE India (Meghalaya Plateau), WG, parts of CI and EC regions. Most of the gridded datasets highly underrepresented the spatial pattern of RX1day and RX5day amounts, especially over EC and northern parts of the EC region, where the average RX1day and RX5day are above 100mm and 200mm respectively (Fig. 4.5 & Fig. 4.6). More specifically, the PERSIANN-CDR, ERA-Interim, MERRA2, NCEP2, PGF, JRA-55 completely failed to replicate the spatial distribution average RX1day rainfall over India, especially over the high rainfall zones of WG, parts of CI and EP and over the orographic rainfall zones over India. Besides, the gauge-based APHRODITE dataset only able to represent the RX1day pattern over the WG, however the same data highly underestimated average RX1day rainfall over CI and EP and the orographic belts of Himalaya (Fig. 4.5). The spatial pattern of RX1day rainfall from other two gauge-based data, namely the CPC and GPCC are also not comparable to the IMD data except for some areas in the CI, EP and NE. Similar findings are noted for these datasets in the spatial distribution of average RX5day rainfall. Overall the performance of ERA5 reanalysis data is spatially comparable with the IMD data, compared to other datasets. Satellite estimated rainfall from CHIRPS better performed than PERSIANN-CDR especially over the high rainfall zones of WG (Fig. 4.5 & Fig. 4.6).

Notably, all of these datasets show dry bias (negative PBIAS) over the NH region for both RX1day and RX5day rainfall amount (Fig. 4.7 & Fig. 4.8). However, CPC, GPCC, CHIRPS, PERSIANN-CDR, ERA-5 and ERA-Interim exhibited wet bias (positive PBIAS) in some

parts of southern, western and southeastern parts of NH. However, the wet bias amount is higher for RX1day over these areas than the wet bias of RX5day rainfall.
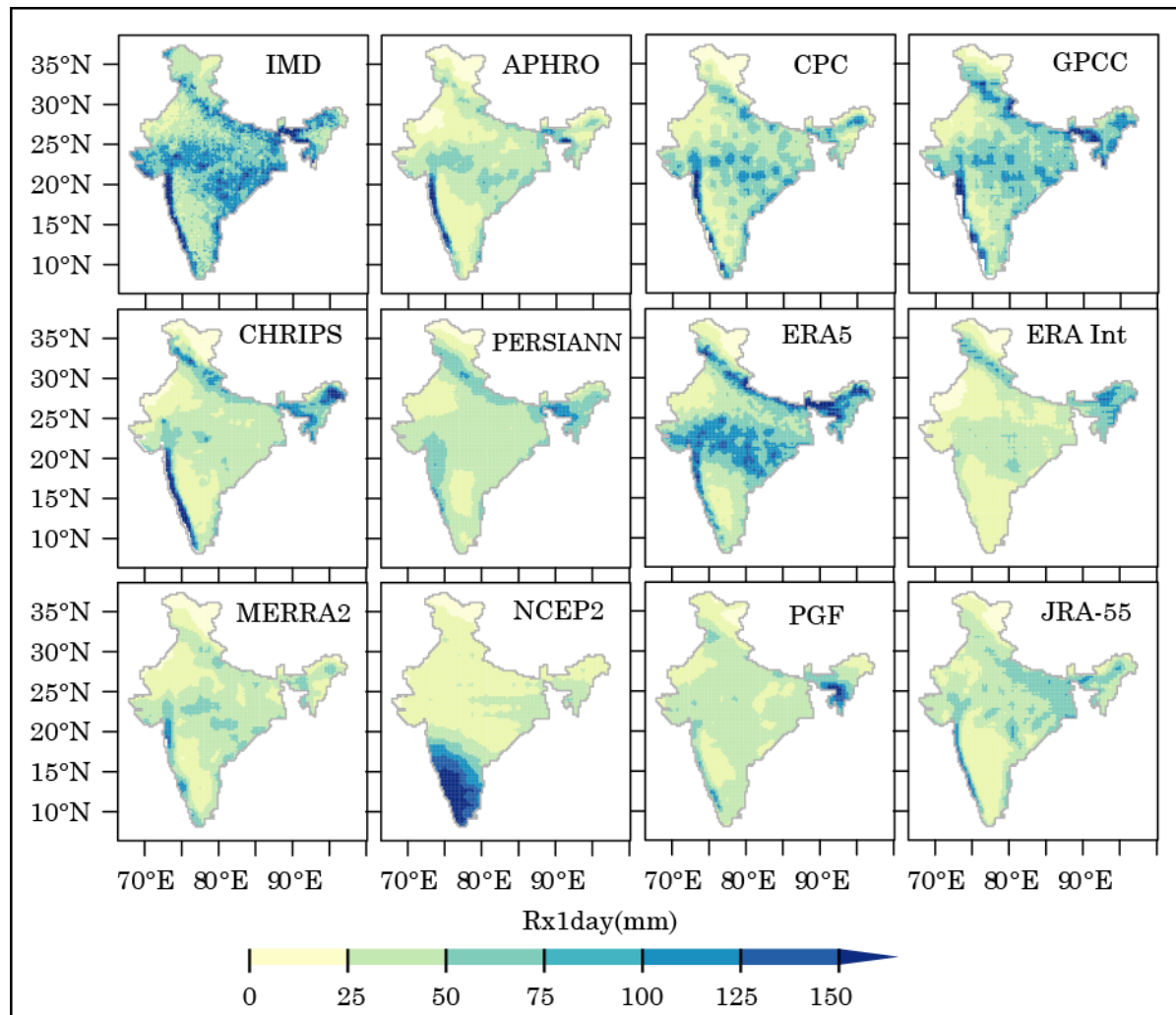
Fig. 4.5. Spatial distribution of average annual RX1day rainfall over India during 1986-2015.
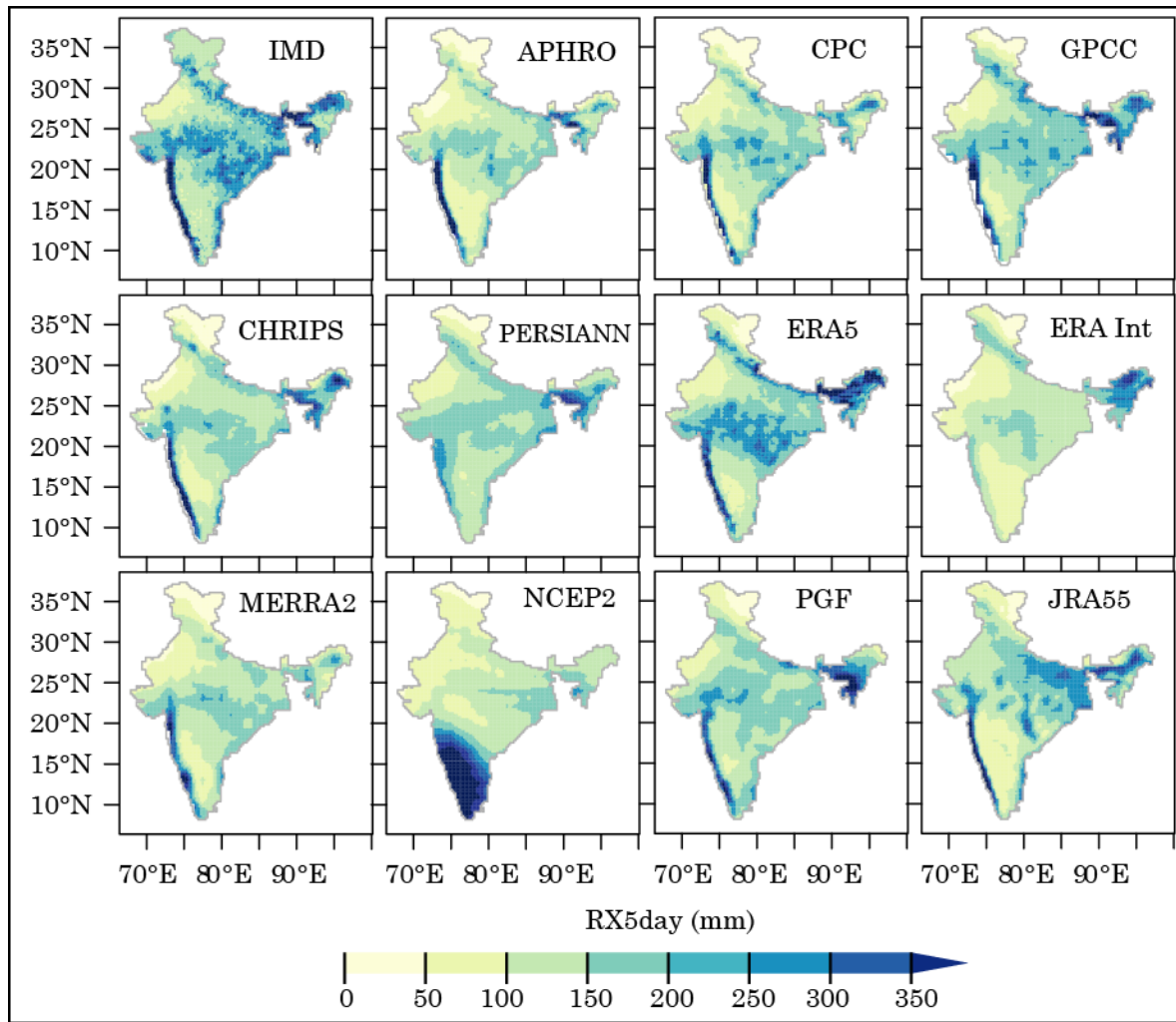
Fig. 4.6 Spatial distribution of average annual RX5day rainfall over India during 1986-2015.

In general, the selected datasets underestimated the RX1day and RX5day rainfall amount over most parts of India which can be seen in Fig. 4.7 and 4.8. Notably, the NCEP2 show the highest overestimation of RX1day and RX5day rainfall in the SP regions, similar to the overestimation of PRCPTOT over this area. Inter-comparison of PDF (Fig. 4.7n & 4.8n) suggests that the ERA5 reanalysis data reasonably well reproduced the spatial pattern of average RX1day and RX5day rainfall amount over India. These PDFs are constructed using the average extreme rainfall amount from all grid cells over India to see how well the datasets can reproduce the occurrence of extreme rainfall over India. The same dataset also better captured the temporal variation in RX1day and RX5day rainfall over India (Fig. 4.7n & 4.8n). Higher overestimation of RX1day and RX5day over NH and NE parts of India is

42

observed in GPCC, CHIRPS, PERSIANN, ERA5, ERA-Interim and PGF datasets. Similar overestimation is observed in the JRA55 dataset over WI and GP.
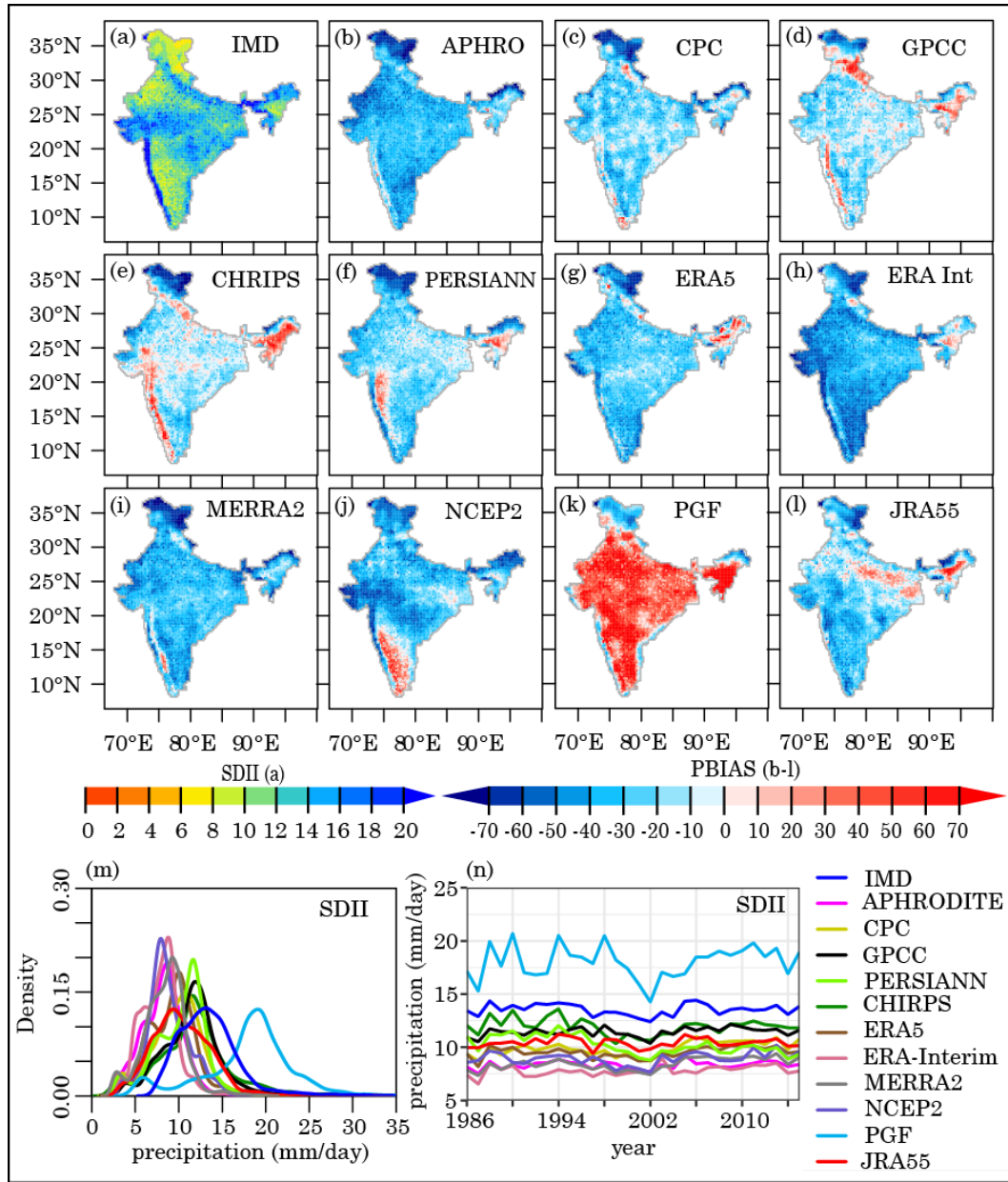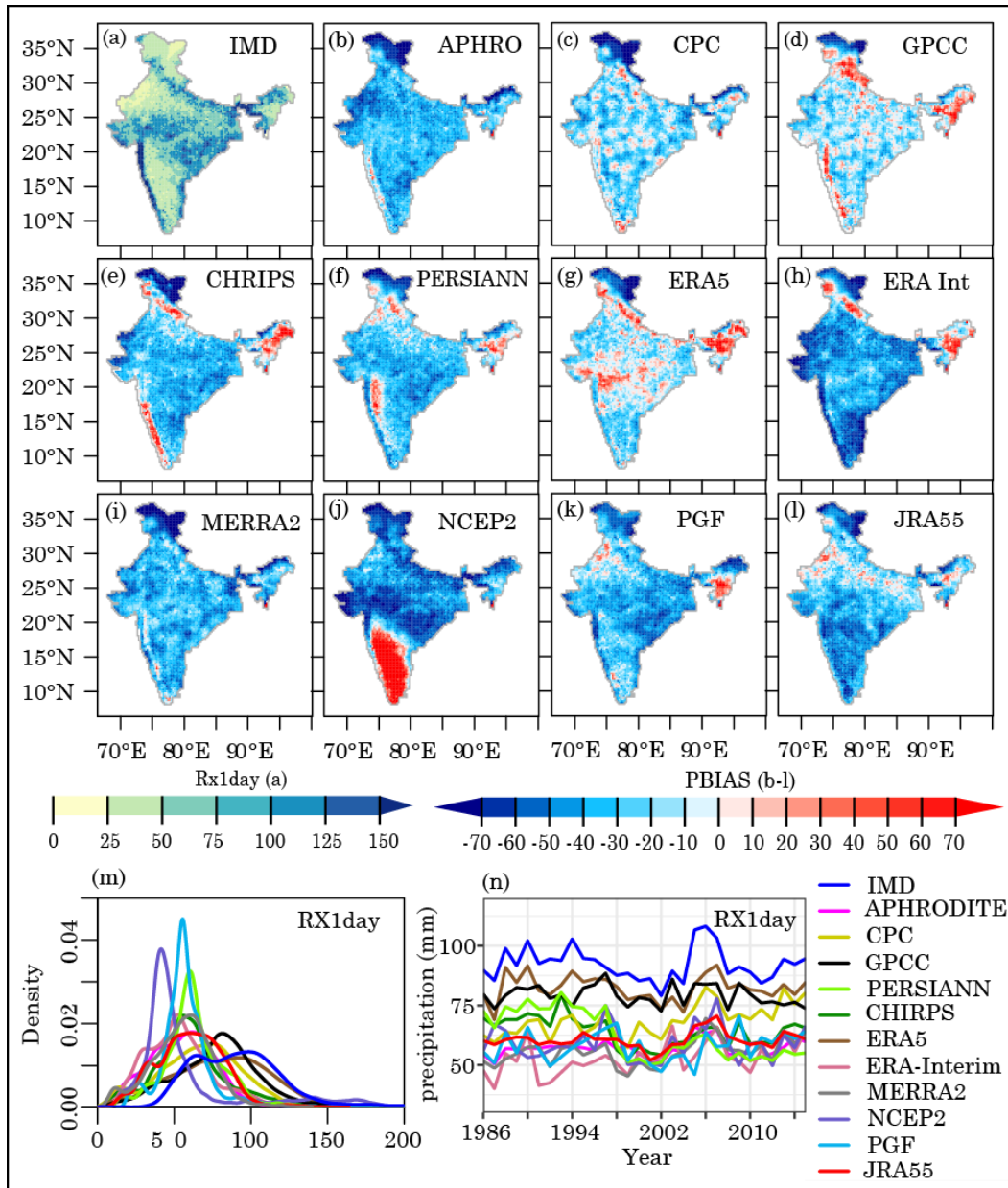

Fig. 4.7 Average RX1day (mm) over India (**a**) during 1986 – 2015. Percentage BIAS in RX1day in different gridded datasets (**b-l**) compared to the IMD. The probability density function (**m**) estimated from annual average values over India and variation of RX1day rainfall during the study period (**n**) are shown in the lower panel.
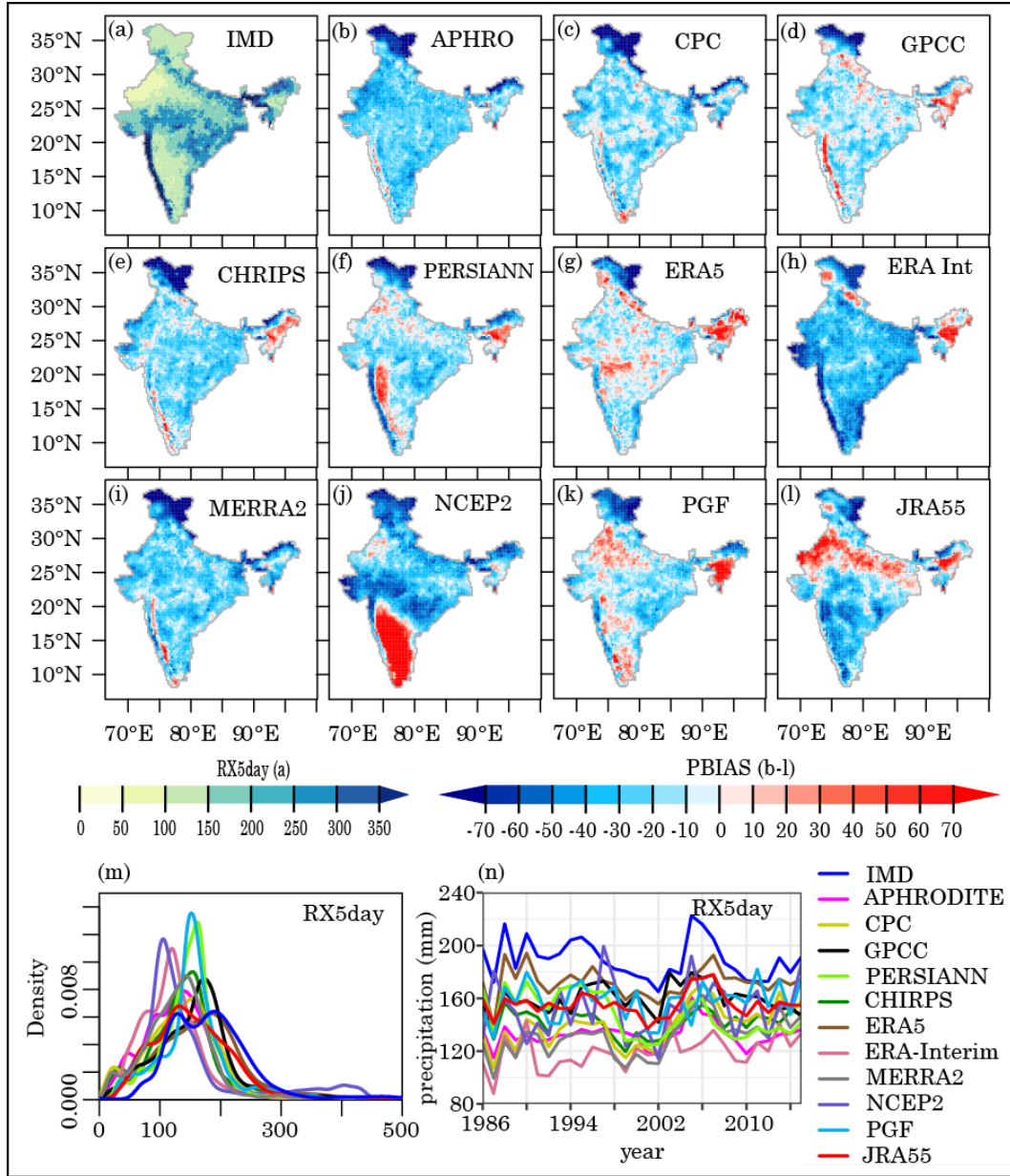
Fig. 4.8 Average RX5day (mm) over India (**a**) during 1986 – 2015. Percentage BIAS in RX5day in different gridded datasets (**b-l**) compared to the IMD. The probability density function (**m**) estimated from annual average values over India and variation of RX5day rainfall during the study period (**n**) are shown in the lower panel.

95ᵗʰ and 99ᵗʰ percentile rainfall

In terms of the percentile-based threshold, the PGF, NCEP2, MERRA2. ERA-Interim and PERSIANN-CDR estimated rainfall thresholds are relatively lower (both for 95ᵗʰ and 99ᵗʰ percentile) over the NH and WG of India in comparison to the IMD data (Fig. 4.9 & Fig.

4.10). Similar underestimation of rainfall amount over most parts of NH is also noticed for other magnitude-based rainfall indices (i.e. PRCPTOT, SDII, RX1day and RX5day) mainly over the northern and north-eastern parts of NH region. Overall, the selected datasets underestimated 95th percentile rainfall amount in areas where the rainfall amount are very high, chiefly over the WG and NE (Meghalaya plateau). Except JRA 55 all other reanalysis datasets mostly underestimated the 95th and 99th percentile rainfall amount over the western sides of WG, while, in the satellite rainfall group the CHIRPS data better performed than PERSIANN-CDR over the same area. Among the gauge based datasets, the CPC and GPCC better reproduce the 95th and 99th percentile rainfall amount over India than the APHRODITE dataset (Fig. 4.9 & Fig. 4.10). However, the GPCC data found to overestimate 95th percentile rainfall amount over some areas of the EP. The PERSIANN-CDR also overestimated 95th percentile rainfall threshold over the EP, GP, parts of CI and over the rain shadow zones of WG (Fig. 4.9). Among the reanalysis, a pattern of over and underestimation is noted for some datasets over certain areas. For example, the PGF dataset estimated 95th rainfall threshold over some parts of GP, EP and CI is between 20mm – 30mm which is well above the IMD estimated thresholds. However, the same dataset underestimates 99th rainfall thresholds, especially in areas where the threshold is above 40mm/day. Estimated rainfall thresholds for 95th and 99th percentile rainfall from the JRA55 datasets over the GP are also higher than the IMD dataset. For both of these rainfall thresholds, an overall underestimation in the ERA-Interim, MERRA2 and NCEP2 reanalysis datasets are observed over most parts of India. The ERA5 data better resembles with the IMD data. However, the dataset overestimated the rainfall threshold over parts of the NE and underestimates these rainfall thresholds over the western parts of the WG. Most of the datasets unable to represent the 99th percentile rainfall threshold over central India and EP, except the GPCC, CPC and ERA-5 dataset. Overall, the GPCC data closely approximates the spatial distribution of 95th and 99th rainfall amount better than the other gauge-based products (CPC and APHRODITE) while the ERA-5 and CHIRPS rainfall estimates are better than the other reanalysis and satellite-derived datasets, respectively. It should be noted that the NCEP2 estimated rainfall amounts are much higher for 99th percentile rainfall than 95th rainfall over the SP region.
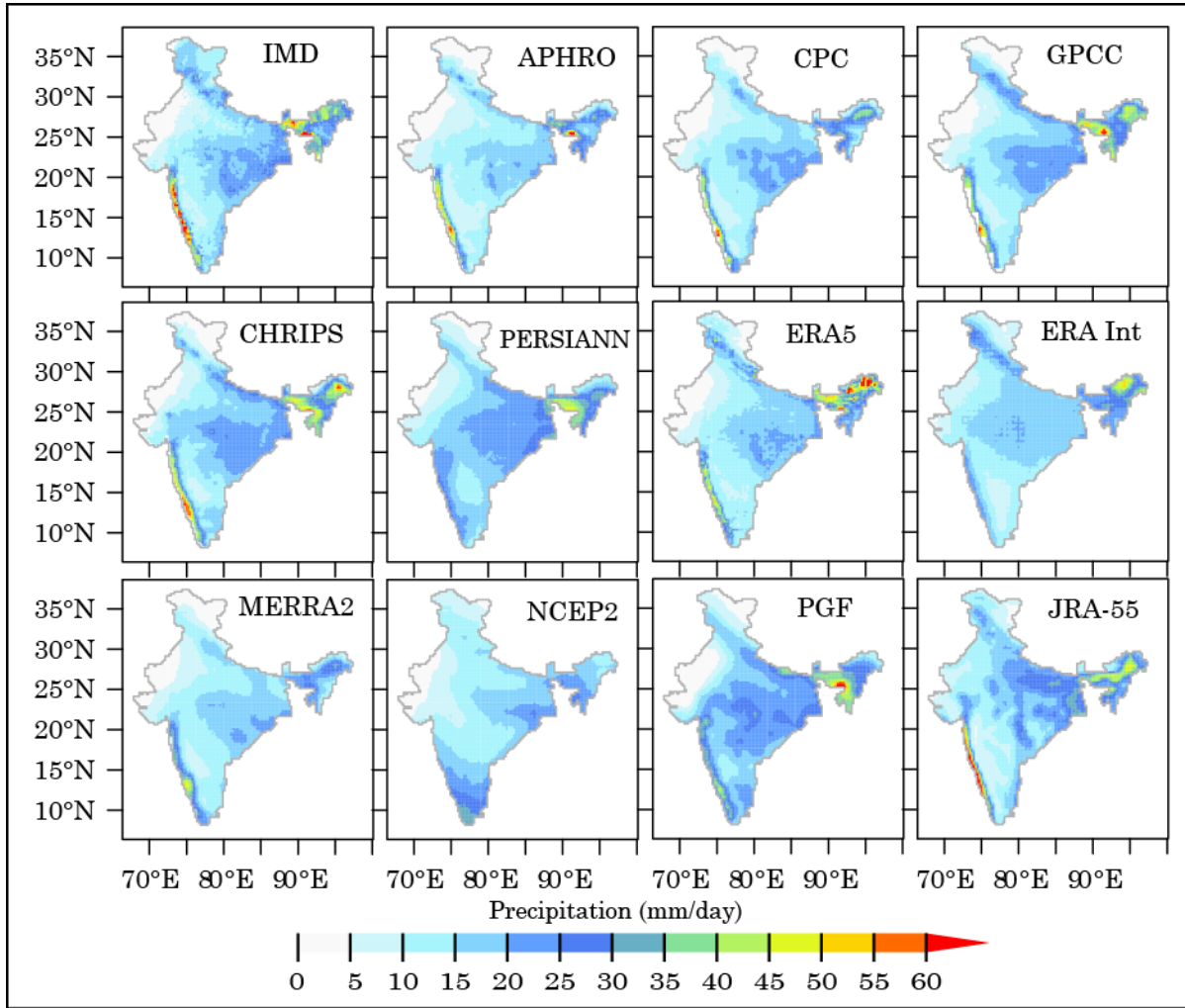
Fig. 4.9. Spatial distribution of annual 95th percentile rainfall over India during 1986- 2015.

Similar to 95th percentile threshold, PERSIANN-CDR and all other reanalysis (except JRA55) underestimated 99th percentile rainfall amount over the WG (Fig. 4.10). Underestimation of 99th rainfall threshold over the Meghalaya plateau is also observed in all of the datasets except GPCC and ERA5. However, the ERA5 data overestimated 99th rainfall amount over most parts of the GP, NE, EC and WG regions.
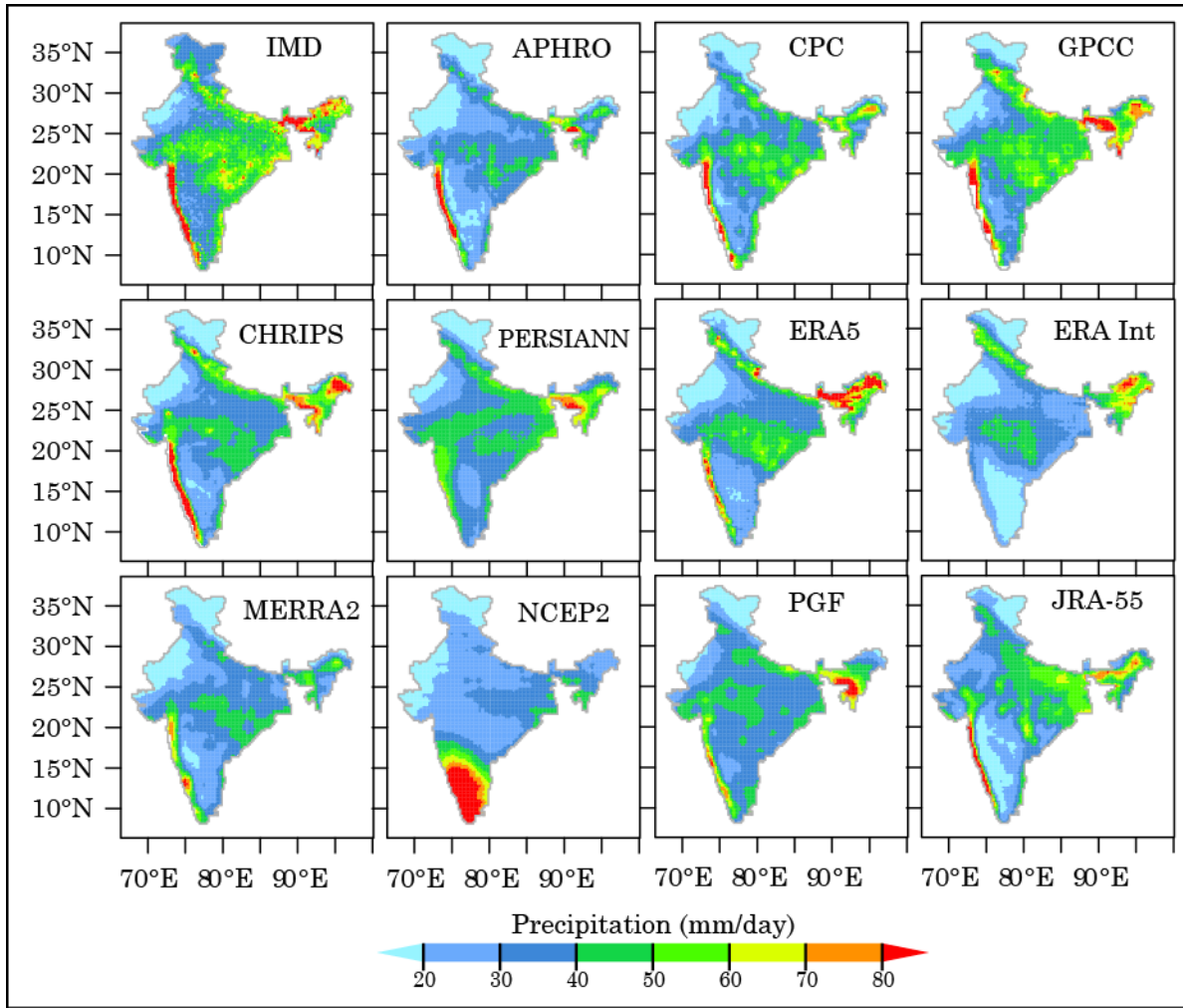
Fig. 4.10. Spatial distribution of annual 99th percentile rainfall over India during 1986-2015.

R95tp and R99tp

The datasets are compared based on their ability on capturing the rainfall amount falling above long term 95th and 99th percentile threshold, referred as R95tp and R99tp respectively (see methodology section for details). The spatial patterns of R95tp and R99tp in the IMD dataset are plotted in Fig. 4.11(a) and Fig. 4.12(a) and the respective PBIAS of other gridded datasets from the IMD are plotted in Fig. 4.11(b-l) and Fig. 4.12 (b-l). During the study period, the average R95tp over India varies between 155.1 mm in the WI dry regions and 4507.57 mm in the NE. Higher R95tp amount (>600 mm) is mainly concentrated over the NE, WG, parts of EP and GP (Fig. 4.11a). R99tp found to vary

between 90.72 mm in the WI dry regions and 1596.76 mm in the NE parts of India. Overall, the distribution of positive and negative PBIAS in 95tp and 99tp are similar to other extreme magnitude-based indices (i.e. RX1day, RX5day) over different regions of India. The analysis of PBIAS indicates that the percentage of dry bias is relatively higher for higher extreme indices (RX1day and R99tp) compared to relatively lower extreme indices (RX5day and R95tp). For example in areas where the dry bias are noted in APHRODITE, PERSIANN-CDR, ERA-Interim, NCEP2 MERRA2 and PGF is found to be higher for RX1day and R99tp than RX5day and R95tp. Opposite to that, the wet bias over parts of SP (in NCEP2), WG (PERSIANN-CDR) and over GP and WI (in JRA-55) is relatively lower for higher extreme indices (RX1day and R99tp) than relatively lower extreme indices (RX5day and R95tp). This emerging pattern of overestimation and underestimation of dry and wet bias of extreme rainfall indices can also be seen in the median PBIAS over India from Table 4.1.

Table 4.1 Median PBIAS in different gridded datasets (from the IMD) for magnitude based extreme indices.

PBIAS	R95tp	R99tp	RX5day	RX1day
APHRODITE	-29.78	-35.91	-27.87	-37.71
CPC	-16.99	-22.22	-21.73	-23.19
GPCC	**-8.08**	**-13.14**	-13.18	-14.24
CHIRPS	-16.71	-31.33	-22.90	-35.18
PERSIANN	-12.14	-28.48	-18.07	-33.98
ERA5	-17.07	-18.11	**-9.17**	**-12.48**
ERA-Interim	**-57.49**	**-61.40**	**-36.93**	-45.63
MERRA2	-26.91	-35.35	-27.70	-38.37
NCEP2	-34.15	-45.41	-33.26	**-49.21**
PGF	-11.60	-30.30	-14.37	-37.74
JRA55	-18.55	-30.47	-18.97	-34.88

The PDF plots suggest that the ERA-5, GPCC and CHIRPS better capture the spatial distribution of R95tp over India (Fig. 4.11m). APHRODITE, ERA-Interim and MERRA2 underestimate R95tp and R99tp over most parts of India (Fig. 4.11 & Fig. 4.12). Consistent

negative PBIAS in these rainfall amounts are found over the NH for all of the datasets. The gridded datasets also underestimated the temporal variations of R95tp and R99tp over India, especially by the ERA-Interim, NCEP2, and JRA55 reanalysis products (Fig. 4.11n and Fig. 4.12n). Lowest median PBIAS over India for R95tp and R99tp is observed in the GPCC while for RX1day and RX5day ERA5 has the lowest median PBIAS (Table 4.1).
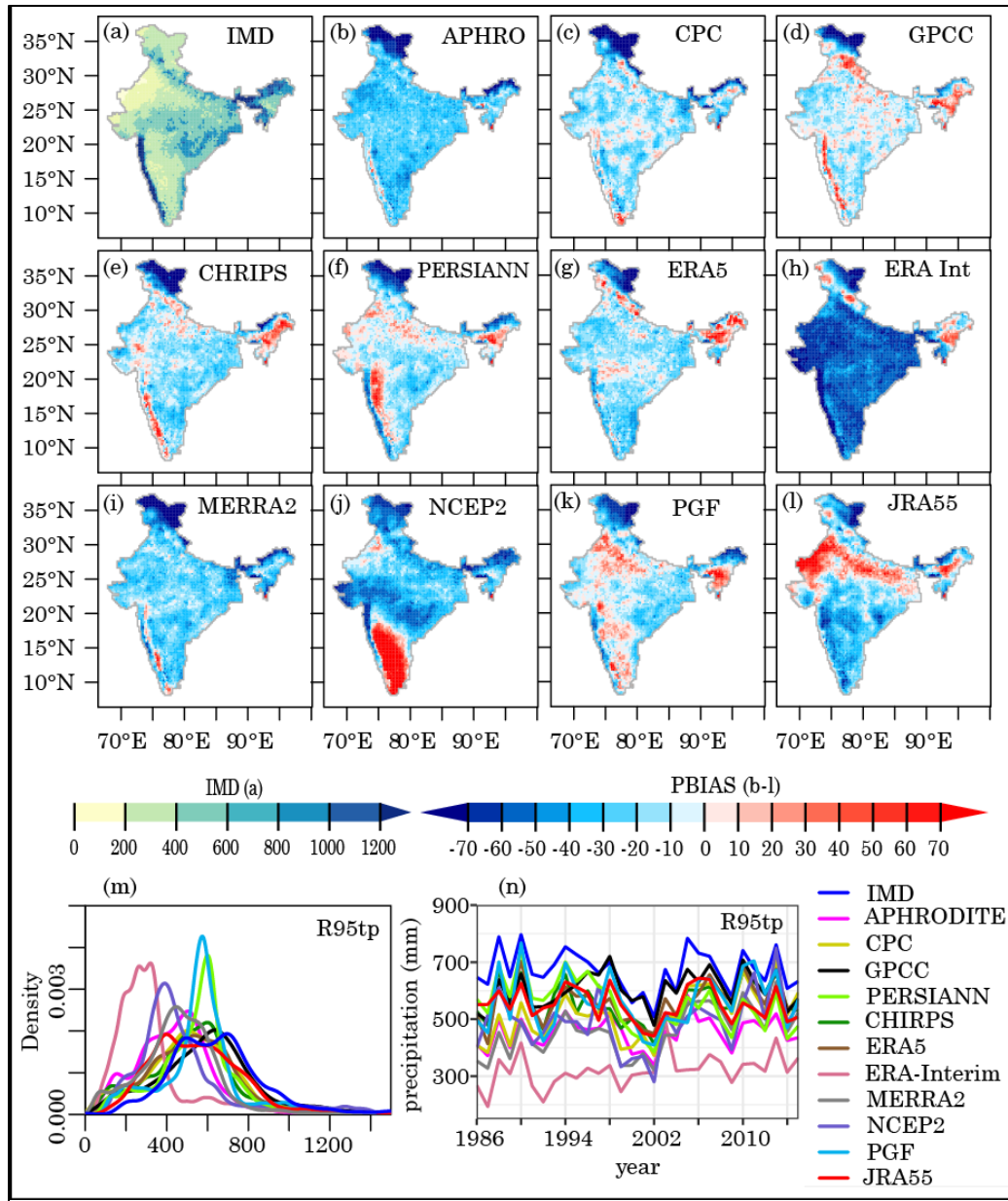
Fig. 4.11 Average R95tp (mm) over India (**a**) during 1986 – 2015. Percentage BIAS in R95tp in different gridded datasets (**b-l**) compared to the IMD. The probability density function

(**m**) estimated from annual average values over India and variation of R95tp rainfall during the study period (**n**) are shown in the lower panel.

Fig. 4.12. Average R99tp (mm) over India (**a**) during 1986 – 2015. Percentage BIAS in R99tp in different gridded datasets (**b-l**) compared to the IMD. The probability density function (**m**) estimated from annual average values over India and variation of R99tp rainfall during the study period (**n**) are shown in the lower panel.

4.2 Frequency of extreme rainfall

In this section, the gridded datasets are evaluated in terms of their ability in identifying frequency (occurrences) of extreme rainfall events based on rainfall thresholds of different magnitudes. As mentioned in the methodology section, in addition to the ETCCDI recommendations of frequency-based lower extreme indices (R10mm, R20mm), we also considered higher extremes indices i.e. heavy (>64.4mm/day), very heavy (>124.4mm/day) and extremely heavy (>244.4mm/day) rainfall days, as per the categorization of IMD (Table 3.1). The last three indices are specifically important considering the spatial variation of extreme rainfall over India and their direct linkages in triggering natural hazards (i.e. floods, landslide) in different parts of India. The consideration of lower rainfall thresholds (R10mm and R20mm) can also enable us to better understand the distribution of rainfall biases with a particular gridded dataset.
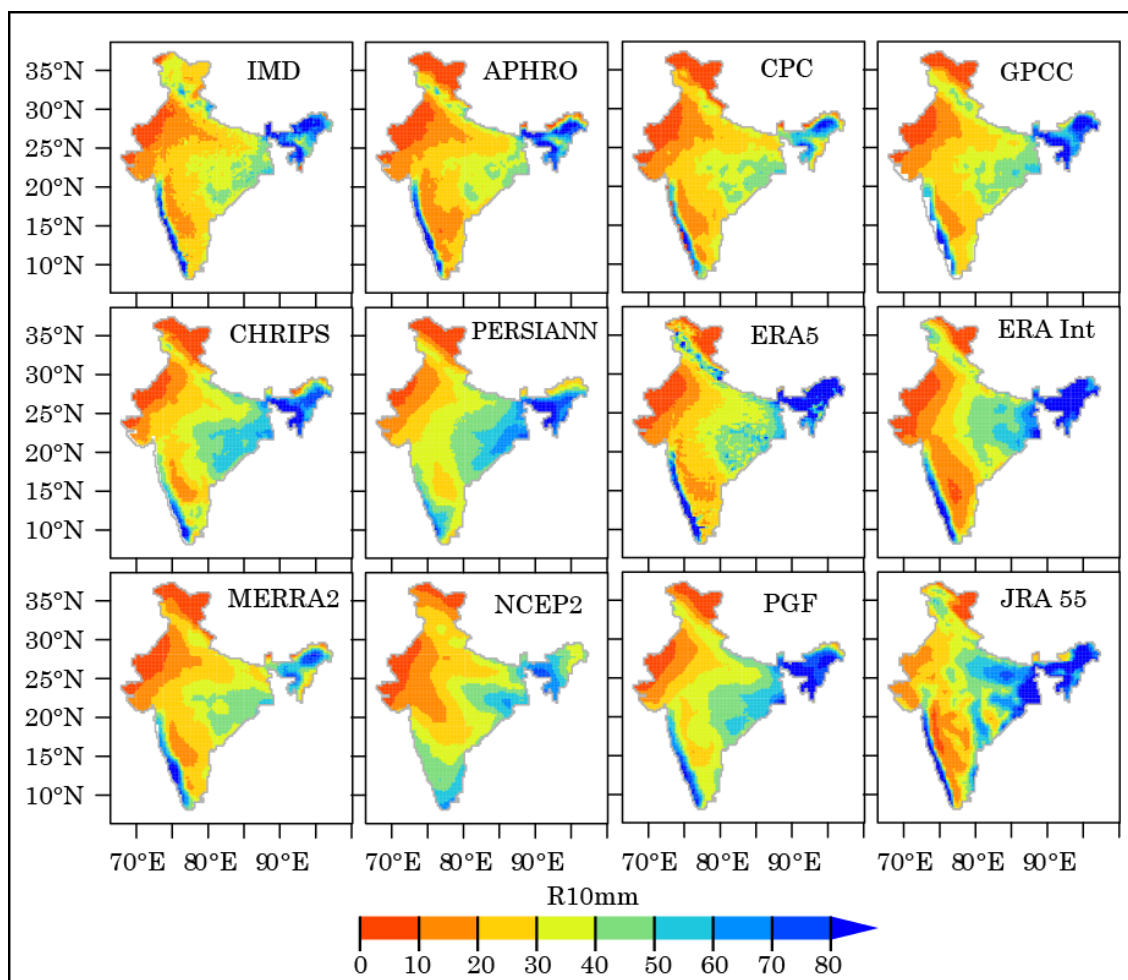
Fig. 4.13. Spatial distribution of average R10mm (days/year) over India during 1986- 2015.

R10mm and R20mm

Distribution of R10mm and R20mm closely follows the spatial distribution of PRCPTOT distribution over India where relatively larger number of R10mm (>50 days/year) and R20mm (>30 days/year) days can be found in areas (Fig. 4.13 & Fig. 4.14) where the average PRCPTOT is above 1200mm, mainly over the orographic belts of WG, NH, NE and in parts of EP. Over most parts of India, the average R10mm and R20mm are below 40 days and 20 days respectively (Fig. 4.13 & Fig. 4.14). Comparatively, in the foothills of the Himalayas and some parts over the EP, EC and lower GP, average R10mm and R20mm are between 40 – 60 days and 25 – 35 days respectively. Over the WG and NE India, average R10mm and R20mm rainfall days are mostly above 60 and 35 days, respectively.

It can be seen that the CHIRPS, PERSIANN-CDR, ERA-Interim, PGF and JRA-55 dataset overestimated the R10mm days over a vast area in the GP and EP when compared to the IMD (Fig. 4.15). However, this overestimation is higher (above 60%) in the PERSIANN-CDR, ERA-Interim and JRA-55 dataset (Fig. 4.15) over these areas. Satellite derived PERSIANN-CDR and the NCEP2 reanalysis are unable to replicate spatial distribution of R10mm and R20mm over the WG and SP (Fig. 4.15 & Fig. 4.16). The ERA-Interim reanalysis exhibited negative PBIAS (-20% to -60%) for R10mm over SP and WI and it was much higher (above -60%) for R20mm in the same areas. Notably, the spatial distribution of R20mm in ERA-Interim highly deviated from the IMD data and it has performed worst compared to other datasets with the highest median PBIAS of -61.3%. Although the APHRODITE and CPC are gauge based dataset, they are less comparable to the IMD especially over the WI and SP and also failed to capture the spatial and temporal variation of R10mm & R20mm rainfall over India (Fig. 4.15m,n & Fig. 4.16m,n). However, the APHRODITE, ERA5 and JRA-55 better performed in the western sides of WG in replicating R10mm and R20mm days. CHIRPS, PERSIANN-CDR and PGF data overestimate R10mm days over most parts of India except some areas located in the WI, NH and NE. Higher concentration of positive PBIAS (above 50%) are noted in PERSIANN-CDR (in SP), JRA-55 (WI, GP and NE), ERA-Interim (GP and NE) and NCEP2 (SP).

Except for APHRODITE, CPC and MERRA2, all the datasets have positive median PBIAS in R10mm over India (Table 4.2). Conversely, except the PGF and PERSIANN-CDR, all other datasets exhibited negative PBIAS over India, implying that a general tendency of

underestimating high rainfall events is a salient feature of these datasets, especially with an increasing rainfall threshold. Overall the GPCC and MERRA2 relatively better capture the temporal variation of R10mm days where the performance of GPCC and CHIRPS for R20mm days is comparable with the IMD as evident from the better resemblances of PDFs (Fig. 4.16m). Beside, similar to the magnitude based indices, the datasets exhibited dry bias in replicating R10mm and R20mm rainfall days over most parts of NH.

Table 4.2 Median PBIAS of gridded datasets from IMD data for selected frequency and duration based indices over India.

PBIAS	R10mm	R20mm	CDD	CWD
APHRODITE	-10.44	-35.58	-11.65	70.53
CPC	-6.02	-16.45	-15.89	14.38
GPCC	1.20	-3.22	-7.56	16.25
CHIRPS	20.33	0.00	-21.29	9.50
PERSIANN	30.05	10.99	-25.32	55.13
ERA5	6.07	-22.04	-18.55	121.98
ERA-interim	0.42	-61.35	-86.03	195.47
MERRA2	-3.18	-28.07	-14.97	79.53
NCEP2	2.33	-37.24	-14.69	109.98
PGF	24.73	34.08	7.47	-29.35
JRA	30.05	-1.23	-21.93	107.09
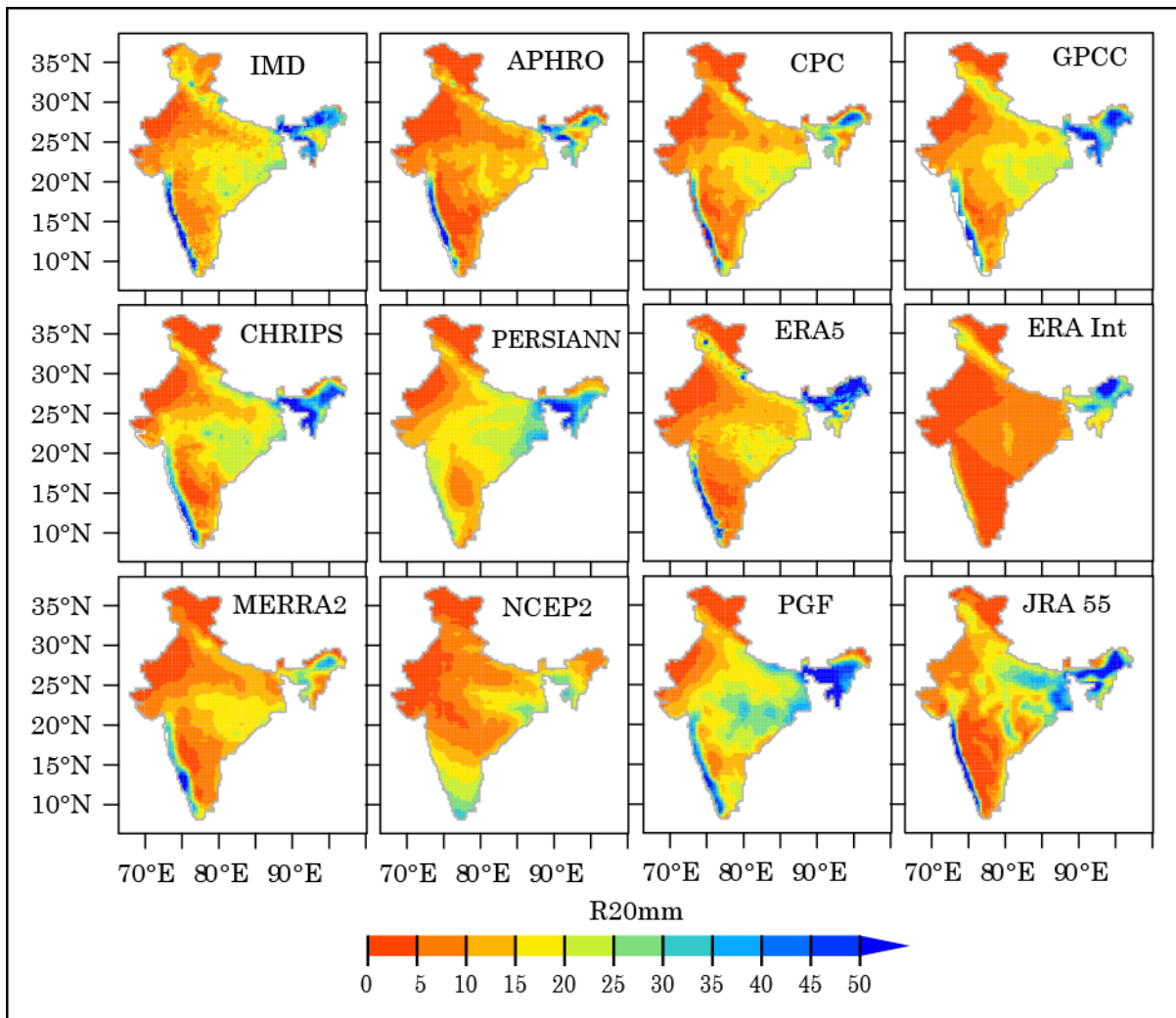
Fig. 4.14 Spatial distribution of average R20mm (days/year) over India during 1986- 2015.
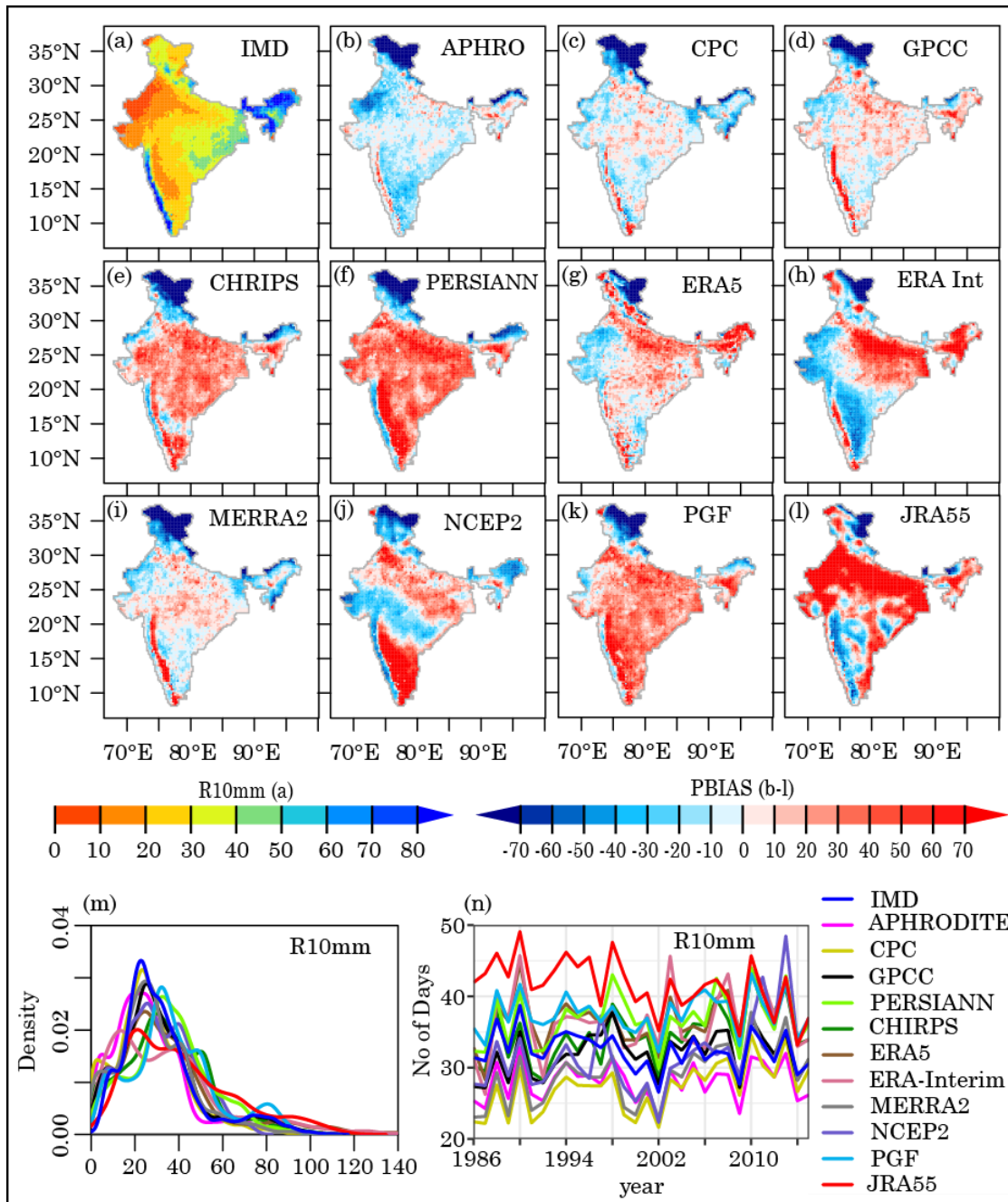
Fig. 4.15 Average R10mm (days) over India (**a**) during 1986 – 2015. Percentage BIAS in R10mm in different gridded datasets (**b-l**) compared to the IMD. The probability density function (**m**) estimated from annual average values over India and variation of R10mm rainfall during the study period (**n**) are shown in the lower panel.
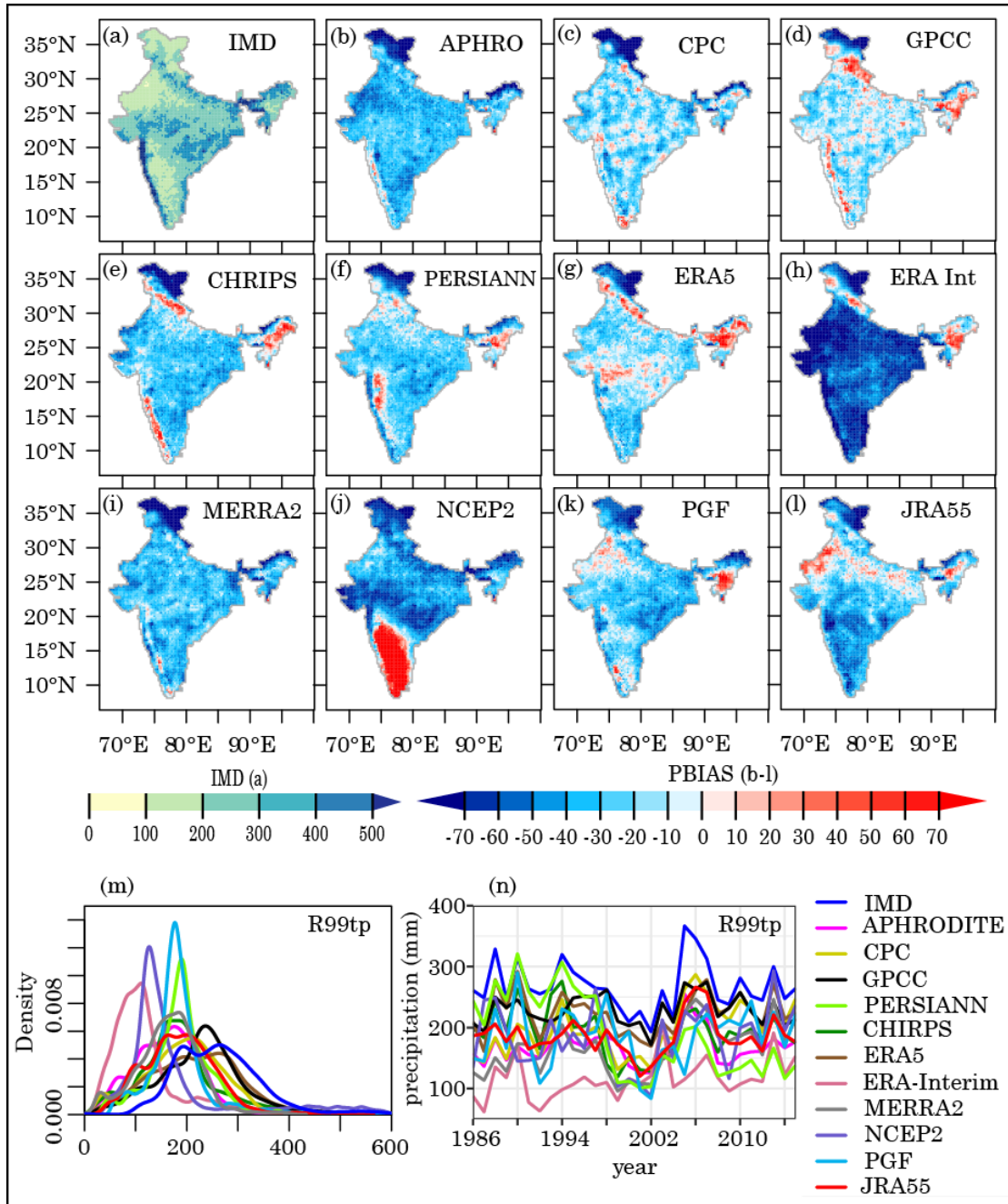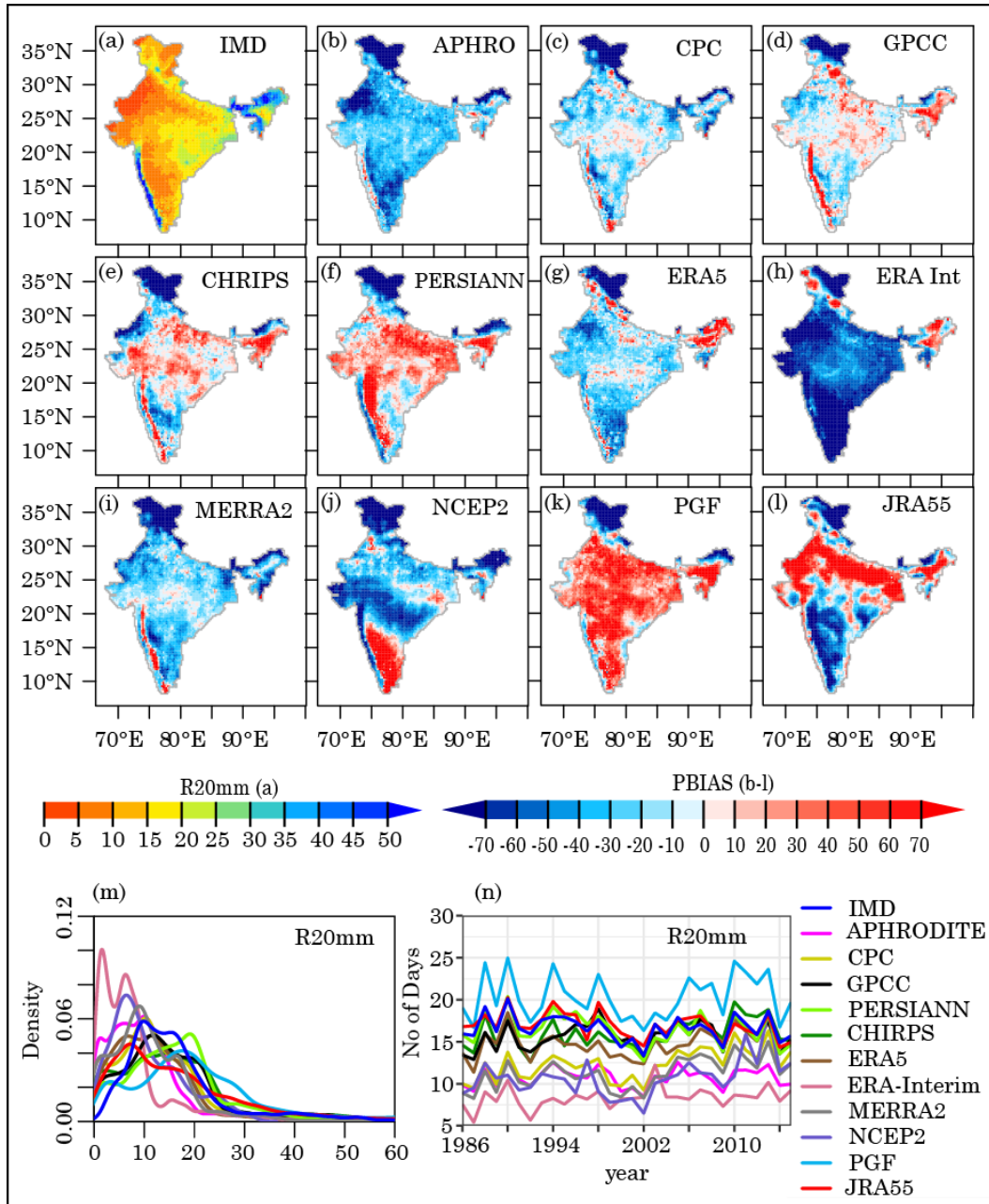
Fig. 4.16 Average R20mm (days) over India (**a**) during 1986 – 2015. Percentage BIAS in R20mm in different gridded datasets (**b-l**) compared to the IMD. The probability density function (**m**) estimated from annual average values over India and variation of R20mm rainfall during the study period (**n**) are shown in the lower panel.

4.3 Heavy, Very heavy and extremely heavy rainfall days

Frequency of Heavy (>64.4 mm/day), very heavy (>124.4 mm/day) and extremely heavy (>244.4 mm/day) rainfall days during the study period (1986 – 2015) are shown in Fig. 4.17, Fig. 4.18 and Fig. 4.19 respectively. Occurrences of heavy rainfall (HR) and very heavy rainfall (VHR) events over India are mainly concentrated in the foothills of the Himalayas, western side of WG, EC, and over parts of the CI and EP region (Fig. 4.17 & Fig. 4.18). Strong orographic control is found to exist in the occurrences of extreme rainfall events over India. Moreover, Heavy and very Heavy rainfall events are less frequent over WI, SP and NH region, resulting in a lower annual rainfall amount in these areas. The selected gridded rainfall datasets mainly underestimate the heavy and very heavy rainfall days over India. In gauge-based datasets, the APHRODITE poorly performed in capturing the heavy rainfall days over India and has all India median PBIAS of -74.6%. In the satellite-based data, the PERSIANN-CDR better capture the heavy rainfall days over WI, CI, and GP but failed to capture the heavy rainfall in the orographic belts of the WG and NH. In contrast, the CHIRPS better capture heavy rainfall over orographic zones and even overestimate rainy days over these areas. Reanalysis datasets, MERRA2, NCEP2 PGF and JRA-55 highly underestimated heavy and very heavy rainfall over NH. The ERA-Interim data failed to capture heavy and very heavy rainfall days over WG and SP. The ERA-5 data better represent HR rainfall days and have relatively low median PBIAS (-37.9%) over India when compared to other satellite-reanalysis datasets. The GPCC outperformed other gridded datasets with a median PBIAS value of -28.6% over India.

Extremely heavy rainfall (EHR) events (>244.5mm) are very rare over India but have relatively greater impacts in damaging infrastructure and crops. ERA-Interim, MERRA2 and JRA-55 reanalysis and the PERSIANN-CDR satellite data completely failed to identify EHR events over India (Fig. 4.19). Only the ERA-5 reanalysis data could partially identify some EHR days over WI, CI and EP. However, the same data is unable to capture the EHR days over WG region. In contrast, NCEP2 data overestimate EHR events over the WG and SP regions, which is a prominent feature of this dataset over this area. Similar overestimation is also found in the CHIRPS data over the WG region.
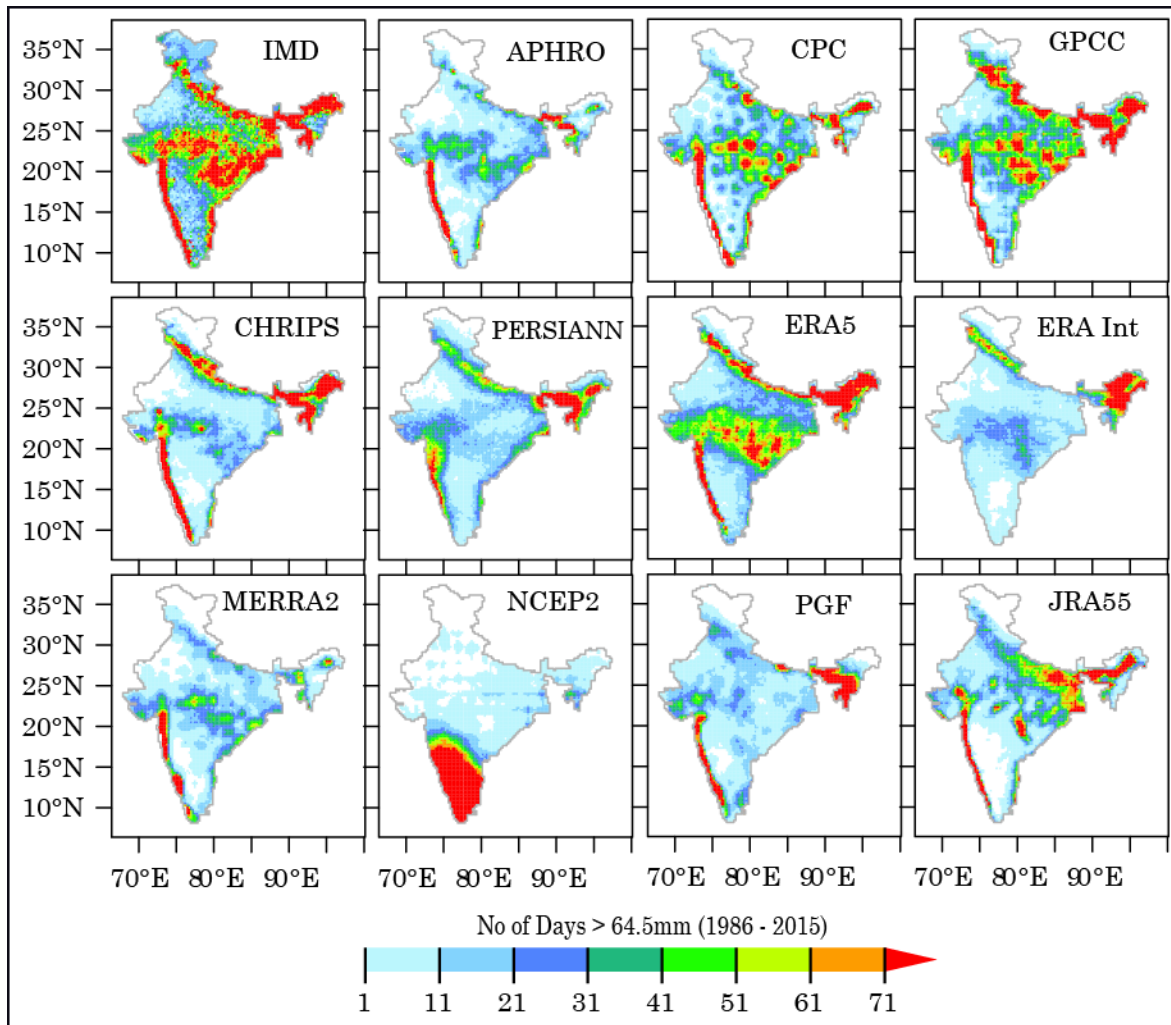
Fig. 4.17 Total number of heavy rainfall days occurred between 1986 and 2015.
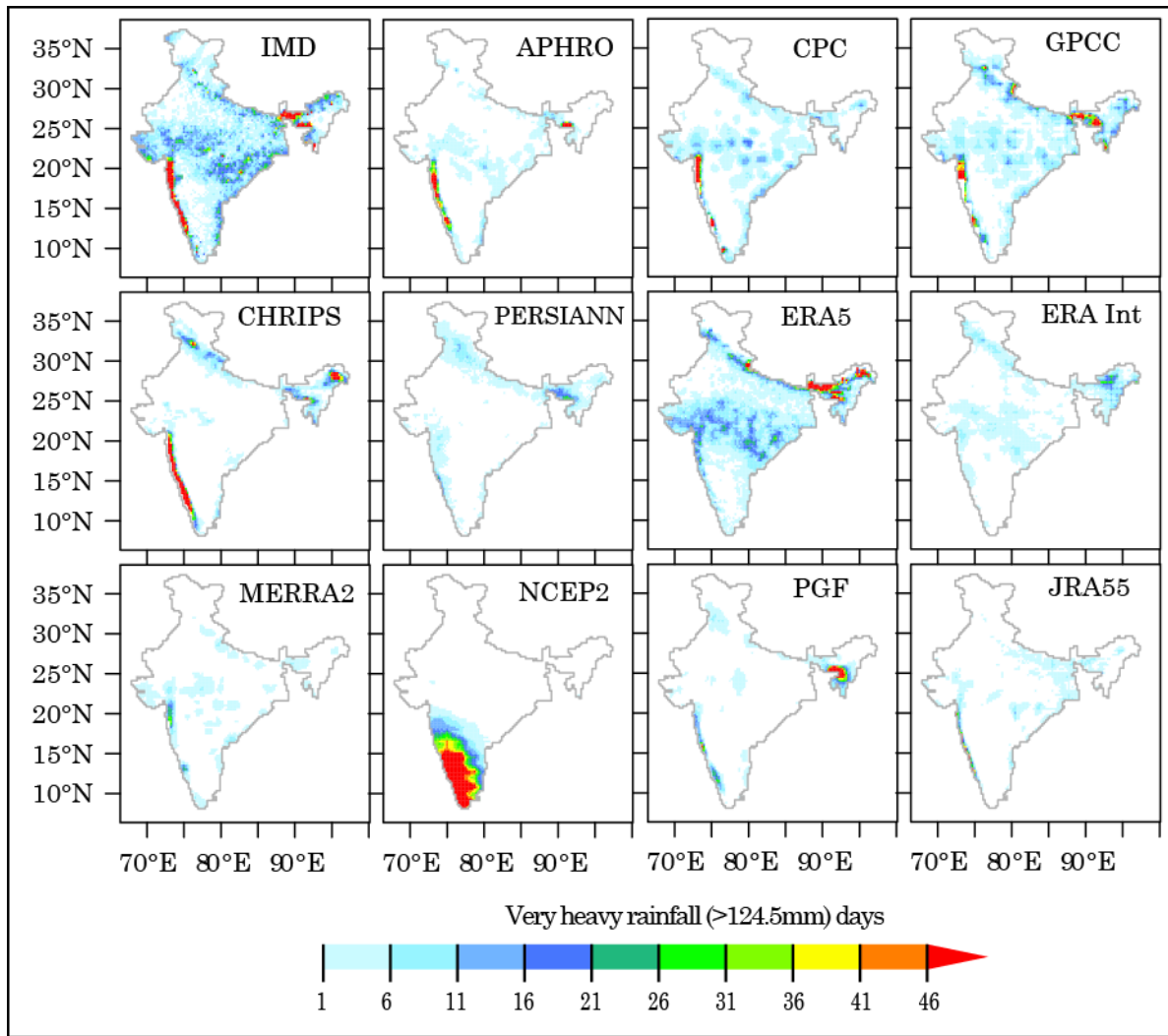
Fig. 4.18 Total number of Very heavy rainfall days occurred between 1986 and 2015.
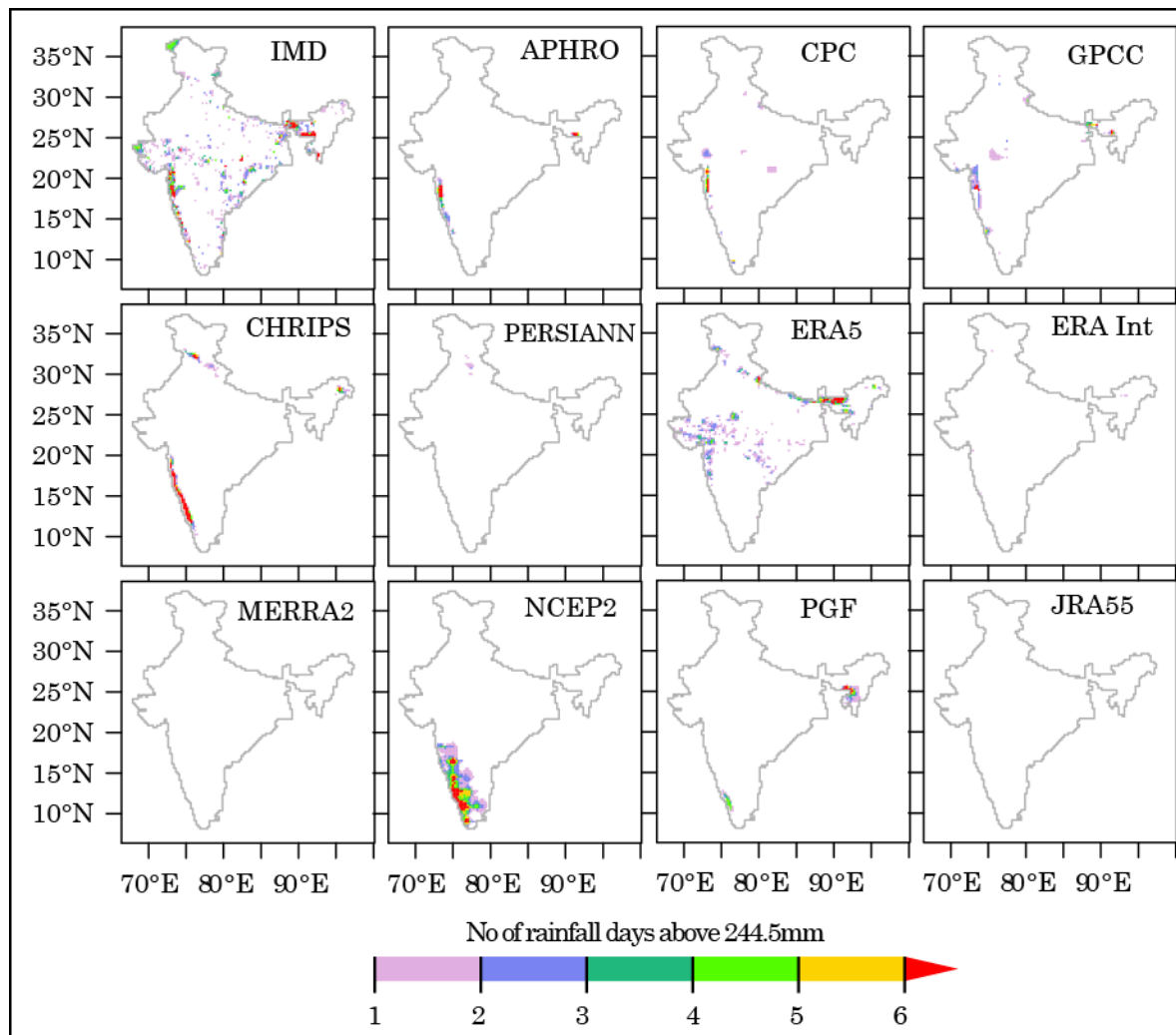
Fig. 4.19 Spatial distribution of extremely heavy rainfall (HER) days over India during 1986- 2015.

4.4 Duration based extreme Indices

Higher number of CDD (>160days) are found over the arid and semi-arid areas of WI, and lower CDD (<40 days) are observed over the NE and NH parts of India (Fig. 4.20). Lower CDD in the NH is due to the intermittent rainfall-snowfall occurrences, once in fortnight, during monsoon-winter continuum, influenced by the monsoon and western disturbances. Compared to the IMD dataset, the PGF reanalysis shows a relatively large number of CDD (>200 days) over the WI. Notably, the ERA-Interim underestimated CDD days with too many wet days, resulting in frequent breaks in CDD and have a median PBIAS of -86.03% over India (Fig. 4.22m). Gauge-based GPCC and the PGF reanalysis data better capture the spatial as well as temporal variation in CDD over India (Fig. 4.22m&n) and have a median

PBIAS value of -7.56% and 7.47% respectively. CHIRPS show good agreement with the reference (IMD) dataset in representing CDD over the WI. Spatial distribution of positive/negative PBIAS is similar in gauge-based (APHRODITE, CPC and GPCC), satellite (CHIRPS) and reanalysis (MERRA2 and PGF) datasets over the NH. Other satellite (PERSIANN-CDR) and reanalysis (ERA-5, ERA-Interim, NCEP2 and JRA-55) datasets mainly underestimated CDD over the same region (NH). Overall, the analyzed gridded products underestimate CDD over most parts of India, except the PGF data.

In contrast to CDD, higher CWD is found over the higher rainfall receiving zones (the WG and NE parts) and lower CWD values are observed over the dry-regions of WI surrounding the TD (Fig. 4.21). Satellite-derived PERSIANN-CDR, CHIRPS; and reanalysis based NCEP2 and PGF rainfall datasets are inadequate in capturing the CWD (>45 days) over the WG (Fig. 4.21) and mainly underestimated the CWD over this region (Fig. 4.21). Negative PBIAS over the NH is observed for the gauge-based (APHRODITE, CPC and GPCC), satellite (CHIRPS) and reanalysis (MERRA2 and PGF) datasets. Except for the PGF (with a median bias of -29.3%), all other rainfall datasets overestimated CWD over India. Overall, satellite-derived CHIRPS and gauge-based CPC and GPCC data are in higher agreement with the IMD data in capturing temporal variations (Fig.4.23n) of CWD over India. Estimated PDFs from these three datasets (CHIRPS, CPC and GPCC) are also close to the PDF of IMD. However, these datasets overestimated CWD over India with corresponding median bias of 9.5%, 14.37% and 16.2% respectively.
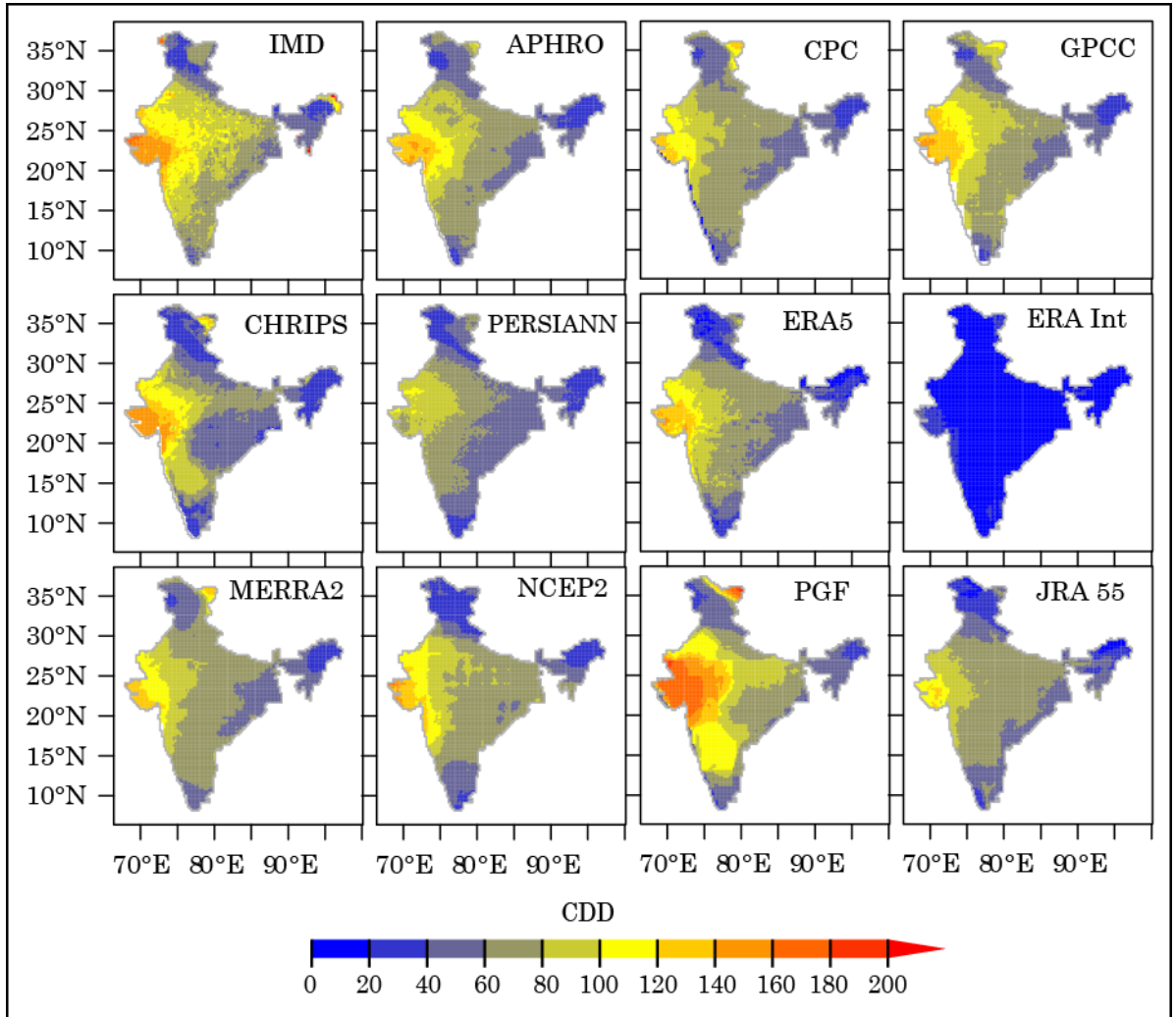
Fig. 4.20. Spatial distribution of average annual consecutive dry days (CDDs) over India during 1986- 2015.
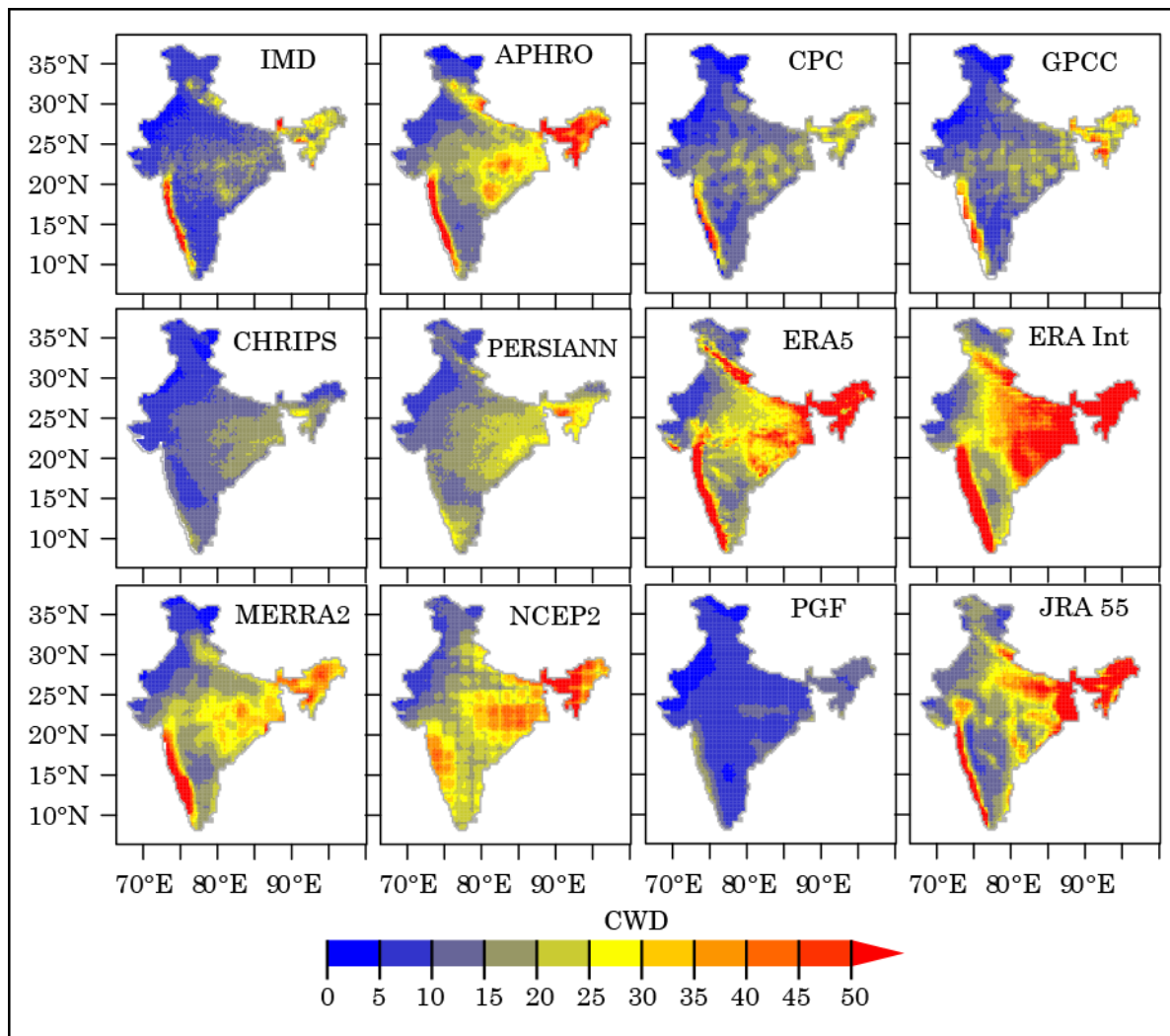
Fig. 4.21 Spatial distribution of average annual consecutive wet days (CWDs) over India during 1986- 2015.
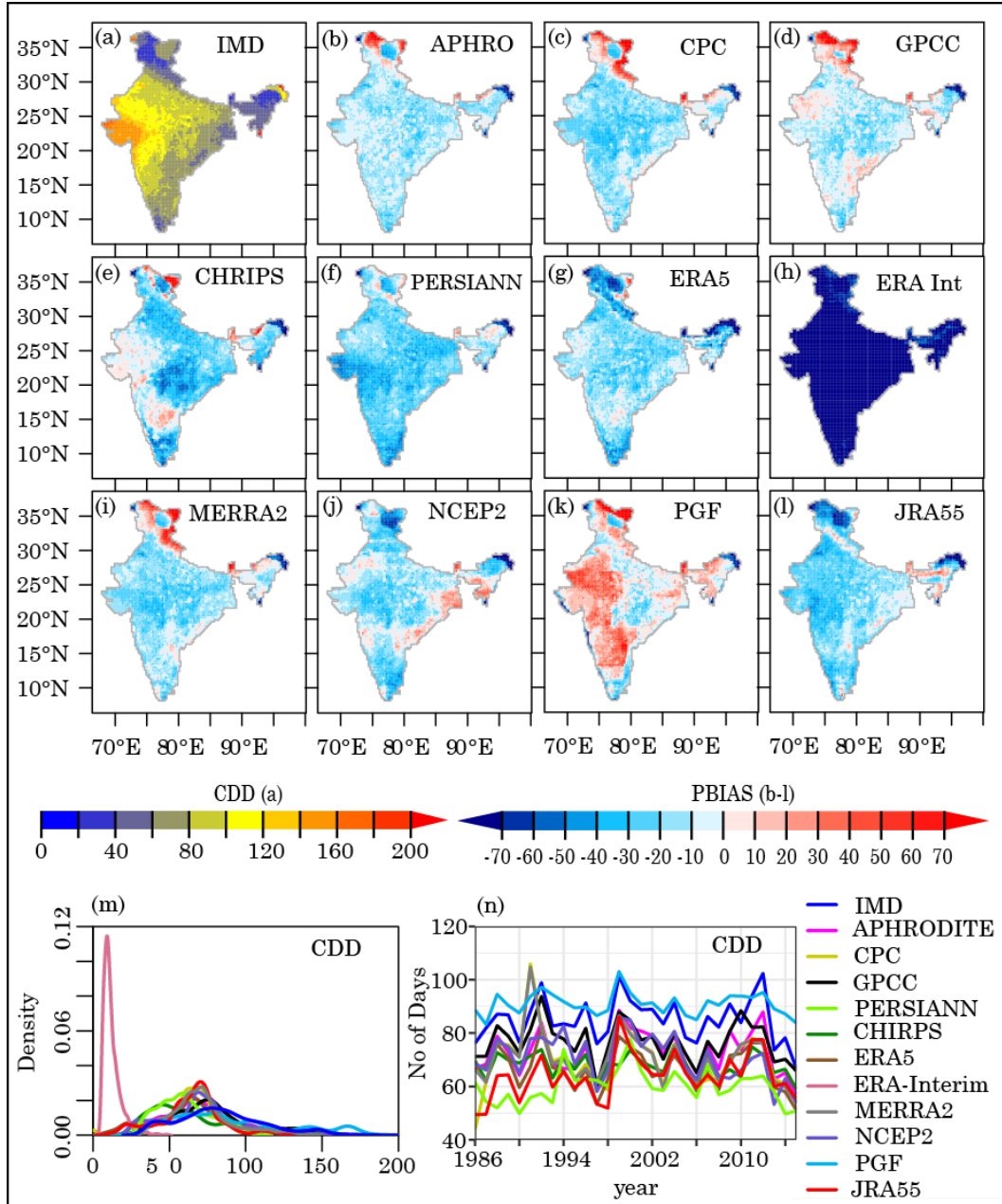
Fig. 4.22. Average CDD (days) over India (**a**) during 1986 – 2015. Percentage BIAS in CDD in different gridded datasets (**b-l**) from IMD. The probability density function (**m**) estimated from annual average values over India and variation of CDD rainfall during the study period (**n**) are shown in the lower panel.
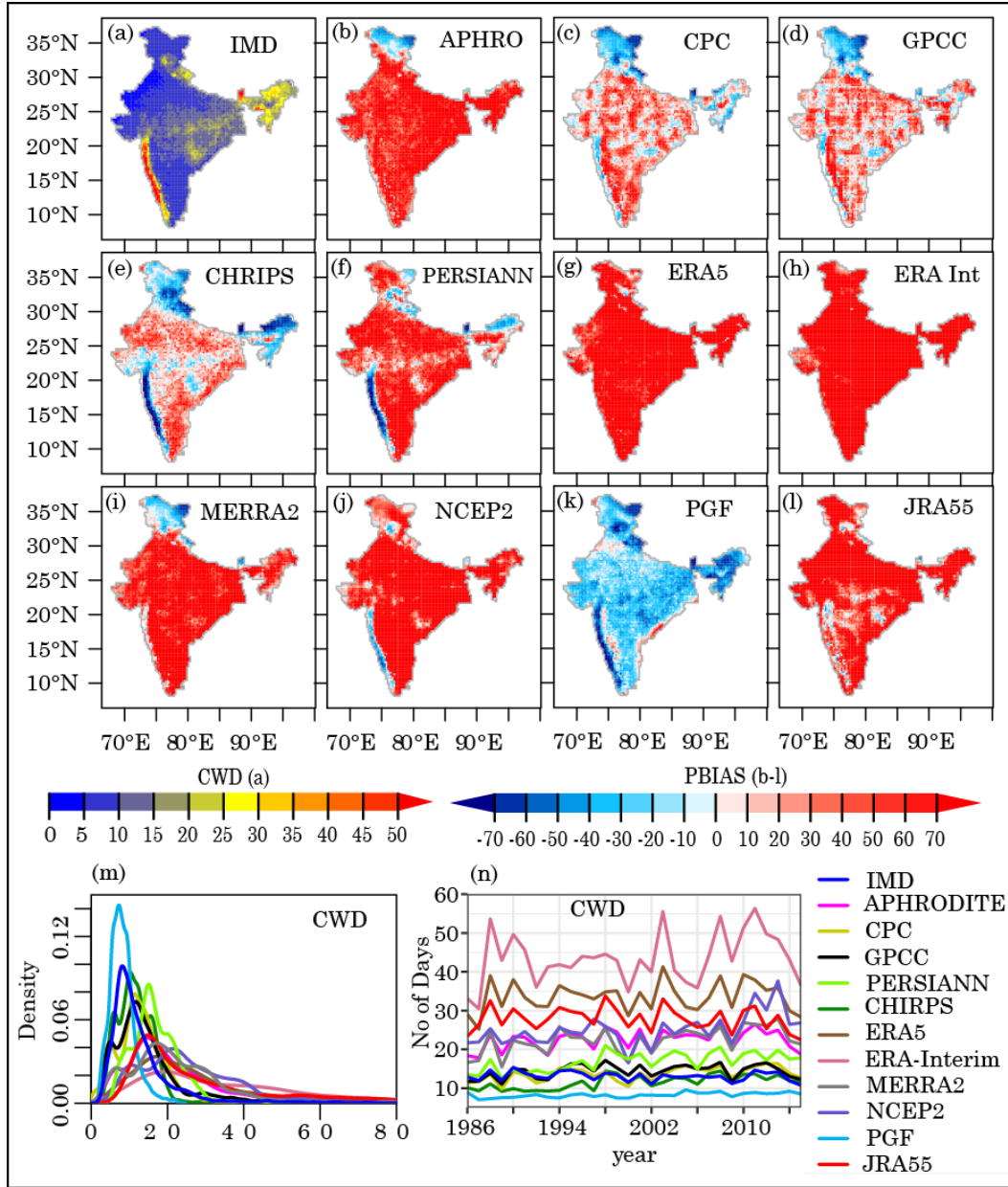
Fig. 4.23. Average CWD (mm) over India (**a**) during 1986 – 2015. Percentage BIAS in CWD in different gridded datasets (**b-l**) from IMD. The probability density function (**m**) estimated from annual average values over India and variation of CWD rainfall during the study period (**n**) are shown in the lower panel.

4.5 Comparison based on different evaluation metrics

As evident from previous results obtained in this study, the performance of these datasets in representing the spatial distribution of average annual extreme rainfall differs widely over India. Relative performance of the gridded datasets in reproducing the spatial distribution of extreme indices over India is compared using the Taylor diagram (Fig. 4.24). Although APHRODITE showed the highest correlation (above 0.75) with the IMD data in representing the spatial occurrences of magnitude based extreme rainfall indices over India (Fig. 4.24a-f), it is unable to capture the spatial variations of extreme rainfall as evident from relatively lower standard deviation (SD) compared to the IMD datasets. On the other hand, the GPCC CHIRPS and ERA5 better captured the spatial variation and closely match with the SD of the IMD dataset. NCEP2 data show the lowest correlation and higher RMSE in all of the six magnitude-based extreme indices and have the worst performance followed by the ERA-Interim dataset. In addition, the GPCC data also showed good performance for R10mm and R20mm rainfall days (Fig. 4.24g-h). Besides, ERA-5 better matches the SD of IMD in representing heavy rainfall (HR) days over India but has a larger RMSE as it overestimates the HR amount.

GPCC and CPC better captured the spatial distribution of CWD over India with CC of 0.8 and 0.6 respectively (Fig. 4.24l). The SD of GPCC (8.6 days) and CPC (7.3 days) nearer to the SD of IMD dataset of 9.4 days for CWD. However, ERA-Interim and PGF derived CDD distributions over India poorly match with the IMD results (Fig. 4.24k). The CPC and the PERSIANN-CDR performed worst among the gauge-based and satellite rainfall group, respectively. Except for CPC, ERA-Interim and PGF, all other datasets have a higher spatial correlation (above 0.8) with the IMD in representing CWD over India. Interestingly, the ERA-5 reanalysis data better approximates the spatial variability than the gauge-based APHRODITE and GPCC data with an SD of 27.8 compared to the IMD derived SD of 29.1 for CDD over India (Fig. 4.24k).
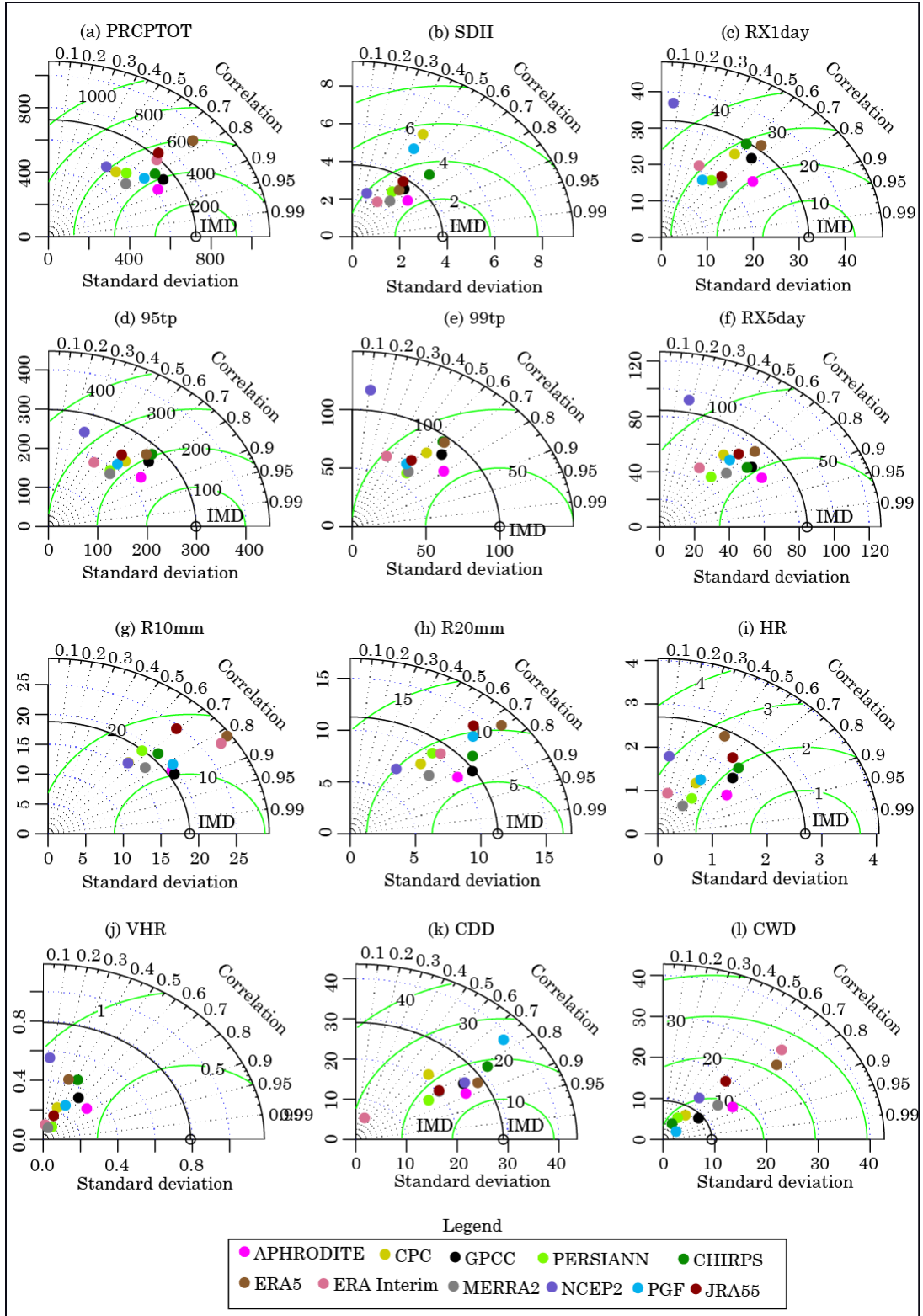
Fig. 4.24. Relative performance of individual datasets in capturing different characteristics of extreme indices over India.

Finally, the normalized values of different evaluation indices (described in the methodology section) are used to compare the datasets while assessing their suitability in representing different rainfall indices over India. The results are presented using 'Portrait diagrams' (Fig. 4.25). The gauge-based datasets have relatively lower normalized error values whereas it is relatively higher for the reanalysis dataset. The ERA-Interim and NCEP2 data show higher error in representing extreme rainfall characteristics over India. Gauge based GPCC exhibited the lowest PBIAS for R95tp, R99tp and HR while the PBIAS in PRCPTOT, SDII, R20mm and CWD is lowest in the CHIRPS datasets. The ERA-5 reanalysis better captures annual one day and five-day maximum rainfall. Besides, lowest median normalized RMSE and MAE are found in the gauge-based APHRODITE and GPCC datasets. The correlation coefficient (CC) and index-of-agreement (d) shows a similar pattern of agreement between IMD and other gridded products.

It is evident from the portrait plot (Fig. 4.25 a-e) that the datasets do not perform consistently well for all the extreme indices over India and also the relative performance of these gridded products vary with the choice of extreme indices. Therefore, a relative skill score (RSC) is obtained by combining the evaluation metrics (see methodology section for details) for the datasets in representing a particular category of rainfall index over India (Fig. 4.25f). The GPCC data obtained the highest score in representing eight out of eleven (excluding the HRE) extreme indices over India (see Table 4.3 for corresponding rank). The APHRODITE data shows the highest score for R99tp, R10mm and CDD. In the satellite rainfall group, CHIRPS performed well in capturing frequency and duration based indices over India while PERSIANN-CDR data has comparatively better efficiency in representing the magnitude of extreme rainfall over India, except for PRCPTOT and SDII which is better captured by the CHIRPS. In the reanalysis group, ERA-5 and MERRA2 performed better than other rainfall datasets. Overall, the NCEP2 and ERA-Interim show the worst performance among the selected gridded datasets in agreeing with the IMD data. Since the rainfall distribution and seasonal concentration varies significantly over India, the results of RSC can be impacted.
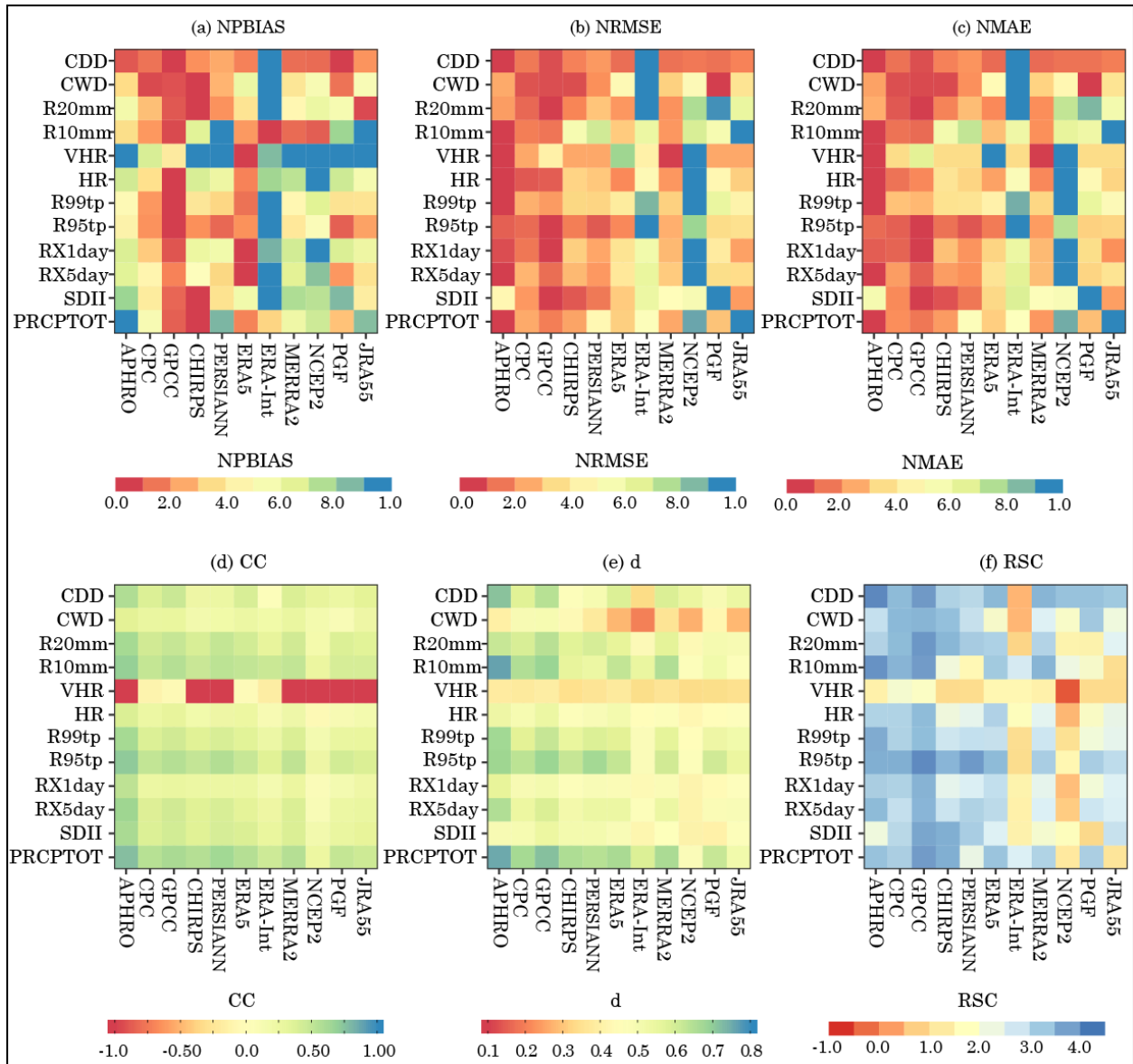
Fig. 4.25 Portrait diagram showing the normalized values of median PBIAS (a), RMSE (b), MAE (c); all India median correlation-coefficient (d), index-of-agreement (e) and relative skill score (f) of different gridded products over India.

Table 4.3 Ranking of gridded datasets in capturing extreme rainfall over India.

Datasets	PRCPTOT	SDII	RX5day	RX1day	R95tp	R99tp	HR	VHR	R10mm	R20mm	CWD	CDD
APHRODITE	3	7	2	2	3	1	4	5	1	6	5	1
CPC	6	4	5	3	4	3	3	1	3	3	2	5
GPCC	1	1	1	1	1	2	1	2	2	1	1	2
CHIRPS	2	2	6	8	5	7	8	9	8	2	3	9
PERSIANN	9	3	3	5	2	4	6	7	10	4	6	10
ERA5	4	6	4	4	6	5	2	3	5	5	9	4
ERA-Interim	8	10	10	10	11	11	10	4	6	11	11	11
MERRA2	7	8	9	7	8	6	5	6	4	7	7	3
NCEP2	10	9	11	11	10	10	11	11	7	9	10	6
PGF	5	11	7	9	7	9	9	10	9	10	4	7
JRA-55	11	5	8	6	9	8	7	8	11	8	8	8

4.6 Comparison based on trends in extreme rainfall

Trend in extreme rainfall indices (using MK test) and its magnitude (using Sen's slope) are estimated to compare the gridded datasets with the IMD at 5% significant level over India.

Trend in PRCPTOT and SDII

Spatial patterns of increasing and decreasing trends of PRCPTOT and SDII are similar in the IMD dataset over India (Fig. 4.26 & Fig. 4.27). Significantly increasing trend at 5% level (hereafter only *significant trend*) in PRCPTOT are observed over WI, WG, SP and parts of EP covering 6.6% of area where SDII is significantly decreasing mostly over west central parts and eastern parts of India. Upward trend in PRCPTOT are also observed mostly over these regions covering 39.4% of total geographical area. Decreasing trends in PRCPTOT are observed over NE, NH, GP and some parts of SP region covering 41.64% of which 11.98% of area show significant downward trend. However, the selected datasets failed to capture the significant negative trends over the western parts of NH which is evident in the IMD dataset. Higher overestimation (underestimation) of significant trend areas is observed for the NCEP2 and JRA-55 (PGF) datasets. Almost all of the selected datasets showed significant increasing trend over the western parts of India, however, the magnitude of trend varies across datasets. PERSIANN-CDR overestimated significant

negative trend areas over GP, NE and WG and SP and positive trend areas in the WI. Among the gauge based datasets the CPC performed worse than APHRODITE and GPCC, by highly over estimating trend magnitude and significant trend zones in PRCPTOT and SDII over southern parts of NH, GP, NE, EP and WI. The MERRA2 and CPC exhibited similar pattern of trend and areas of significant trend over India (Fig. 4.26). The estimated significant trend zones from the ERA-Interim NCEP2 and JRA-55 largely deviate from the IMD (Fig. 4.26). Overestimation of significant positive trend in the WI and SP is not in agreement with the IMD.

Fig. 4.26. Trend in PRCPTOT during 1986 – 2015 over India. Black-dots showing grid-cells with significant trend at 5% level.

Fig. 4.27 Trend in SDII rainfall during 1986 – 2015 over India. Black-dots showing grid-cells with significant trend at 5% level.

The PERSIANN-CDR show significant increase in SDII over WG, SP, NH, GP and parts of NE. Similar to PRCPTOT, the NCEP2 indicates significant increase in SDII over CI and parts of EP and significant decrease in SDII over SP. Significant increase in SDII over the WI is also observed in the CPC, GPCC, CHIRPS, ERA5, MERRA2 and PGF datasets, similar to the IMD dataset.

Trend in RX1day and RX5day

RX1day and RX5day rainfall has significantly increased in parts of WI, EP, NE and south-eastern Parts of NH during the study period, covering 4.9 % area and 3.4% area respectively. Significant decreasing trend, covering 7.1% (RX1day) and 10.4% (RX5day) of India are prominent over NH, GP, NE and parts of SP (Fig. 4.28 & Fig. 4.29). The ERA-5 reanalysis and gauge-based GPCC data better resemble the significant trend areas in comparison to the IMD dataset. The PERSIANN-CDR and NCEP2 data noticeably overestimated significant areas of positive and negative trend over India, respectively.

Fig. 4.28 Trend in RX1day rainfall during 1986 – 2015 over India. Black-dots showing grid-cells with significant trend at 5% level.

Fig. 4.29 Trend in RX5day rainfall during 1986 – 2015 over India. Black-dots showing grid-cells with significant trend at 5% level.
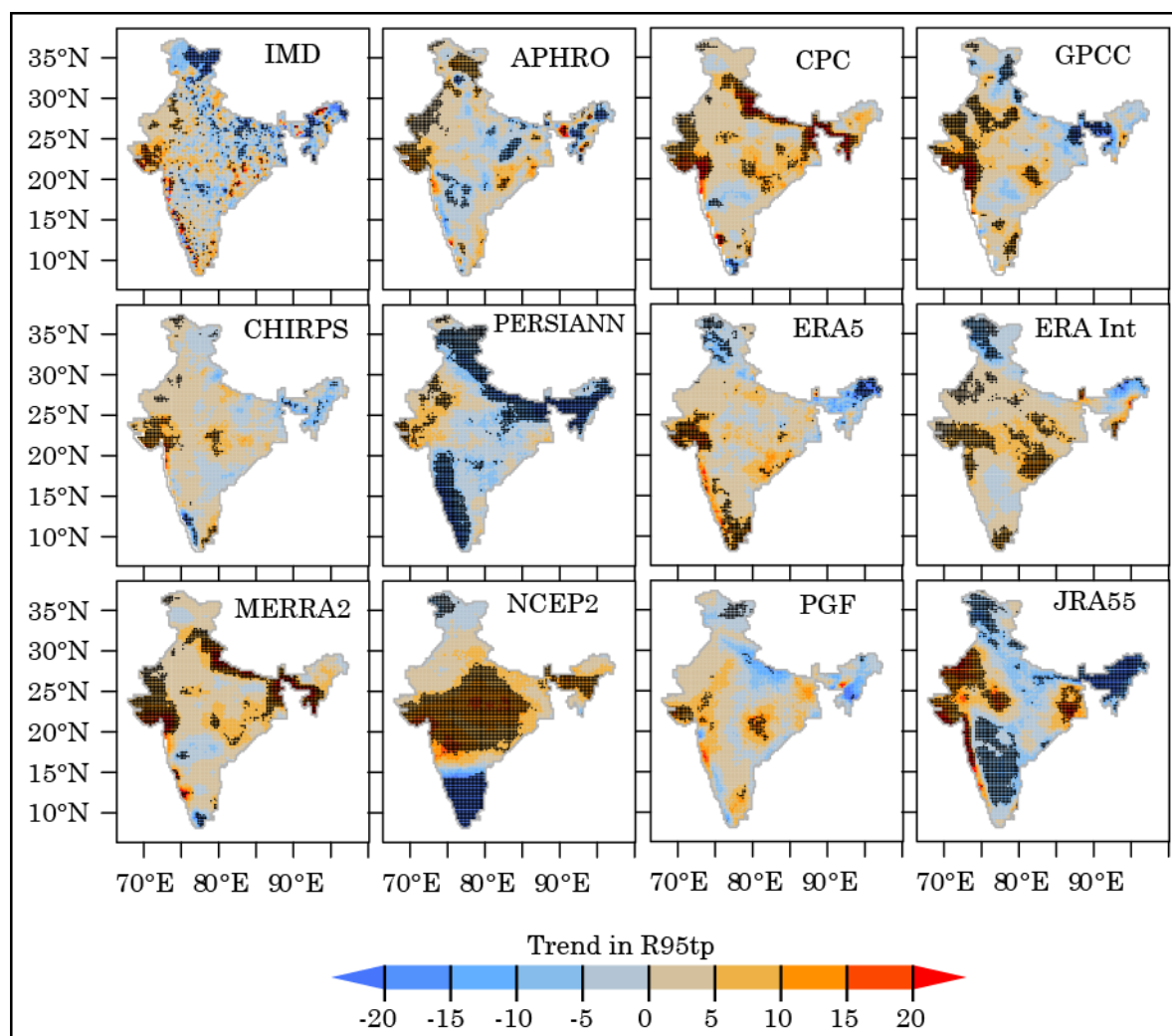
Fig. 4.30 The trend in R95tp during 1986 – 2015 over India. Black-dots showing grid-cells with a significant trend at the 5% level.

Trend in R95tp and R99tp

The pattern of over/underestimation of trend is also similar both in R95tp (Fig. 4.30) and PRCPTOT (Fig. 4.31), indicating that the changes in total precipitation are mostly contributed as increase/decrease in extreme rainfall (R95tp). ERA5 data was found to better reproduce the trend pattern in R95tp over India, except over SP and GP, compared to other datasets. The CHIRPS estimated trend in R99tp closely resembles the spatial pattern as derived from the IMD with ERA5 being the next best performing data set. PERSIANN-CDR underestimated trend magnitude in R95tp and R99tp over orographic belts of WG and

Himalaya (Fig. 4.30 & Fig. 4.31). NCEP2 failed to reproduce the spatial pattern of R95tp and R99tp over CI and SP, with consistent over and underestimation of increasing and decreasing trends of extreme rainfall over these regions, respectively.
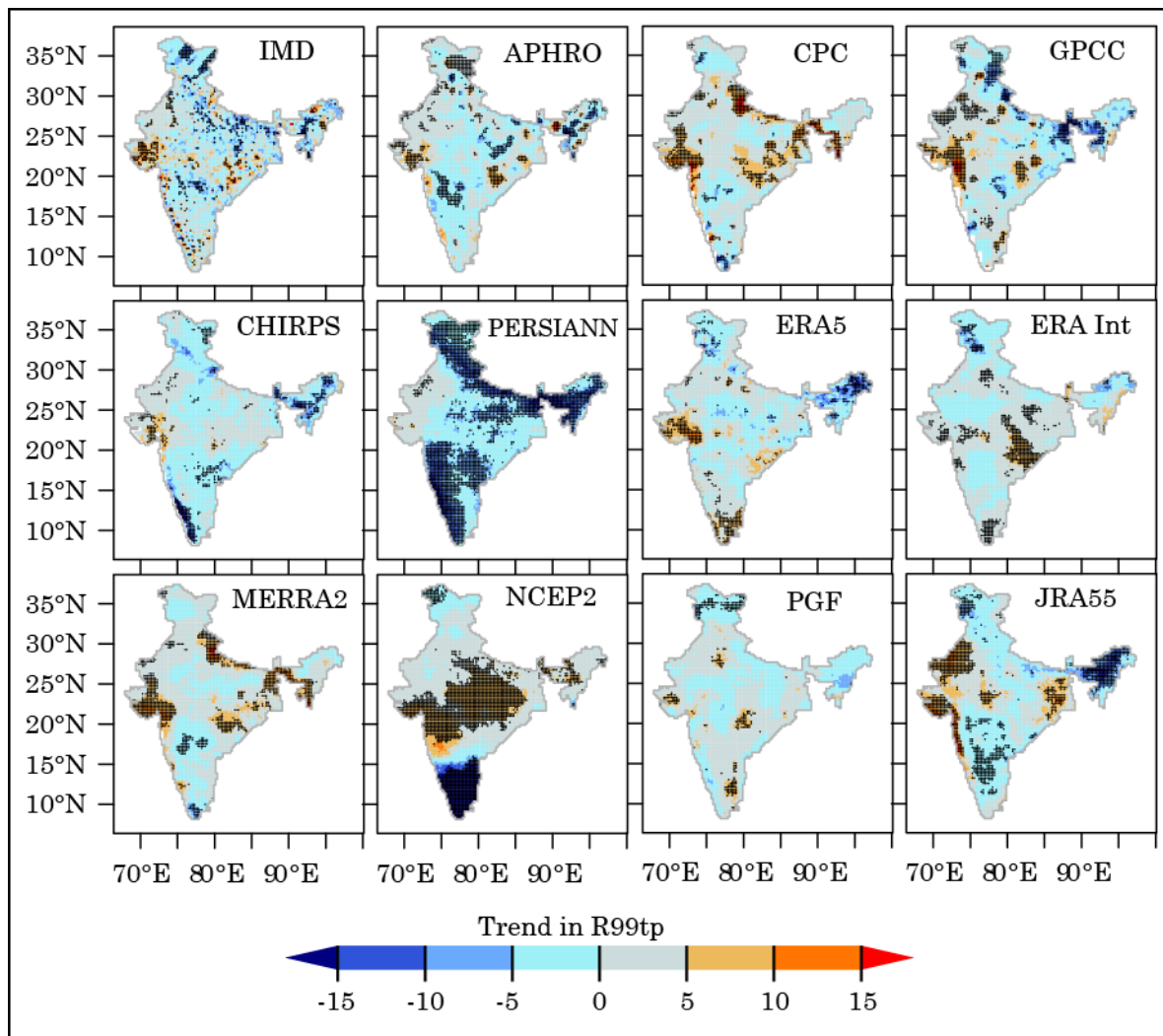
Fig. 4.31 Trend in R99tp rainfall during 1986 – 2015 over India. Black-dots showing grid-cells with significant trend at 5% level.

Trend in CDD and CWD
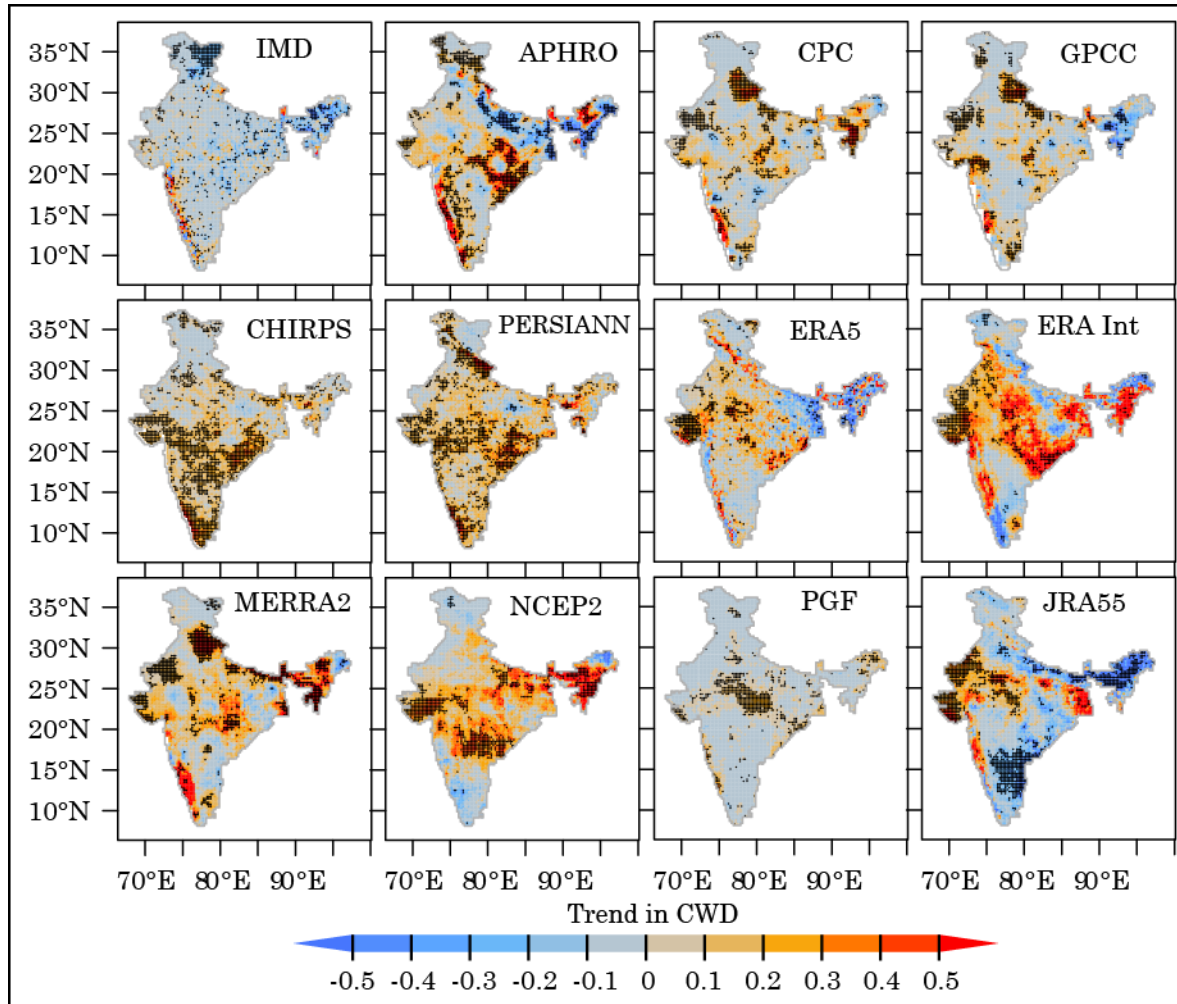
Fig. 4.32. Trend in CWD during 1986 – 2015 over India. Black-dots showing grid-cells with significant trend at 5% level.

CWD has not changed significantly over most parts of India in the IMD datasets, The grids of significant trend are mostly dispersed over India, while it is mostly grouped in other gridded datasets (Fig. 4.32). Significant negative trend in CWD is mostly observed over the eastern parts of NH, NE and parts of EP and GP. A decreasing trend in CWD is found in the WG and foothills of Himalaya. The gauge-based APHRODITE performed more poorly than CPC and GPCC. Satellite-derived CHIRPS and PERSIANN-CDR overestimated significant positive trend areas over southern India. The higher mismatch is observed over NE, EP, and WI for ERA-Interim, APHRODITE, PERSIANN-CDR and NCEP2 datasets.

Trends of CWD estimated from the ERA-5 reanalysis better resembles IMD than other reanalysis products. The gauge based datasets better captured the trend pattern in CDD compared to other gridded datasets (Fig. 4.33). The APHRODITE better matches with IMD in representing CDD trends, except for the NH region. The JRA-55 highly overestimated trend magnitude of CDD in the SP region with a value of 2 days/year. APHRODITE, CPC and GPCC data showed a decreasing trend over NH and foot-hills of Himalaya which is in contrast to the IMD.
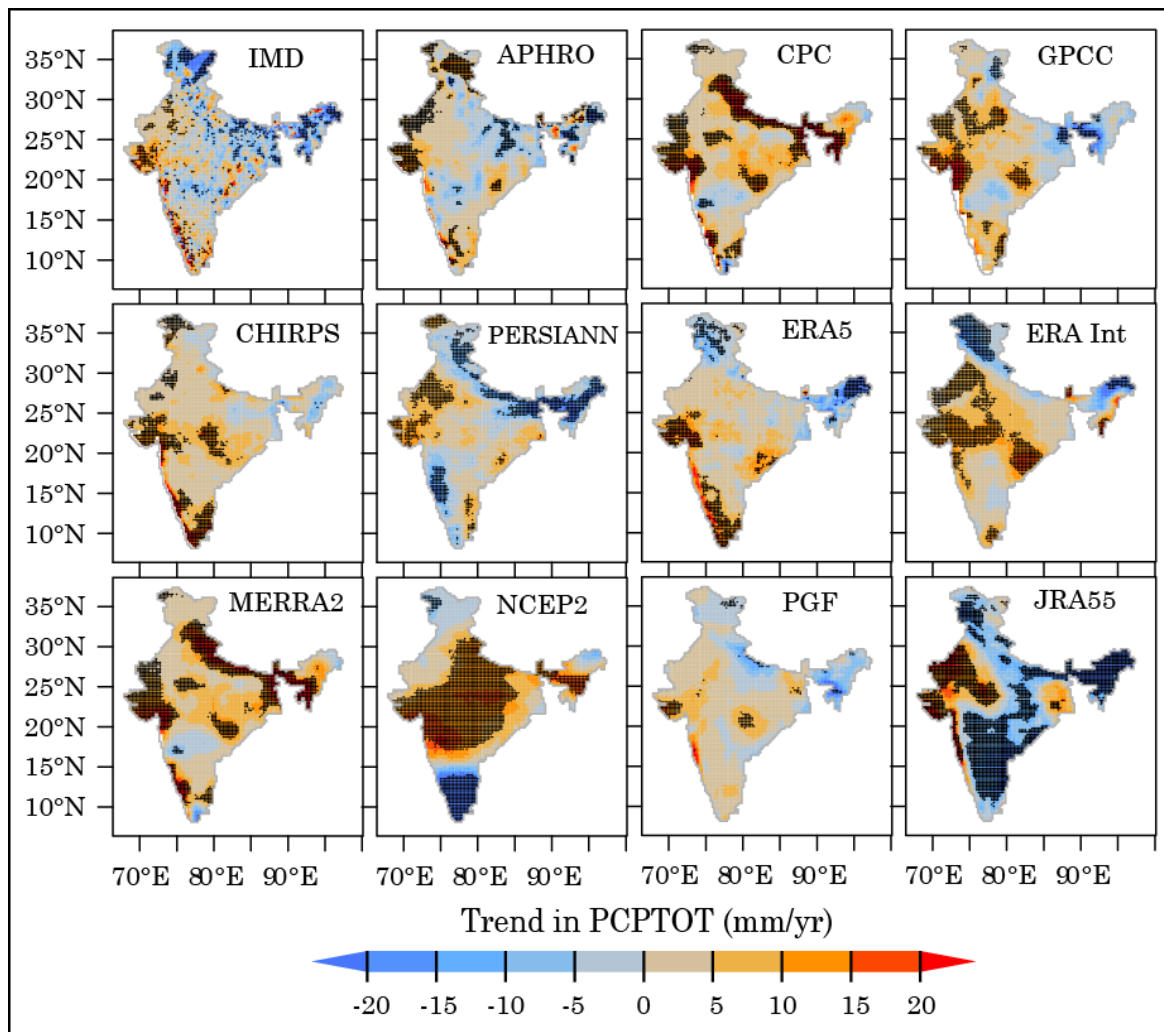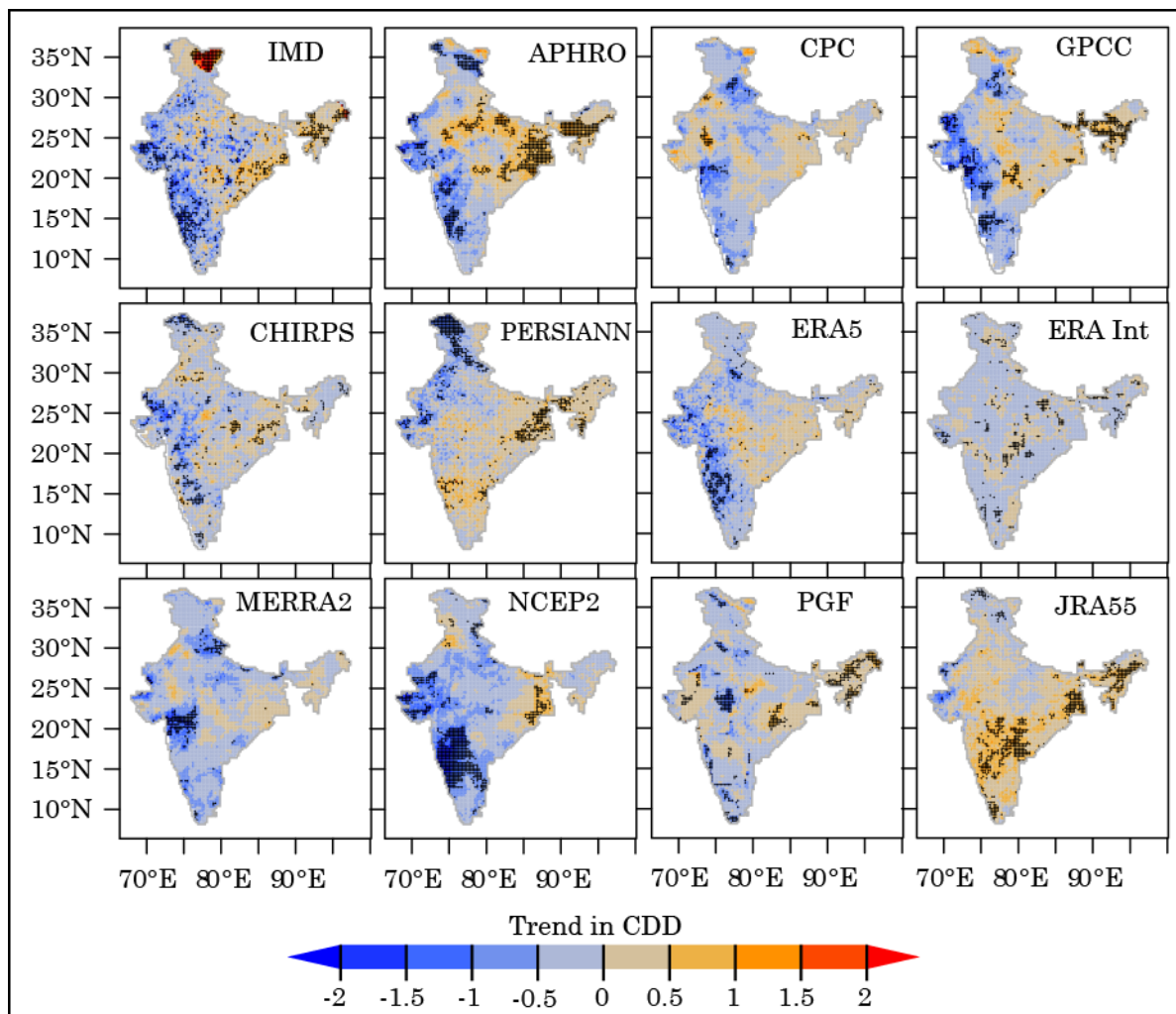

Fig. 4.33. Trend in CDD during 1986 – 2015 over India. Black-dots showing grid-cells with significant trend at 5% level.
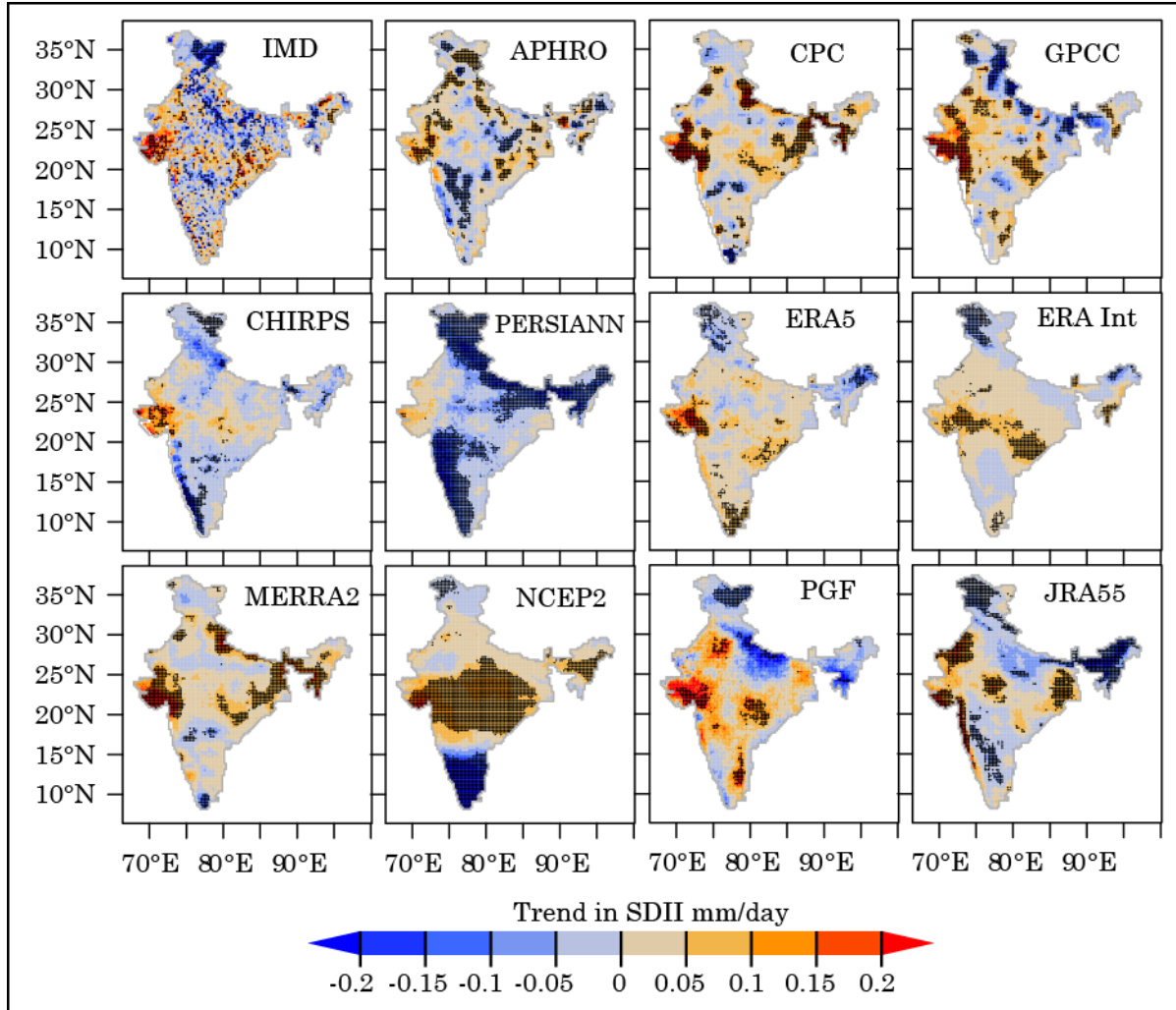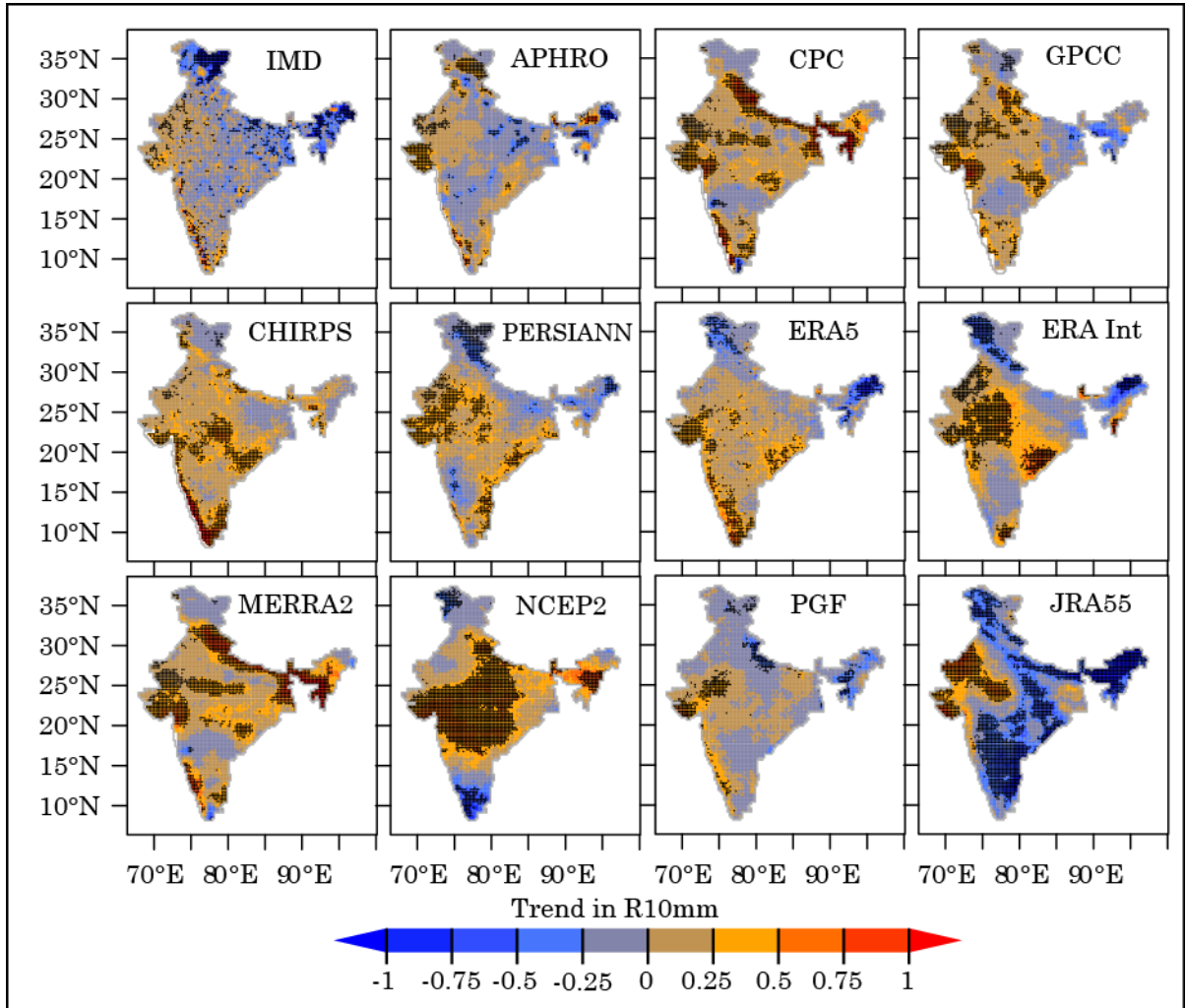
Fig 4.34. Trend in R10mm rainfall during 1986 – 2015 over India. Black-dots showing grid-cells with significant trend at 5% level.

Trend in R10mm and R20mm

Significant decreasing trends in R10mm (Fig. 4.34) and R20mm (Fig. 4.35) rainfall days are observed mostly over NH, GP and NE India whereas increasing trends are found over the WG region of India. ERA-5 better captures the decreasing trend areas over NH and NE, however, slightly overestimated areas of significant increasing trend that are observed over EP and WI. In contrast, CPC, MERRA2, NCEP2 exhibited opposite trend pattern to the IMD in the foothills of Himalaya, NE and GP. Besides, the estimated magnitude of negative trend over these regions is also higher in JRA-55 (R10mm) and PERSIANN-CDR (R20mm) datasets. NCEP2 showed positive trends in R10mm and R20mm over CI, EP and SP which

is contrast to the negative trend found in IMD data. JRA-55 (NCEP2) data highly overestimated negative (positive) trend areas R10mm rainfall days over India.
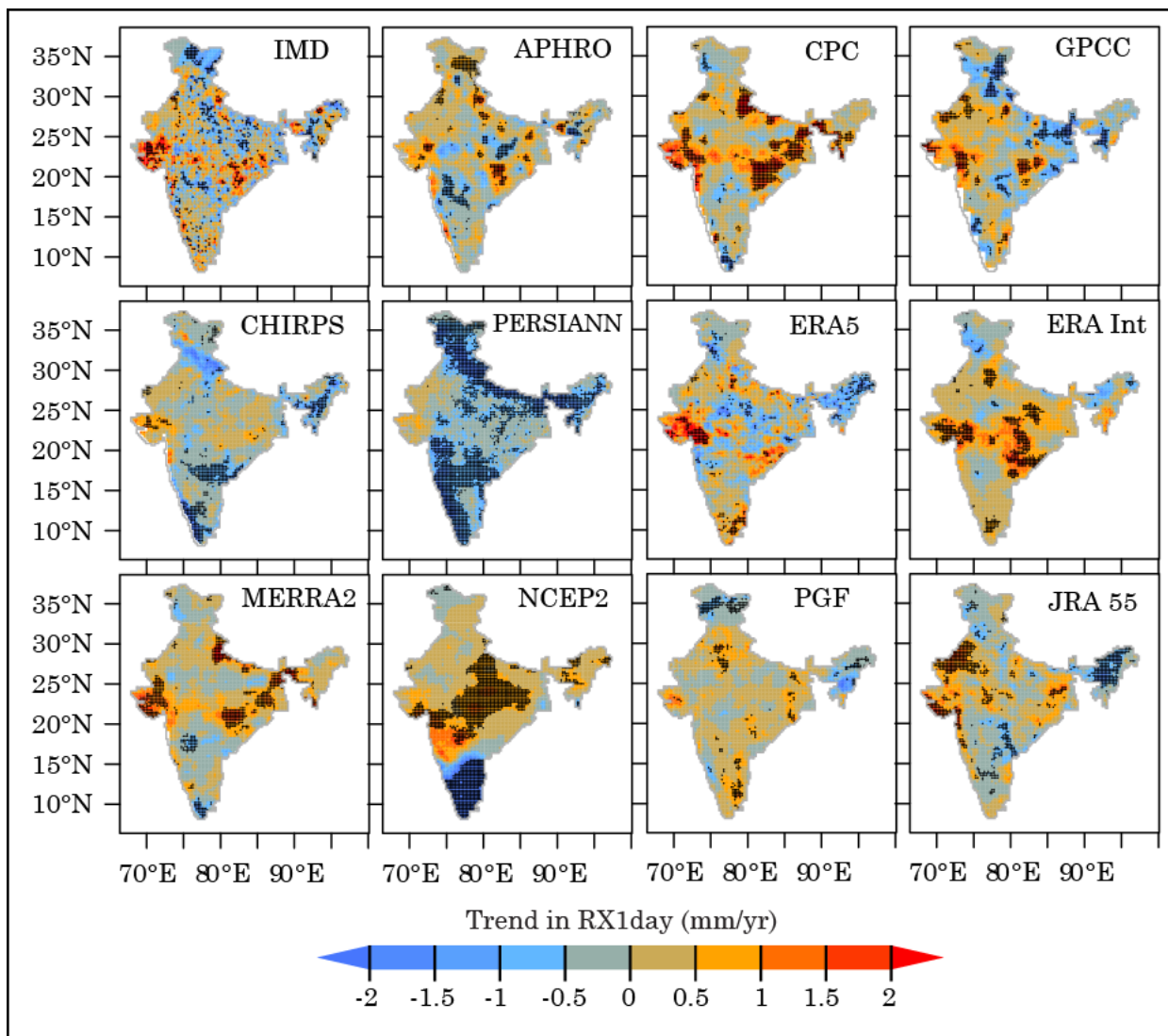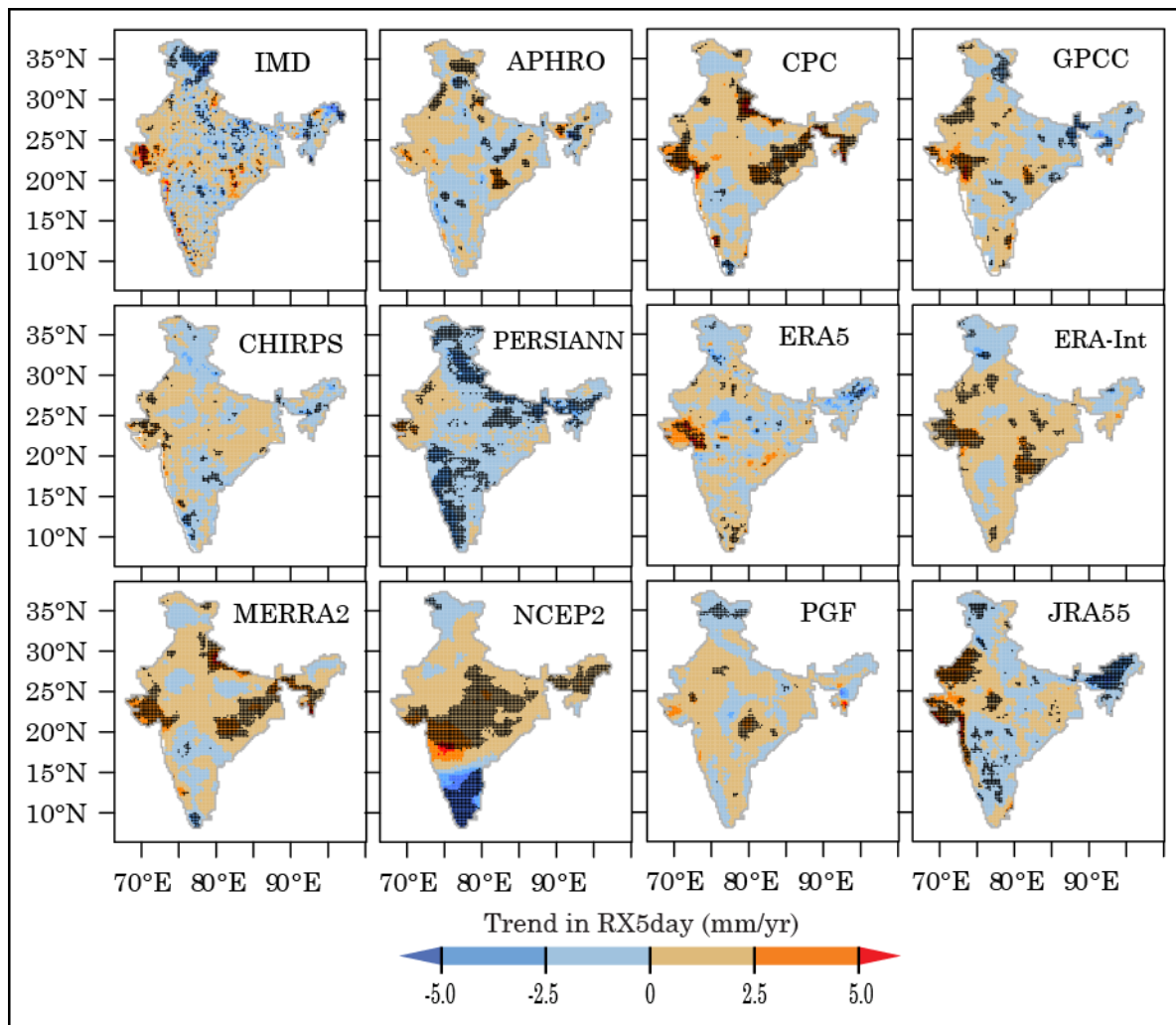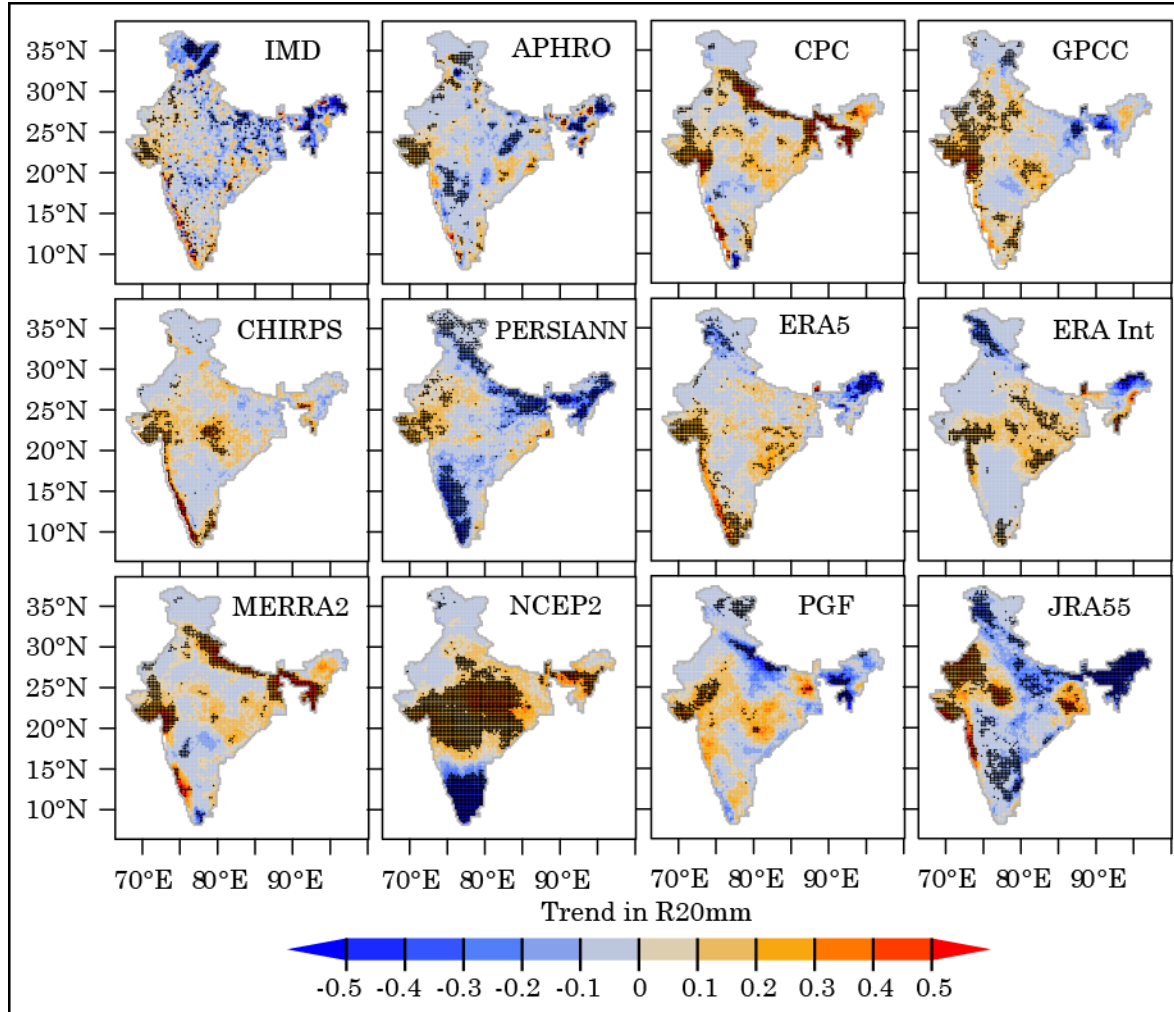

Fig. 4.35. Trend in R20mm rainfall during 1986 – 2015 over India. Black-dots showing grid-cells with significant trend at 5% level.

The gridded datasets largely deviated in estimating trends in extreme rainfall amount and rainfall days, especially areas of significant increase or decrease in reference to the IMD dataset. Higher inconsistency is noted for the PERSIANN-CDR, NCEP2, and JRA-55 datasets. Besides, the gauge-based CPC and MERRA2 reanalysis data exhibited similar pattern of trend magnitude and significant trend zones over various parts of India.

4.7 Discussion

From the above analysis, it is evident that the relative performance of gridded rainfall datasets varies over India and with the choice of extreme rainfall indices. Relative performance of the selected gridded rainfall datasets varied markedly in capturing extreme rainfall characteristics over India. Overall, the selected datasets underestimated the magnitude of extreme rainfall (RX1day, RX5day, R95tp and R99tp) over India. Among the gauge-based gridded datasets GPCC shows the best agreement with the IMD dataset ahead of APHRODITE and CPC. This is because of the differences in gauge-records used in these datasets during construction: GPCC has a higher station density and a homogenous spatial coverage over India (especially in CI and EP region) compared to APHRODITE and CPC (Rana et al., 2015; Schneider et al., 2014). Therefore, GPCC obtained the highest-ranking score for most of the extreme indices and also better preserve the spatial variation rainfall extreme over India. Another source of uncertainty may be due to the differences in interpolation techniques used to construct these datasets. The Sheremap interpolation technique used by GPCC and APHRODITE is found to more robust over complex terrain than the optimal interpolation technique used in CPC (Ahmed et al., 2019; Salman et al., 2019). However, the gauge based datasets failed to capture extreme rainfall dynamics over orographic belts, mainly in the eastern parts of the NH. This is mainly due to the mere absence of gauge records in these gridded datasets in this region during construction (Pai et al., 2014).

Among the satellite rainfall datasets, CHIRPS performs better than PERSIANN-CDR in reproducing extreme rainfall behaviour over India. Similar finding for CHIRPS is also reported by Gupta et al., (2019) in reproducing extreme rainfall over India. Inadequate representation of extreme rainfall over the WG and foothills of Himalaya is another limitation of satellite-derived rainfall as the remotely-sensed precipitation measurements failed to detect orographic rainfall resulting from atmosphere-mountain interactions (Gupta et al., 2019). Additionally, the decrease in reflective sensitivity of satellite estimates over rugged terrain can also contribute to this bias. PERSIANN-CDR uses Infrared (IR) measurements of cloud top temperature and its relationship with precipitation rates for providing daily precipitation estimates. To avoid large unrealistic estimates of precipitation, maximum estimates are capped in PERSIANN-CDR system by setting an arbitrary limit which can explain underestimation in extreme precipitation. Another

constrain is that the training of artificial neural network relies solely on the IR measurement and a high-resolution data which is limited over the continental United States only. On the other hand, the CHIRPS precipitation estimates are derived by subsuming data from multiple sources (gauge-based, IR measurements, T3B42 and CFS2). Besides, the CHIRPS uses gauge-based GPCC data for calibration, while, the PERSIANN-CDR estimates are calibrated using the GPCP satellite-derived precipitation product. However, these two datasets are inadequate in representing the spatial pattern of extreme rainfall trends over India. The PERSIANN-CDR and CHIRPS are mainly developed to provide temporally homogeneous precipitation records rather than best instantaneous estimates of precipitation rates.

The reanalysis datasets showed the largest discrepancies among other precipitation products when compared with the IMD dataset. NCEP2 showed very high positive PBIAS over the SP region which is in line with the findings of Ghodichore et al (2018). Systematic positive PBIAS in representing extreme rainfall by NCEP2 is reported in previous data comparison studies (Huang et al. 2016; Chen et al. 2019). Overestimation of extreme rainfall over the GP in JRA-55 may be due to the spin-down problem which simulates excessive precipitation at the start at the forecast (Kobayashi et al., 2015). Overestimation (underestimation) of CWD (CDD) is highest in ERA-Interim datasets and may be due to the presence of too many wet days with little rainfall (Belo-Pereira et al 2011; Zhu 2017). The PGF reanalysis highly overestimated SDII, CWD and underestimated CDD over India which may be due to the presence of too little wet days in the dataset. Subdued monsoon season precipitation over India in ERA-Interim is also reported by Kim et al. (2019). The ERA-Interim data highly underestimates the R20mm rainfall days over India. Kim et al. (2019) also reported similar findings over the same region where the ERA-Interim estimated rainfall days above 30mm/day is near zero over most parts of India. Performance of MERRA-2 is comparatively better than the ERA-Interim, NCEP2 and JRA-55 reanalysis, especially in capturing heavy rainfall amount and frequency of R10mm and CDD days over India. Mahato and Mishra et al. 2019 also find similar results while analyzing extreme monsoon season precipitation over in India. An improved precipitation correction algorithm and incorporation of merged gauge-satellite data may be the reason for that (Reichle et al. 2017). Being the fifth generation reanalysis product, the ERA-5 shows improvements with the sophisticated data assimilation methods and has benefited from improvements in model

physics and core development of forecast models (Nogueira, 2020). As discussed above, the difference in grid-resolution also reduces the performance of reanalysis datasets in reproducing extreme rainfall. However, the dataset failed to capture CDD and CWD over India.

Grid-resolution of the gridded datasets has a substantial effect in representing extreme rainfall. Plotting of the overall scores of datasets against their base resolutions (Fig. 4.36) reveal that high-resolution datasets performed better than relatively lower resolution datasets. The effects of resolution-dependent are more prominent among the reanalysis datasets. Degradation of relative skill score in representing higher extremes (RX1day, 99tp and R20mm) is higher than lower extremes (RX5day, 95tp and R10mm). Choice of higher threshold i.e. 99tp and R20mm reveals greater dependence on grid-resolution as they lie on the higher end of the PDF therefore difficult to capture by relatively low-resolution datasets.
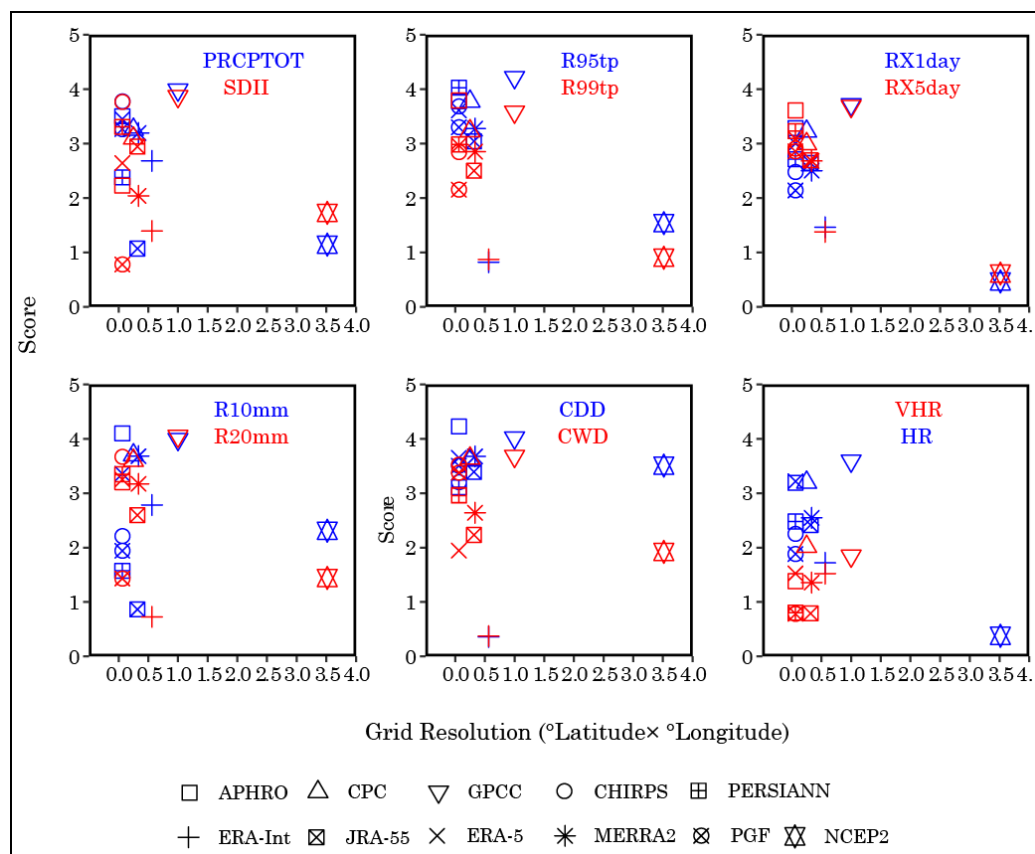
Fig. 4.36 Overall score of each rainfall datasets over India vs. grid-resolution of the gridded datasets in selected extreme rainfall indices.

4.8 Conclusion

Understanding extreme precipitation characteristics is crucial as they can have great societal impacts especially under recent warming. Gridded rainfall datasets for studying extreme rainfall are quite an attractive choice as they provide daily precipitation estimates at a high spatial resolution over most parts of the globe. However, their performance must first be assessed before use in hydro-climatological studies. In this study, we assessed the performance of eleven daily gridded rainfall datasets in terms of their suitability for characterizing extreme rainfall and its trends over India. The gauge based GPCC better captures extreme rainfall over India than the other datasets. In the satellite-reanalysis group, CHIRPS and ERA-5 outperformed other datasets. Duration based indices are better captured by the gauge-based datasets than the satellite and reanalysis datasets. Spatial-resolution may have some effects while representing spatial occurrences of extreme rainfall over India. We found that reanalysis datasets are more resolution sensitive, as the higher resolution gridded datasets (i.e.ERA5) better captured the extreme characteristics than low-resolution reanalysis datasets (ERA-Interim and NCEP2). However, the gridded datasets failed miserably in capturing trends in different rainfall indices over India. Given the recent warming of the atmosphere and increasing frequency and magnitude of extreme precipitation observed in parts of the world, it is important to accurately monitor these events as they have great societal impact. Moreover, some of the gridded datasets used in this study are often used to validate global and regional climate models for climate change impact assessment studies and the underestimation of extreme rainfall which is inherent in these datasets may introduce larger uncertainties in climate change studies, especially those with an emphasis on extreme precipitation. Therefore, we argue that assessment of the relative performance of gridded datasets over the region of interest is a prerequisite before conducting any research on changing extreme rainfall characteristics in a warming world. This study also provides some useful insights into the performance of gridded rainfall products over India.

Chapter 5

Evaluation of gridded precipitation datasets for characterizing precipitation concentration index (PCI) over India.

In this chapter, the analysis of PCI is presented. First, the annual and seasonal distribution of PCI over India is studied based on the IMD gridded dataset. Then the role of geographical factors (i.e. latitude, longitude and elevation) in the spatial distribution of PCI over India is explored. Following that the gridded data comparisons results are presented and discussed.

5.1. Spatial pattern of annual and seasonal PCI over India

The average APCI over India exhibits a strong irregular distribution (APCI> 20) of precipitation with a mean value of 24.66. Average SPCI over India during winter, summer, monsoon and post-monsoon seasons were 13.96, 16.82, 11.45 and 19.32 respectively indicating moderate distribution of precipitation during winter and monsoon season and irregular precipitation distribution during summer and post-monsoon. On annual scale, highest irregularity (APCI value of 52.1) is observed in Northern parts of WI covering the areas surrounding the TD. This part receives the lowest amount of rainfall compared to other regions of India and has a more uneven distribution of annual precipitation, falling mainly in few months of the year. In contrast, the lowest APCI value (12.64) is found over the western part of NH. According to De Luis et al., (2011) APCI value less than 16.7 indicates that the total precipitation is concentrated in half of the period (six months) and are found over parts of NH (associated with winter snowfall and monsoon precipitation); NE, southern parts of SP and south-western parts of WG (Fig. 5.1A). During the Monsoon season, uniform to moderate distribution of precipitation concentration (PCI < 15) mainly prevails over India, because of the south-west monsoon wind which brings maximum amount of rainfall over Indian landmass compared to other seasons.
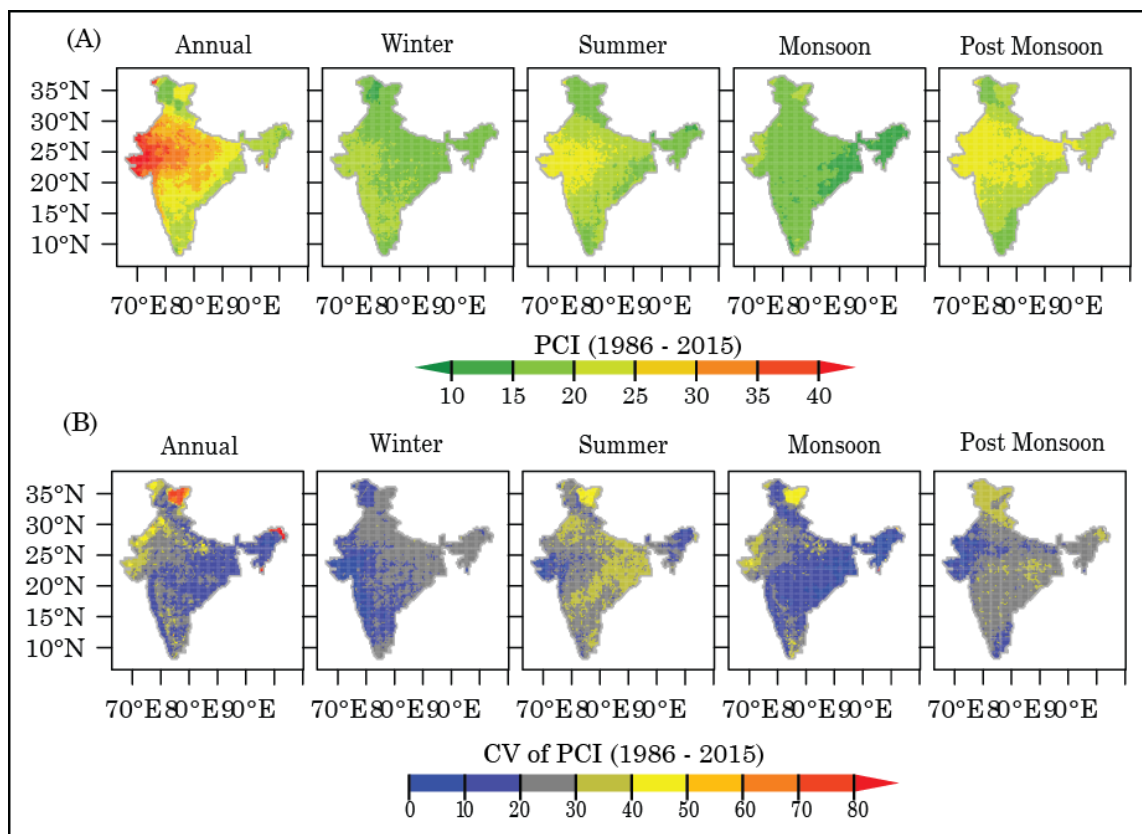
Fig. 5.1. Precipitation Concentration Index (A) and its coefficient of variation (B) over India (1986 – 2015).

Spatial distribution of average PCI values over India and its coefficient of variation (CV) are presented in Fig. 5.1B. Annual average PCI values are moderately distributed over parts of NE and NH during this study period (1986 – 2015). Irregular distribution (15 < PCI > 20) prevails in the contiguous region of the Bay of Bengal and SP region. During the winter, a uniform distribution of PCI is found over parts of NH which may be attributed to the winter snowfall activities over this region (Bhutiyani et al., 2010). During the monsoon season, uniform distributions of PCI prevail over the Indian state of West Bengal (Fig. 5.1A) which is consistent with the study conducted by Chatterjee et al., (2016). Besides, Thomas and Prasannakumar (2016) found that annual precipitation concentration is irregularly distributed over the Indian state of Kerala which is in line with the present study.

An East-West gradient in the distribution in APCI exists from NE to the WI, with a continuous increase from the NE parts to the TD, indicating that PCI is inversely related to

precipitation amount (Fig. 5.1A). To verify this, we calculated Pearson's product-moment correlation between average precipitation and average PCI over India on annual and seasonal scale. They are negatively correlated at 95% level of significance on both annual and seasonal scale. On an annual scale, a weak but significant negative correlation (r = -0.42) exists between these two variables. Seasonally, the highest negative correlation (r = -0.76) is found during winter, followed by summer, post-monsoon and monsoon seasons with respective r values of-0.71 -0.70 and -0.49 respectively.

Higher variation (CV) of APCI (Fig. 5.1B) is found over the eastern part of the NH, parts of GP and in the dry regions of WI. On an annual scale, the WC, NE, EP, EI and parts of the CI and SP are characterized with lesser variability of PCI (Fig. 5.1B). Seasonally, only during monsoon season, during which maximum rainfall occurs over the Indian landmass, a uniform to moderate PCI prevails over a major part of the country. Monsoon season is also marked with a lesser variation of PCI, except some parts of WI, NH and the southern tip of India.

5.2 Correlation of PCI with geographical factors

Geographical factors such as latitude, longitude and altitude are the main controlling factors in influencing on the distribution of precipitation over global land surfaces. Average APCI values are found to be positively correlated with latitude, indicating that the heterogeneity of APCI over India generally increases (from South-North) with latitude (Table 5.1). However, average APCI over India is found to be negatively correlated (P > 0.01) with longitude and elevation with a corresponding correlation coefficient of -0.59 and -0.33. The Indian landmass/subcontinent is dominated by the monsoon circulation system, having two branches, also has a northerly course during monsoon season, which contributes over 80% of the annual rainfall (Gadgil, 2018). These influences are evident as we can find a significant positive correlation between latitude and average APCI over India. A similar finding is also reported by Zhang et al (2018) over China. Longitudinal decrease of APCI from the WI to the NE is mainly due to the coupling effects of the direction of the south-west monsoon wind, orographic influences and large scale atmospheric circulations that prevails over India. The decrease in APCI with altitude is supported by the process of orographic lifting and subsequent increase in precipitation amount with altitude which are common over the western and southern parts of the WG and NH.

Table 5.1 Pearson's correlation coefficient of the APCI with latitude, longitude and altitude over India for the period of 1986 – 2015.

	Latitude	Longitude	Altitude
APCI	0.057*	-0.587*	-0.334*

* significant at 1% level.

5.3 APCI in different precipitation datasets

Based on IMD gridded dataset, maximum, mean and minimum APCI over India during the study period (1986 – 2015) are 12.6, 24.6 and 52.1 respectively. All of the selected gridded datasets underestimate the minimum APCI value, except the GPCC gridded data, with a minimum value of 12.8. Similar to GPCC data, the PGF reanalysis product also closely approximates the minimum APCI value over India, with a value of 12.4. The mean APCI value is also underestimated by all of the gridded precipitation datasets considered in this study when compared to IMD data (Fig. 5.2). Most of these datasets well captured the spatial variability of APCI distribution, especially over the EC, and eastern part of CI, except the NCEP2 reanalysis data where large deviations are observed near the northern parts of the EC. However, the spatial distribution of APCI values over the NH and NE India are under/overestimated by most of these datasets. This deviation is caused by the undulating terrain, which introduces additional uncertainties in the satellite/reanalysis derived rainfall products since they failed to capture orographic variations in precipitation distribution. According to the IMD gridded dataset, about 8.52%, 24.10% and 67.38% of the geographical area are under moderate, irregular and highly irregular precipitation distribution, respectively. Among the selected gridded datasets, the GPCC and PGF reanalysis results were spatially comparable with IMD data (Fig. 5.3A).
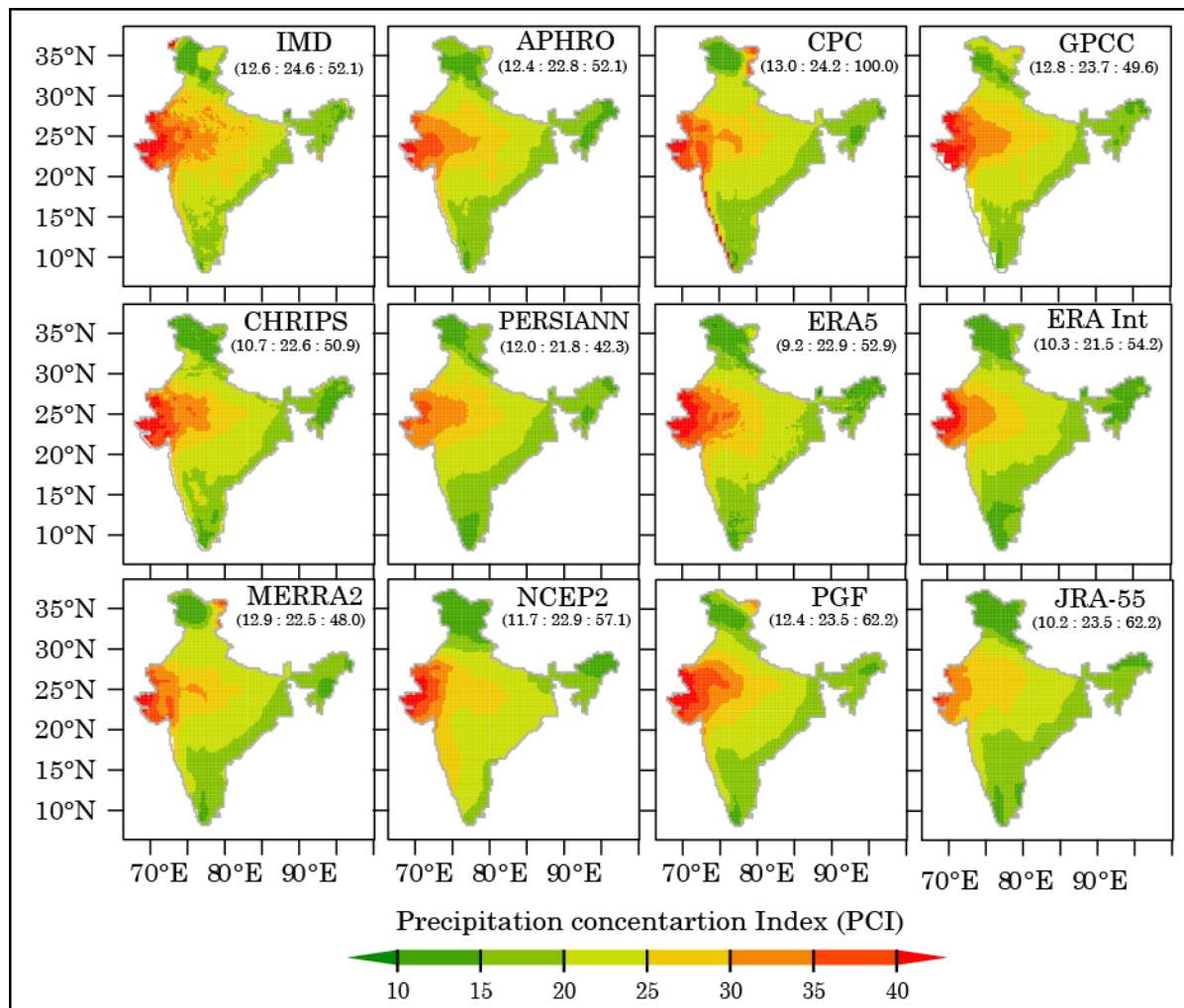
Fig. 5.2. Spatial variability of average APCI values across different gridded precipitation products over India (1986- 2015).
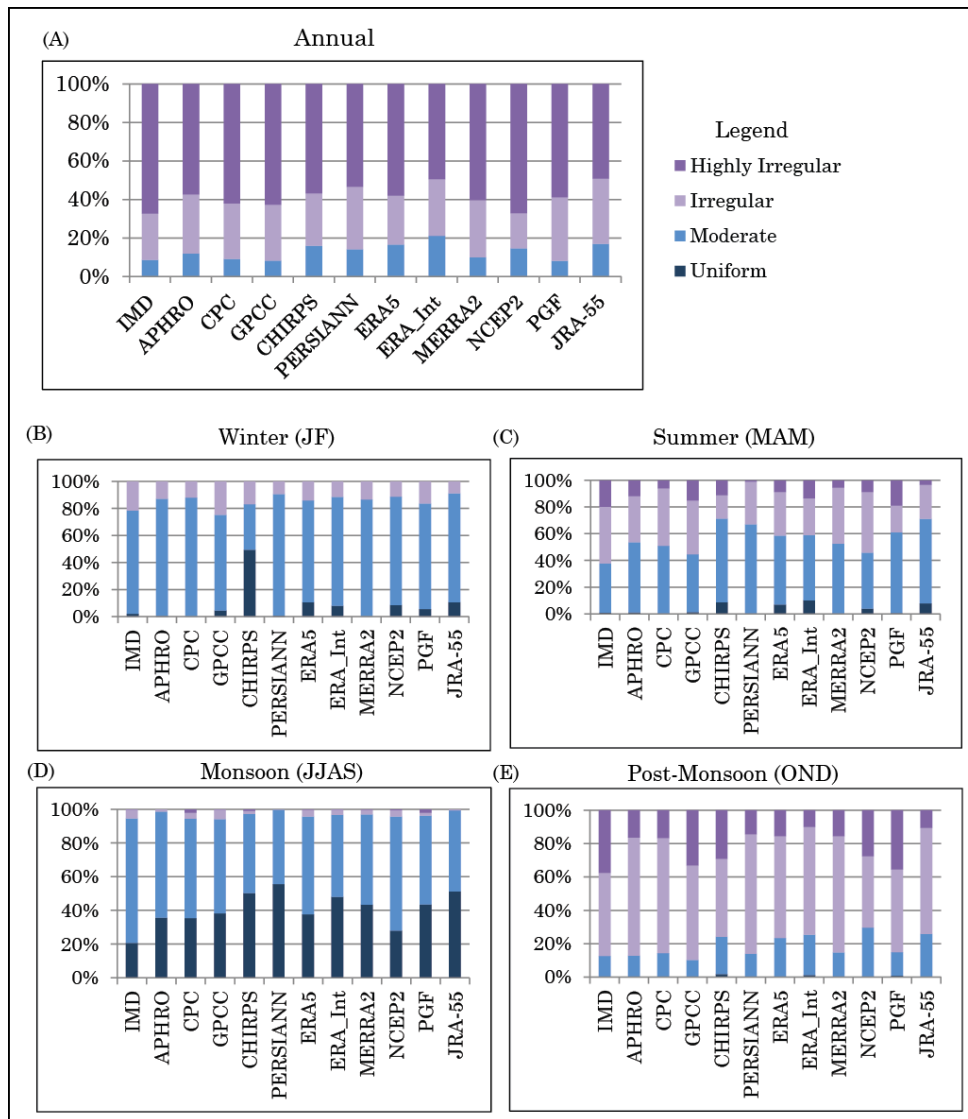
Fig. 5.3. Inter-comparison of different gridded precipitation dataset based on spatial coverage area (%) under different PCI categories on annual (A) and seasonal scale (B-E) over India.

5.4 Seasonal PCI on different precipitation datasets

5.4.1 Winter season

According to the IMD gridded dataset, about 76.34% and 21.62% of the area (Fig. 5.3B) during the winter season are under moderate and irregular precipitation distribution respectively. Uniform to moderate PCI distribution are observed over the NH, GP, NE and parts of SP regions of India (Fig. 5.4A). Irregular distribution of precipitation concentration

is found over the WC, north western parts, and central parts of the SP. Compared to the IMD dataset, almost all the gridded precipitation products well captured the spatial distribution of PCI during the winter season (Fig. 5.4A). However, the satellite-derived CHIRPS rainfall data highly overestimates uniform rainfall distribution over India and perform worst compared to the PERSIANN-CDR satellite-derived product. This may be due to the difference in calibration datasets used to construct the satellite rainfall products or estimating fog/smog, which is common during winter months in north India, as precipitation. The CHIRPS is developed using the Tropical Rainfall Measuring Mission Multi-satellite Precipitation Analysis version 7 (TMPA 3B42 v7) datasets (Funk et al., 2015) whereas the PERSIANN-CDR data is developed using Gridded satellite infrared data (GridSat-B1) and calibrated against the GPCP rainfall product (Ashouri et al., 2015). The accuracy of CHIRPS estimate depends on correct differentiation of clouds from smog and other atmospheric pollutants which are very common in Northern India. Also, the CPC, MERRA2 and JRA-55 datasets are unable to capture the uniform PCI distribution over parts of NH.

5.4.2 Summer season

Compared to the winter season, increased irregularity of precipitation during summer is observed over India(Fig. 5.4B), especially due to an increase in highly irregular distribution (PCI > 20) in the WI. Pockets of uniformly distributed PCI values were observed over the northern parts of NE India in the IMD dataset, which was also observed in the APHRODITE, GPCC, CHIRPS, ERA5 and ERA-Interim datasets. However, ERA5, ERA-Interim and NCEP2 reanalysis datasets overestimated summer PCI values over parts of NH. Besides, the reanalysis datasets (except PGF) and the satellite-derived PERSIANN-CDR data are unable to capture the highly irregular distribution of PCI in parts of WI (Fig. 5.4B). Gauge based GPCC data better represent the summer PCI over India as revealed by their spatial coverage when compared to the IMD dataset (Fig. 5.3C). Based on IMD gridded data, about 36.7% and 42.5% of the total geographical area are under moderate and irregular PCI classes, whereas, the GPCC data shows about 43.2% and 40.3% area under moderate and irregular PCI classes respectively (Fig. 5.3C). Besides, the PGF and CHIRPS can well capture the dynamics of summer PCI values compared to other reanalysis and satellite datasets (Fig. 5.4B).
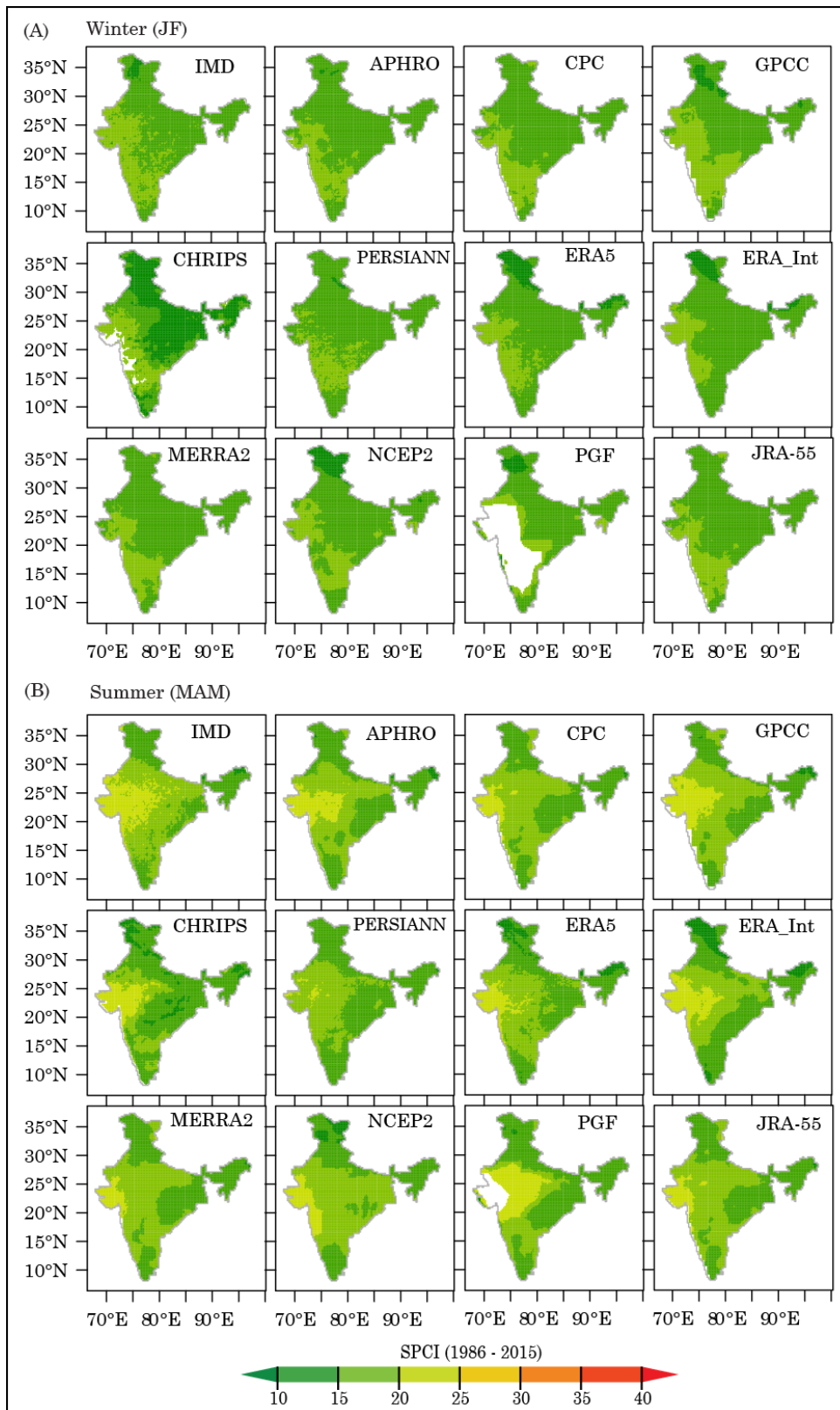
Fig. 5.4 Average winter (A) and summer (B) seasons PCI based on different gridded precipitation datasets over India (1986 – 2015).

5.4.3 Monsoon Season

During the monsoon season, uniform and moderate precipitation concentration prevail over India (Fig. 5.5A) covering about 20.7% and 73.9% of the area respectively (Fig. 5.3D). Uniform precipitation concentration (PCI < 10) mainly concentrated in the windward side of the WG, NE and the northern parts of the EC, and mainly associated with the south-west monsoon wind, which brings maximum proportion of annual rainfall over India. Gauge-based gridded datasets better perform in capturing the spatial dynamics of PCI during the monsoon period compared to reanalysis and satellite precipitation datasets. Most of these datasets, especially PERSIANN-CDR, CHIRPS, ERA-Interim, MERRA2, PGF and JRA-55 underestimate monsoon PCI values over large parts of the SP region. This indicates that these datasets are unable to capture the rainfall patterns, mainly by overestimating monsoonal precipitation over the rain shadow zones of the WG, which has also been discussed in previous studies (Ghodichore et al., 2018; Mondal et al., 2018).

5.4.4 Post-monsoon

According to the IMD dataset, during the post-monsoon season, irregular and highly irregular PCI distribution prevail over major parts of India, covering 49.8% and 37.5% of the area respectively (Fig. 5.5B). About 12.6% of area are found to be under moderate PCI distribution and mainly covers the SP and parts of western parts of NH (Fig. 5.5B). This pattern closely follows the rainfall distribution during the post-monsoon period over India and the snowfall activity that prevails over the NH. The eastern part of the SP region receives significant rainfall during the post-monsoon season, associated with the North-East monsoon wind and explains the moderate PCI distribution over this region. Highly irregular concentration of precipitation is observed over the GP, CI and WI. Rest of the country, which covers the eastern part of NH, parts of the EP and SP region are characterized with irregular distribution of precipitation.
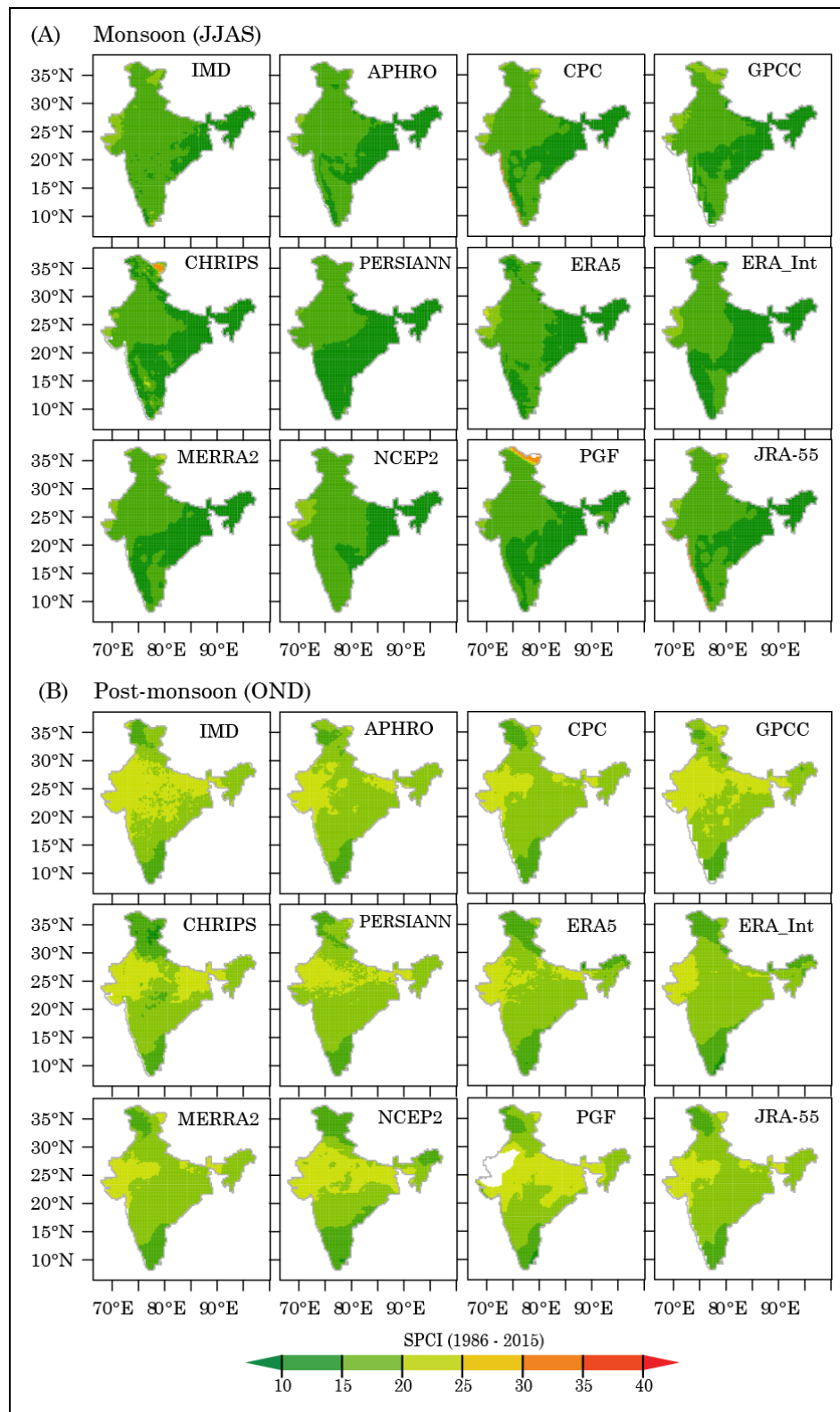
Fig. 5.5 Average monsoon (A) and Post-Monsoon (B) seasons PCI based on different gridded precipitation datasets over India (1986 – 2015).

Gauge based APHRODITE, CPC, GPCC; the PGF and JRA-55 reanalysis data aptly captured the uniform PCI areas during the post-monsoon season. However, CHIRPS, ERA-5, ERA-Interim and NCEP2 overestimated area under uniform PCI distribution (PCI >10), especially over the high elevation areas of NH. It is noted that most of the gridded datasets can reasonably capture the spatial distribution of moderate PCI distribution over India during the post-monsoon season, especially over the SP and EC regions. In contrast, few of them i.e. the gauge based GPCC, satellite-derived CHIRPS and NCEP2 and PGF reanalysis datasets appropriately captured the spatial distribution of highly irregular over the GP and WI during post-monsoon season.

5.5 Comparison of PCI among different datasets

To check the temporal consistency of different precipitation products, the Pearson's product-moment correlation coefficient (CC) of APCI has been calculated for each precipitation products by comparing them with the IMD gridded data across India (Fig.5.6A). The APHRODITE showed a higher degree of co-linearity over India, followed by the GPCC and PERSIANN-CDR data, with corresponding median CC value of 0.73, 0.58 and 0.57 respectively over India (Table 5.2). In general, the gauge-based gridded datasets exhibit a higher degree of co-linearity compared to satellite and reanalysis products. All the selected gridded precipitation products show very low CC (<0.25) over parts of NH, GP and western parts of NH. In addition, NCEP2 performs worst among the satellite/reanalysis datasets, with a low correlation value of 0.27 over India (Table 5.2). Calculated correlation values over India on different temporal scale (Fig. 5.7) also suggest that the APHRODITE and GPCC have better agreement with the IMD dataset in capturing the spatial dynamics of PCI over India during the study period. On seasonal scale, the overall performance of the gridded precipitation datasets was relatively higher during the post-monsoon season (Fig. 5.7. 2d). However, performance of NCEP2 data is worst (both on annual and seasonal scale) as revealed by consistently lower CC value during most of the year.
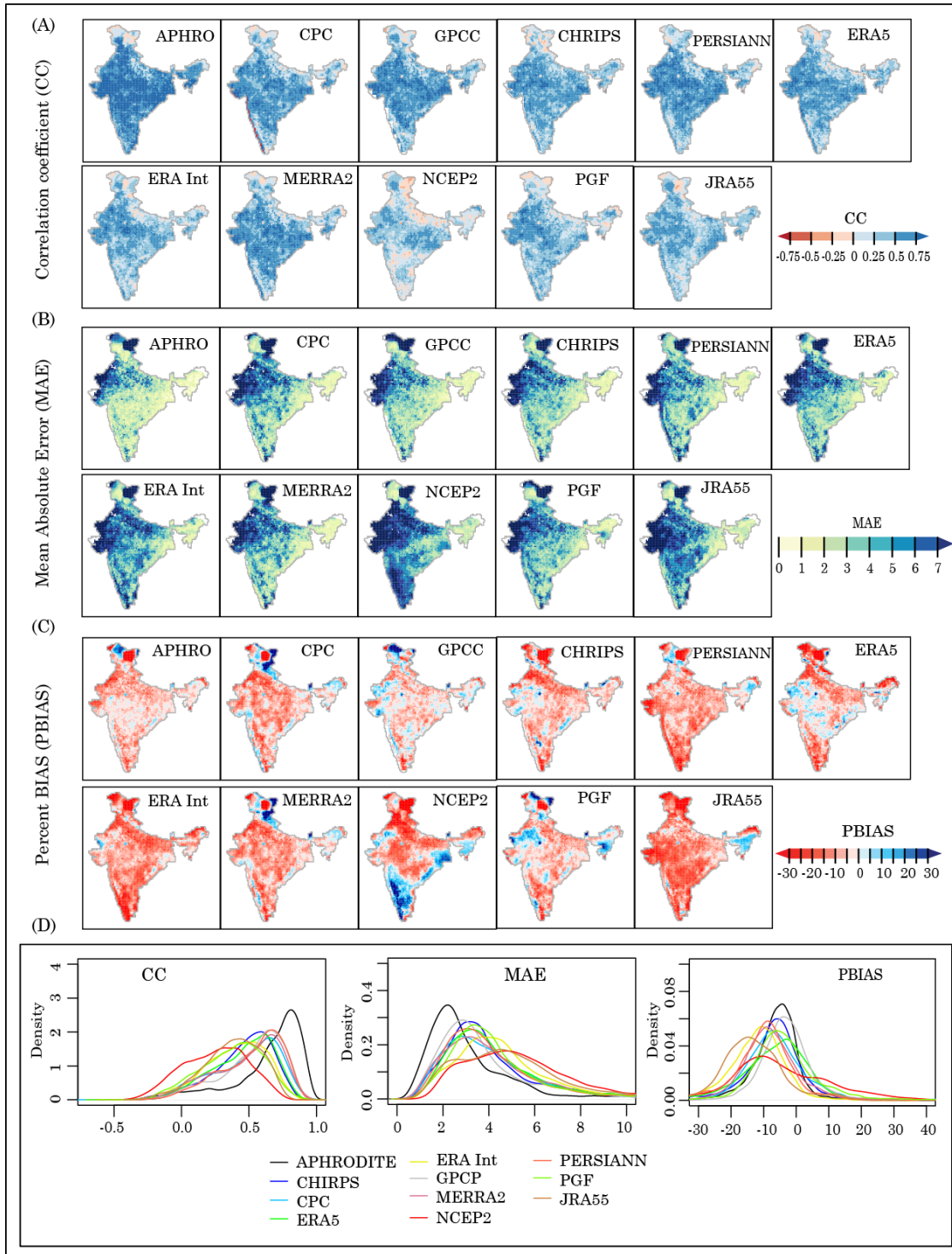
Fig. 5.6 Correlation coefficient (CC), Mean Absolute Error (MAE) and PBIAS of APCI between IMD and other gridded product over India (1986 – 2015). Lower panel (D) shows the probability density function (PDF) of CC, MAE and PBIAS for individual gridded datasets.

Table 5.2 Mean absolute error (MAE), correlation coefficient (CC) and percent bias (PBIAS) for APCI of different precipitation datasets compared to the IMD gridded dataset over India.

Data Set	MAE	CC	PBIAS
APHRODITE	2.60	0.73	-5.78
CPC	3.73	0.52	-6.79
GPCC	3.27	0.58	-3.33
CHIRPS	3.54	0.49	-6.46
PERSIANN	3.61	0.57	-9.49
ERA5	3.76	0.49	-5.68
ERA-Interim	4.28	0.42	-11.61
MERRA2	3.71	0.54	-8.25
NCEP2	5.07	0.27	-7.21
PGF	3.86	0.40	-4.92
JRA55	4.48	0.39	-13.98
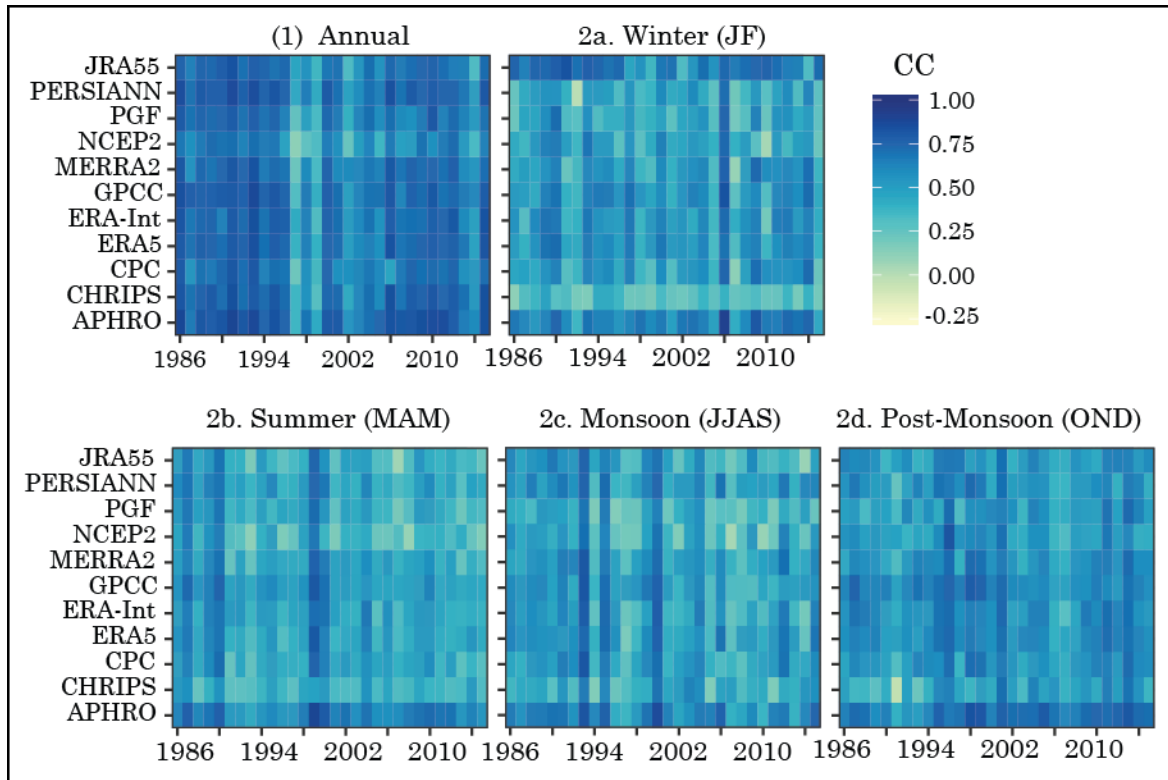
Fig. 5.7 Correlations between IMD and other gridded dataset on annual and seasonal scale over India (1986 – 2015).

Higher MAE values are mainly found over the dry areas of West India (WI) and NH and in some pockets over the rain shadow zone of WG (Fig. 5.6B). Most of these precipitation products show a lower MAE over NE India and parts of CI and EP. APHRODITE, GPCC, CHIRPS, PGF and ERA5 data better captured the APCI over CI, SP and parts of EC when compared to other gridded precipitation datasets. APHRODITE showed the lowest median MAE over India (2.60), followed by GPCC (3.27) and CHIRPS (3.5), where the NCEP2 showed highest median MAE of 5.07 over India (Table 5.2).

Spatial distribution of PBIAS indicates that most of the gridded precipitation datasets inadequately represents the precipitation concentration over the rain shadow zone as well as in low rainfall areas over India (Fig. 5.6C). Overall, underestimation/overestimation of PCI values is mainly found in the dry regions of WI, NH and in the rain shadow zone of WG. Most of these gridded datasets underestimate rainfall amounts over the mountain and dry areas of India, resulting in negative PBIAS. In contrast, NCEP2, highly overestimated rainfall over the SP and parts of the EC region, southern parts of NE those results in a large underestimation of PCI over these areas, which is also highlighted in Ghodichore et al., (2018). However, most of the gridded precipitation datasets well captured the APCI in areas where annual rainfall is above 1400mm/yr. The gauge based GPCC product better performed when compared to other gridded datasets as revealed by the respective median PBIAS of -3.33% over India which is followed by the PGF (-4.92%) and CHIRPS (-6.45%) rainfall data (Table 5.2). The PDF plot of CC, PBIAS and MAE (Fig. 5.6D) also confirms that the gauge based APHRODITE has better agreement with the IMD where the NCEP2 reanalysis data performed worst among these datasets.

The performance of selected gridded precipitation products in capturing the spatial distribution of annual and seasonal PCI over India is further evaluated using the Taylor diagram (Fig. 5.8). On annual scale, the APHRODITE product better performed in capturing the APCI values over India. During monsoon season, the performance of APHRODITE, CPC and MERRA2 is better compared to other gridded datasets. The GPCC data better performs during the post-monsoon season. Besides, during summer and winter gauge based APHRODITE, GPCC and the ERA-5 reanalysis product well captured the PCI dynamics over India.

In general, the gauge based APHRODITE, GPCC and the satellite-derived CHIRPS datasets are found to better capture the spatial and temporal variability of APCI over India when compared with the IMD gridded datasets. Prakash (2019) also reported that the CHIRPS rainfall product better approximates monthly precipitation climatology over India compared to other satellite based rainfall datasets. Similarly, the gauge based APHRODITE and GPCC products are also found to better capture daily/monthly precipitation over India (Prakash et al., 2015; Rana et al., 2015) which is in line with the present study. However, majority of the selected precipitation datasets are unable to capture the PCI dynamics over orographic rainfall zones such as the WG and NH as revealed by the error matrices (Fig. 5.6 B & C).
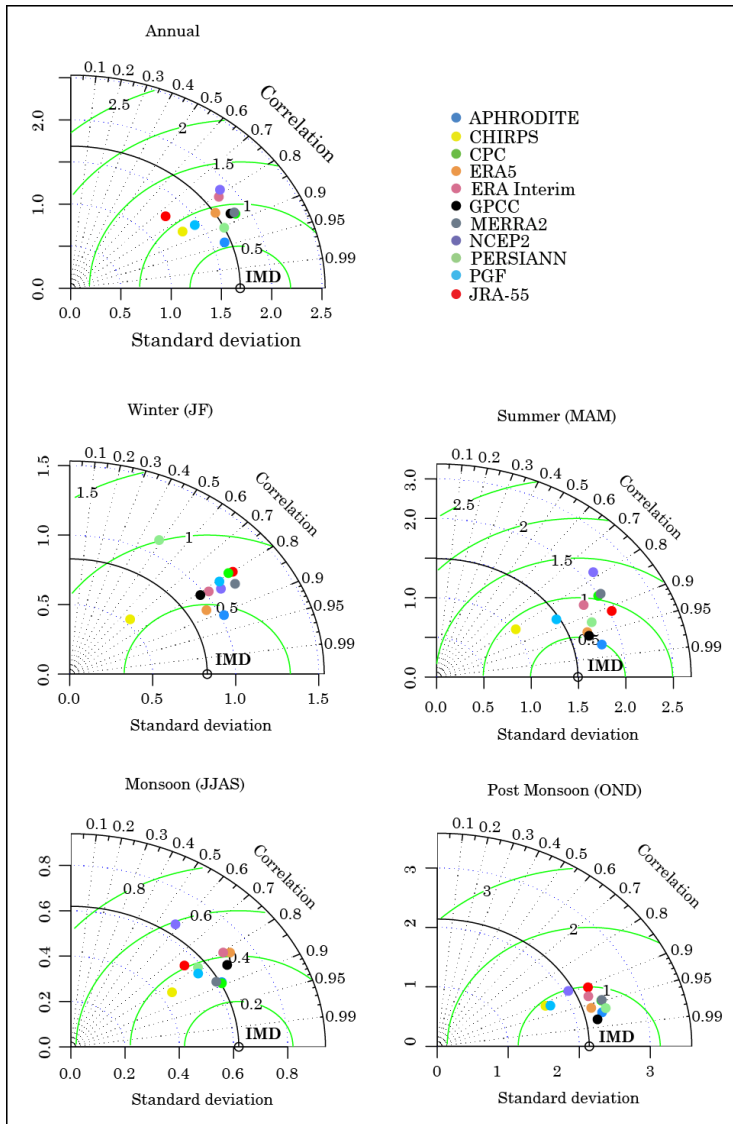
Fig. 5.8 Taylor diagrams for the annual and seasonal PCI over India from eleven precipitation datasets compared to the IMD gridded data for the period 1986-2015. Standard deviation is on the radial axis, correlation is on the angular axis and semi-circle lines indicate RMSD.

5.6 Trends in APCI over India

According to the IMD gridded dataset, about 61.61% of area showed negative trend in APCI and covers most of the GP, WC, SP and WI implying that APCI is declining in these areas (Fig. 5.9). Pockets of significantly negative trend zones, which comprises about 4.2% of the area, are found in the WC, SP, WI and in parts of CI and EP. The highest decreasing trend in APCI is observed over the WI. Decreasing PCI (> -0.5/ year) coupled with the wetter climate in the future (Kumar et al., 2013) may reduce the higher irregular nature of APCI over this region.

The positive trend of APCI covers about 38.39% of the area and are mainly concentrated in the NE, northern parts of the EC and NH region (Fig. 5.9). Besides, the increasing trends in APCI are also observed in parts of the CI, SP and WI (over the Aravalli Range). Significantly increasing trend (at 95% significant level) of APCI is found in areas of the EC, NE, and NH covering about 3.6% of geographical area. Therefore, proper regional water management practices are needed to be developed to cope up with the negative impacts associated with the increasing irregularity of precipitation on the hilly and coastal areas of India.

Based on the IMD dataset, the median APCI trend value over India is about -0.30/10 year. Lowest and highest median Sen's slope value in APCI are found in the ERA5 and CPC datasets with a corresponding value of -0.18/10year and -0.44/10 year respectively. The PERSIANN-CDR and the GPCC better approximate the median slope value over India with a corresponding value of -0.30/10year and -0.33/10year respectively.

The spatial pattern of increasing/decreasing trends in APCI can be explained by the increasing/decreasing trends in annual precipitation and trends in heavy precipitation amount over the respective areas. We already have explained that PCI is inversely related to precipitation amount therefore changes in annual precipitation amount can affect the PCI values. The decreasing trend in precipitation over the NE and SP region is reported by many previous studies (Mondal et al., 2018; Mondal et al., 2015; Kumar et al., 2010) which may increase the APCI over these regions. While decreasing trend in APCI over parts of the GP, WI and SP is in line with the increasing trends in annual precipitation as reported by previous studies (Mondal et al., 2018; Kumar et al., 2010).

Fig.5.9 Trend in APCI over India during 1986 – 2015 based on different gridded precipitation datasets. Grid cells with significant trends (at 95% significance level) are represented in black dots.

APHRODITE, GPCC, ERA5, ERA-Interim and PGF datasets well captured the negative trend areas over the WI. However, estimated significant trend magnitude by these datasets differs from the reference (IMD) dataset (Fig. 5.9). Furthermore, most of the precipitation products overestimated areas significantly negative trend zone over CI, with exception to the APHRODITE, PGF and JRA-55 datasets. Similar overestimation of negative trend areas in APCI over the NH is observed for most of the selected gridded precipitation products, except the ERA-5, ERA-Interim and NCEP2 reanalysis datasets. In comparison to the IMD and other gridded precipitation datasets, the GPCC data contrastingly shows a zone of significant positive trend in APCI over the western parts of the NH. This may be attributed to the quality of data used (i.e. no of gauging stations, record length) in this

gauge based gridded dataset over this region. Among the reanalysis and satellite rainfall products respectively, ERA5 and CHIRPS better perform in capturing positive trend areas over India (Fig.5.10) with a corresponding value of 37.61% and 35.62% respectively when compared to their IMD data-based counterparts of 38.39% area. The APHRODITE data better performs among the gauge-based gridded precipitation products, with a positive trend area of 39.24% (Fig.5.10) which closely approximates the IMD gridded data-based area. Notably, the JRA-55 reanalysis data highly overestimate positive APCI trends areas over India, covering about 75.5% of total grid-cells of which 17.8% are significant at 95% level.
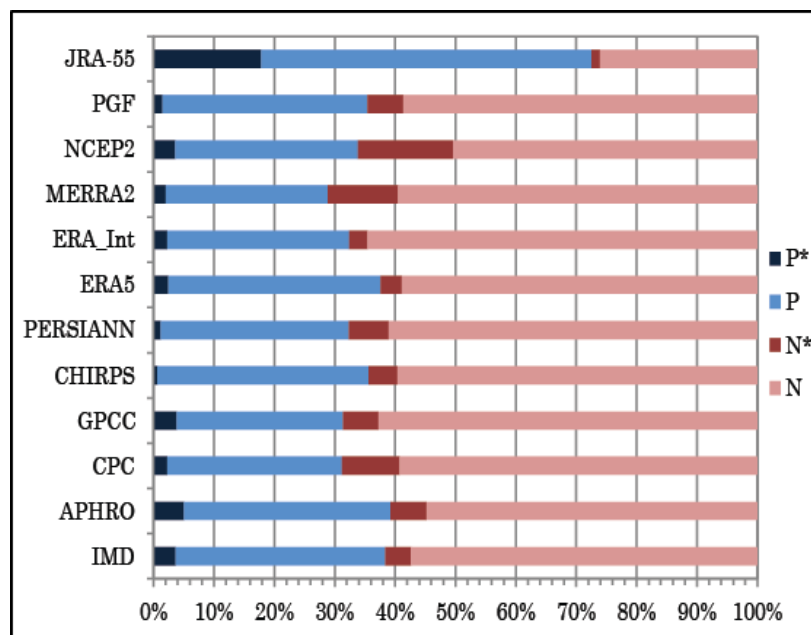
Fig. 5.10 Percentage of area under positive (P) and negative (N) APCI trends over India among different gridded precipitation datasets during 1986-2015. P/N with * marks means significant at 95% level.

5.7 Trend in SPCI over India

A significant increasing trend during the winter season is observed over parts of the SP, EC, EP and NE (Fig. 5.11A). Pockets of significantly decreasing trends during winter are found to be located on the WI. The gauge based and reanalysis products better captured the spatial pattern of increasing and decreasing trends during winter. According to the IMD

gridded datasets, increasing SPCI trend area over India during the summer season is higher as compared to the winter season (Fig. 5.11B). The APHRODITE better captures the spatial pattern of trends in summer PCI over India followed by the ERA-5 and CPC datasets. However, the NCEP2 and PERSIANN-CDR data highly overestimate significant negative trend areas mostly over the WI.

According to the IMD gridded dataset, SPCI during monsoon season is significantly increasing over the flood-prone areas of Assam valley (NE India) and in the northern part of the EC (Fig. 5.12A). A significant decreasing trend during monsoon is found over parts of the SP, WI and NH. Besides, a large part of the GP and southern part of NE India exhibit significant increasing trend during the post-monsoon period and is consistent across the gridded datasets (Fig. 5.12B). This may be due to the decreasing precipitation amount during the post-monsoon season over these areas as reported by Mondal et al., 2018 and Bisht et al., 2018.

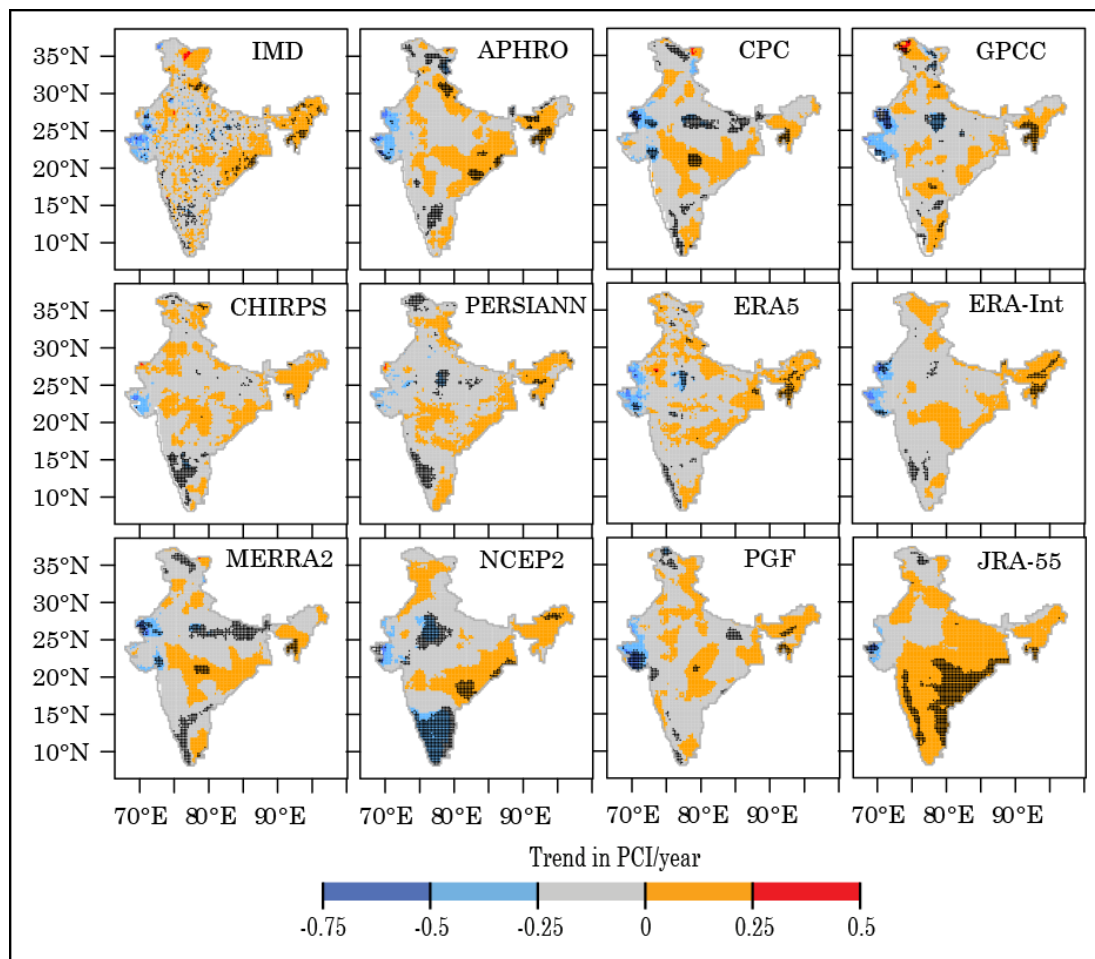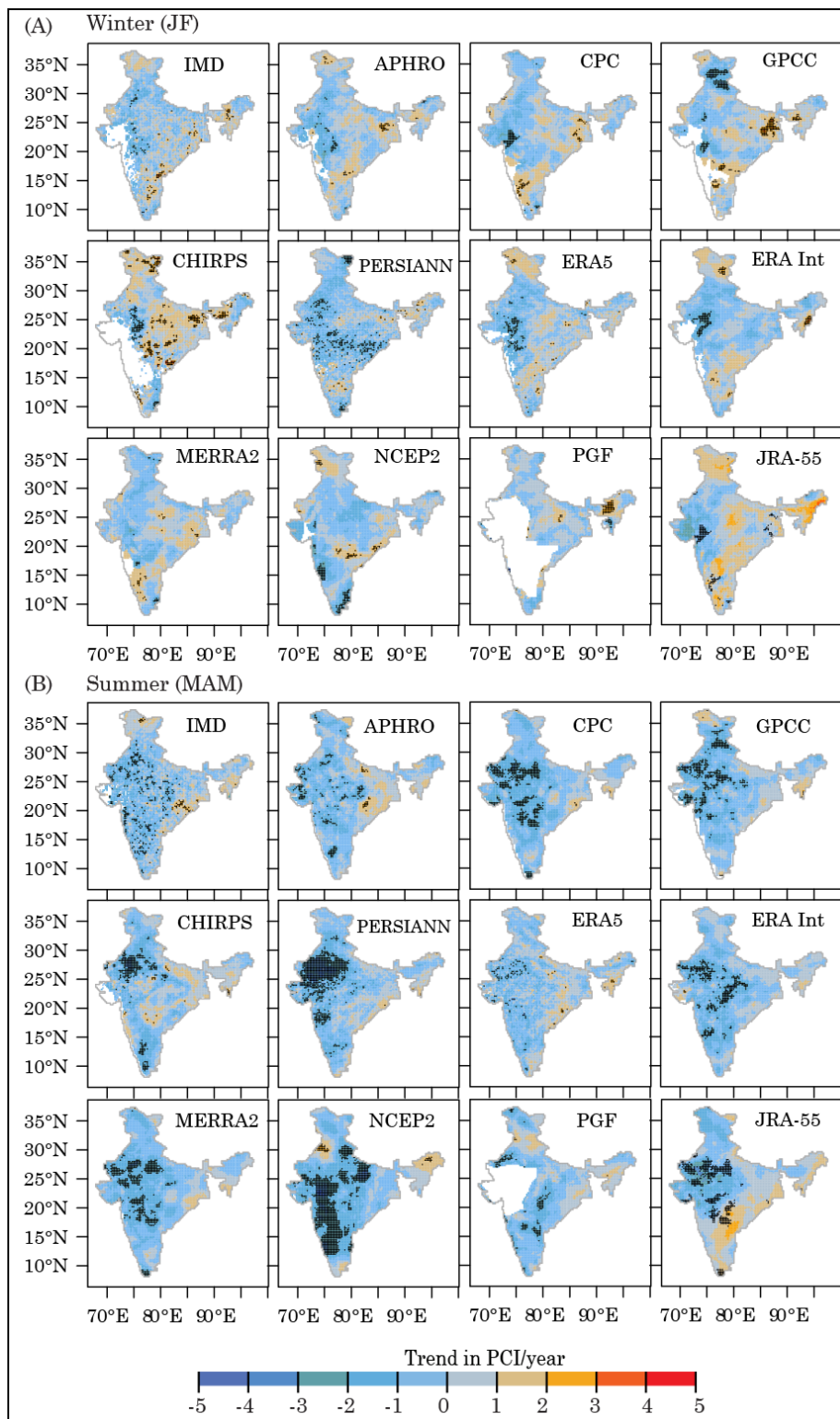Fig. 5.11 Trend in winter (A) and summer (B) PCI over India during 1986 – 2015 based on different gridded precipitation datasets. Grid cells with significant trends (at 95% significance level) are represented in black marks.
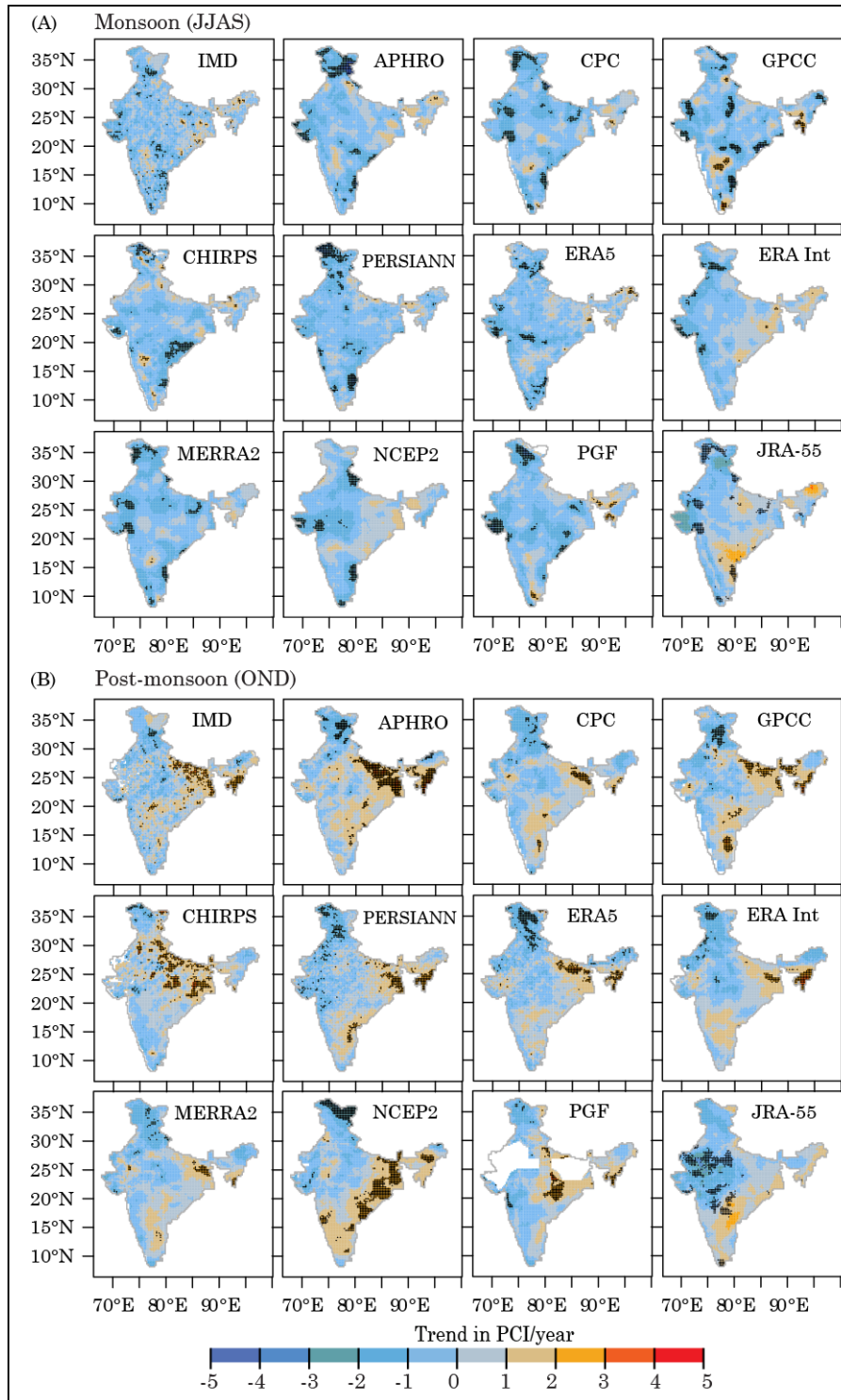
Fig. 5.12 Trend in monsoon (A) and post-monsoon (B) seasons PCI over India during 1986 – 2015 based on different gridded precipitation datasets. Grid cells with significant trends (at 95% significance level) are represented in black marks.

5.8 Conclusion

Understanding the spatio-temporal variations in precipitation concentration is of utmost importance for managing water resource, irrigation planning, hydropower development, flood management, and reducing the risk of soil erosion. This study, analyzed different characteristics of annual and seasonal PCI over India (1986 – 2015) based on the IMD gridded precipitation dataset and compared the results with eleven other gridded datasets. The IMD gridded data analysis indicated that the precipitation concentration in India is highly irregular, with an average APCI value of 24.6 during the study period. On the annual scale, About 67.38%, 24.10%, and 8.52% of the total geographical area of India are under highly irregular, irregular, and moderate precipitation distributions, respectively. This indicates that the uniform precipitation distribution is absent over India. It is more important to note that in spite of India's tropical location, especially in the southern part, the precipitation is seasonally concentrated. The southern part of the peninsular region should have experienced conventional precipitation throughout the year since it is located within 10° N latitude. However, the topographical characteristics and the prevailing wind system over the region control the current precipitation pattern which is distributed between moderate to highly irregular concentration classes. On the other hand, the very high concentrations of precipitations are found in the north-western part of the country surrounding the TD. In general, the entire EP and the NE of India reported moderate to irregular precipitation concentration. Uniform to moderate precipitation distribution prevails over the country only during the monsoon, covering about 20.71% and 73.88% of the area respectively. Uniform precipitation distribution is found over NE India, lower GP, northern parts of EC and southern WG. It is also to be noted that North-West Himalaya receives uniform precipitation during the winter season. This region is under the influence of westerlies (regionally called western disturbances) during this part of the year. The westerlies bring regular precipitation to the region during the winter season.

The APCI decreased over India with a magnitude of -0.30/10 year during 1986-2015. This indicates that the irregularity of precipitation is marginally decreasing, which is in tune with the reported increase in precipitation in different parts of India (Mondal et al., 2018; Kumar et al., 2010). The amount of precipitation and average PCI, across spatial and temporal scale over India, is negatively related as evident from significant negative correlation coefficient. This means, higher the amount of precipitation lower will be the

concentration of precipitation, as the precipitation amount increases PCI moves towards uniform distribution. The reported increase in precipitation in certain regions of India indicates that precipitation in India is moving towards lesser concentrations.

Calculated PCI from eleven other gridded datasets are compared against their IMD counterparts using model evaluation indices (i.e. CC, MAE, and PBIAS), PDF, and Taylor diagram. Among the gridded datasets analyzed in this study, the gauge based APHRODITE and GPCC data effectively capture the spatial pattern of annual and seasonal PCI over India in comparison with the reference IMD gridded dataset. Besides, the CHIRPS and PGF better-performed as compared to other selected satellite and reanalysis rainfall datasets respectively. Least agreement is found in the satellite-derived PERSIANN-CDR and NCEP-2 reanalysis datasets. Performance of individual gridded precipitation products is poor in data-sparse regions, especially over complex topography like Himalaya. This may introduce additional uncertainties while analyzing the reliability of reference (IMD) and other gridded datasets. Therefore, the strength of these gridded data sets can be enhanced by putting additional gauge derived information along with suitable interpolation algorithm that may reduce input data uncertainties. All the evaluation indices (i.e. CC, MAE PDF and Taylor diagram) are in agreement to indicate that the APHRODITE closely approximate PCI values estimated from IMD since APHRODITE is a purely a gauge based dataset where the NCEP2 reanalysis showed the least agreement with the IMD dataset.

The analysis helped to understand different characteristics of precipitation concentration over India. The results of this study are of considerable importance in taking effective decisions in taking water and soil conservation measures, disaster preparedness and reducing the risk associated with drought and floods. It also aids in selecting suitable gridded precipitation datasets while analyzing precipitation characteristics over India.

Chapter 6

Conclusion

6.1 General conclusion

The study explored the feasibility of eleven different precipitation products for studying different characteristics of annual extreme precipitation and precipitation concentration over India in comparison to a high resolution gridded rainfall dataset obtained from the IMD.

In general, the study found that the relative performance of the gridded datasets tends to vary in different parts of India and also with the choice of indices, used for comparing the datasets. A general drawback of these gridded datasets is that mostly all the datasets are unable to capture the extreme precipitation climatology over northern Himalaya, indicating the influence of orography on capturing extreme rainfall. In the gauge-based gridded datasets, the GPCC better performed in representing extreme whereas the APHRODITE better captures PCI over India while compared to IMD dataset. The ERA-5 reanalysis data better performed in the reanalysis group and the CHIRPS data better performed than PERSIANN-CDR among satellite rainfall data in representing extreme precipitation and PCI over India. The NCEP2 reanalysis performed worst among the all selected datasets especially over southern India and highly overestimated rainfall which is line with other recent studies (Ghodichore et al., 2018). Besides, the selected datasets are inconsistent with each other in representing trends in extreme and annual rainfall indices as well as PCI over India. However, commenting on the robustness and ability of satellite and reanalysis rainfall products requires further investigation. Overall, a tendency of underestimating higher extreme rainfall indices, located far right end of the PDF of daily rainfall (i.e. RX1day and R99tp) is a general feature of these datasets. This underestimation decreases with lower rainfall thresholds (i.e. RX5day, R95tp) and finally, these datasets overestimate the lower rainfall days (R10mm and R20mm). Therefore, a pattern of underestimation of extreme excess rainfall and overestimation of lower rainfall amount is a common attribute of the gridded datasets.

Regional variation in topography also found to have impacts on the spatial distribution of bias in extreme rainfall. Higher concentration of PBIAS over WG, NH signifies that the

datasets underestimate extreme rainfall over the orographic belts. Similar findings are also reported by Bharti et al., (2016); Kim et al., (2019) over NH and WG.

Besides, the spatial resolution of the gridded datasets has a substantial effect in representing extreme rainfall over India. The effects of resolution-dependent are more prominent among the reanalysis datasets. Degradation of relative skill score in representing higher extremes (RX1day, 99tp and R20mm) is higher than lower extremes (RX5day, 95tp and R10mm). Choice of higher threshold i.e. RX1day and 99tp reveals greater dependence on grid-resolution as they lie on the higher end of the PDF, therefore difficult to capture by relatively low-resolution datasets.

Nonetheless, the best approach in doing gridded precipitation data would be considering all gridded products and extracting maximum possible information from them while commenting on their relative strength and weakness for hydro-climatological studies.

6.2 Limitations and suggestion for further work
Consideration of lower extreme events, which stems from the deficiencies of precipitation are also equally important given the recurrent and chronic drought events in different parts of India. Besides, the selection of a study period spanning a minimum of 30-year also limits the inclusion of recent satellite precipitation products which may give some useful insights about the recent developments in satellite rainfall retrieval. To facilitate grid to grid comparison of the selected gridded datasets with the IMD data, all the datasets are re-gridded into a common 0.25° grid size which can introduce additional uncertainties in these daily precipitation values. Therefore, one can address this limitation of gridded data comparison. Investigating the choice of resampling technique and the choice of grid resolution of the different rainfall characteristics can also help future work in this direction.

The outcome of this work will benefit the data users, model developers, and researchers in the field of hydrology and climatology in understanding the relevant precipitation characteristics over different parts of India as well as about the relative strength and weakness of these gridded precipitation products used in this study while selecting their own.

References

Ahmad, I., Zhang, F., Tayyab, M., Anjum, M.N., Zaman, M., Liu, J., Farid, H.U. and Saddique, Q., 2018. Spatiotemporal analysis of precipitation variability in annual, seasonal and extreme values over upper Indus River basin. Atmos. Res., 213, 346-360. https://doi.org/10.1016/j.atmosres.2018.06.019

Ahmed, K., Shahid, S., Wang, X., Nawaz, N. and Khan, N., 2019. Evaluation of gridded precipitation datasets over arid regions of Pakistan. Water, 11(2), p.210. https://doi.org/10.3390/w11020210

Ajayamohan, R.S., Merryfield, W.J. and Kharin, V.V., 2010. Increasing trend of synoptic activity and its relationship with extreme rain events over central India. J. Clim., 23(4), pp.1004-1013. https://doi.org/10.1175/2009JCLI2918.1

Alexander, L.V., Bador, M., Roca, R., Contractor, S., Donat, M.G. and Nguyen, P.L., 2020. Intercomparison of annual precipitation indices and extremes over global land areas from in situ, space-based and reanalysis products. Environ. Res. Lett., 15(5), p.055002. https://doi.org/10.1088/1748-9326/ab79e2

Allen, M.R. and Ingram, W.J., 2002. Constraints on future changes in climate and the hydrologic cycle. Nature, 419(6903), pp.228-232. https://doi.org/10.1038/nature01092

Asadieh, B. and Krakauer, N.Y., 2015. Global trends in extreme precipitation: climate models versus observations. Hydrol. Earth Syst. Sci., 19, 877–891. https://doi.org/10.5194/hess-19-877-2015

Ashouri, H., Hsu, K.L., Sorooshian, S., Braithwaite, D.K., Knapp, K.R., Cecil, L.D., Nelson, B.R. and Prat, O.P., 2015. PERSIANN-CDR: Daily precipitation climate data record from multisatellite observations for hydrological and climate studies. Bull Am Meteorol Soc, 96(1), pp.69-83. https://doi.org/10.1175/BAMS-D-13-00068.1

Awange, J.L., Ferreira, V.G., Forootan, E., Andam-Akorful, S.A., Agutu, N.O. and He, X.F., 2016. Uncertainties in remotely sensed precipitation data over Africa. Int. J. Climatol., 36(1), pp.303-323. https://doi.org/10.1002/joc.4346

Awange, J.L., Hu, K.X. and Khaki, M., 2019. The newly merged satellite remotely sensed, gauge and reanalysis-based Multi-Source Weighted-Ensemble Precipitation: Evaluation over Australia and Africa (1981–2016). Sci. Total Environ., 670, 448-465. https://doi.org/10.1016/j.scitotenv.2019.03.148

Bador, M., Alexander, L.V., Contractor, S. and Roca, R., 2020. Diverse estimates of annual maxima daily precipitation in 22 state-of-the-art quasi-global land observation datasets. Environ. Res. Lett., 15(3), p.035005. https://doi.org/10.1088/1748-9326/ab6a22

Bailey, L.D. and van de Pol, M., 2016. Tackling extremes: challenges for ecological and evolutionary research on extreme climatic events. J Anim Ecol, 85(1), pp.85-96. https://doi.org/10.1111/1365-2656.12451

Balsamo, G., Dutra, E., Albergel, C., Munier, S., Calvet, J.C., Munoz-Sabater, J. and de Rosnay, P., 2018. ERA-5 and ERA-Interim driven ISBA land surface model simulations: which one performs better?. Hydrol. Earth Syst. Sci, 22(6), pp.3515-3532. https://doi.org/10.5194/hess-22-3515-2018

Bartolini, G., Grifoni, D., Magno, R., Torrigiani, T. and Gozzini, B., 2018. Changes in temporal distribution of precipitation in a Mediterranean area (Tuscany, Italy) 1955–2013. Int. J. Climatol., 38(3), 1366-1374. https://doi.org/10.1002/joc.5251

Basheer, M. and Elagib, N.A., 2019. Performance of satellite-based and GPCC 7.0 rainfall products in an extremely data-scarce country in the Nile Basin. Atmos. Res., 215, 128-140. https://doi.org/10.1016/j.atmosres.2018.08.028

Belo-Pereira, M., Dutra, E. and Viterbo, P., 2011. Evaluation of global precipitation data sets over the Iberian Peninsula. J. Geophys. Res. Atmos., 116(D20). https://doi.org/10.1029/2010JD015481

Bharti, V., Singh, C., Ettema, J. and Turkington, T.A.R., 2016. Spatiotemporal characteristics of extreme rainfall events over the Northwest Himalaya using satellite data. Int J Climatol, 36(12), pp.3949-3962. https://doi.org/10.1002/joc.4605

Bhattacharyya, S. and Sanyal, J., 2019. Impact of different types of meteorological data inputs on predicted hydrological and erosive responses to projected land use changes. J. Earth Syst. Sci., 128(3), p.60. https://doi.org/10.1007/s12040-019-1076-y

Bhutiyani, M.R., Kale, V.S. and Pawar, N.J., 2010. Climate change and the precipitation variations in the northwestern Himalaya: 1866–2006. Int. J. Climatol., 30(4), 535-548. https://doi.org/10.1002/joc.1920

Bisht, D.S., Chatterjee, C., Raghuwanshi, N.S. and Sridhar, V., 2018. Spatio-temporal trends of rainfall across Indian river basins. Theor. Appl. Climatol., 132(1-2), 419-436. https://doi.org/10.1007/s00704-017-2095-8

Bohlinger, P., Sorteberg, A. and Sodemann, H., 2017. Synoptic conditions and moisture sources actuating extreme precipitation in Nepal. J. Geophys. Res. Atmos, 122(23), pp.12-653. https://doi.org/10.1002/2017JD027543

Bosilovich, M.G., Chen, J., Robertson, F.R. and Adler, R.F., 2008. Evaluation of global precipitation in reanalyses. J Appl Meteorol Climatol, 47(9), pp.2279-2299. https://doi.org/10.1175/2008JAMC1921.1

Brooks C.E.P., and Carruthers N.B., 1953. Handbook of Statistical Methods in Meteorology Met. O, 538, H.M. Stationery Off. http://refhub.elsevier.com/S0169-8095(16)30714-1/rf0020

Caloiero, T., Coscarelli, R., Gaudio, R. and Leonardo, G.P., 2019. Precipitation trend and concentration in the Sardinia region. Theor. Appl. Climatol., 137(1-2), 297-307. https://doi.org/10.1007/s00704-018-2595-1

Cavalcante, R.B.L., da Silva Ferreira, D.B., Pontes, P.R.M., Tedeschi, R.G., da Costa, C.P.W. and de Souza, E.B., 2020. Evaluation of extreme rainfall indices from CHIRPS precipitation estimates over the Brazilian Amazonia. Atmos Res, 238, p.104879. https://doi.org/10.1016/j.atmosres.2020.104879

Chatterjee, S., Khan, A., Akbari, H. and Wang, Y., 2016. Monotonic trends in spatio-temporal distribution and concentration of monsoon precipitation (1901–2002), West Bengal, India. Atmos. Res., 182, 54-75. https://doi.org/10.1016/j.atmosres.2016.07.010

Chaudhary, S., Dhanya, C.T. and Vinnarasi, R., 2017. Dry and wet spell variability during monsoon in gauge-based gridded daily precipitation datasets over India. J. Hydrol., 546, pp.204-218. https://doi.org/10.1016/j.jhydrol.2017.01.023

Chen, A., Chen, D. and Azorin-Molina, C., 2018. Assessing reliability of precipitation data over the Mekong River Basin: A comparison of ground-based, satellite, and reanalysis datasets. Int. J. Climatol., 38(11), 4314-4334. https://doi.org/10.1002/joc.5670

Chen, A., He, X., Guan, H. and Zhang, X., 2019. Variability of seasonal precipitation extremes over China and their associations with large-scale ocean–atmosphere oscillations. Int J Climatol, 39(2), pp.613-628. https://doi.org/10.1002/joc.5830

Chen, M., Shi, W., Xie, P., Silva, V.B., Kousky, V.E., Wayne Higgins, R. and Janowiak, J.E., 2008. Assessing objective techniques for gauge-based analyses of global daily precipitation. J. Geophys. Res. Atmos., 113(D4). https://doi.org/10.1029/2007JD009132

Chen, S., Gan, T.Y., Tan, X., Shao, D. and Zhu, J., 2019. Assessment of CFSR, ERA-Interim, JRA-55, MERRA-2, NCEP-2 reanalysis data for drought analysis over China. Clim. Dyn., 53(1-2), pp.737-757. https://doi.org/10.1007/s00382-018-04611-1

Chen, S., Liu, B., Tan, X. and Wu, Y., 2020. Inter-comparison of spatiotemporal features of precipitation extremes within six daily precipitation products. Clim. Dyn., 54(1), pp.1057-1076. https://doi.org/10.1007/s00382-019-05045-z

Cortesi, N., Gonzalez-Hidalgo, J. C., Brunetti, M., and Martin-Vide, J.: Daily precipitation concentration across Europe 1971–2010, Nat. Hazards Earth Syst. Sci., 12, 2799–2810, https://doi.org/10.5194/nhess-12-2799-2012

CWC. (2018). State wise flood damage statistics. New Delhi: Flood Forecast Monitoring Directorate, Central Water Commission of India, Government of India

Dash, S.K., Nair, A.A., Kulkarni, M.A. and Mohanty, U.C., 2011. Characteristic changes in the long and short spells of different rain intensities in India. Theor. Appl. Climatol, 105(3-4), pp.563-570. https://doi.org/10.1007/s00704-011-0416-x

Dash, S. and Maity, R., 2019. Temporal evolution of precipitation-based climate change indices across India: contrast between pre-and post-1975 features. Theor. Appl. Climatol., 138(3-4), pp.1667-1678. https://doi.org/10.1007/s00704-019-02923-8

Dee, D.P., Uppala, S.M., Simmons, A.J., Berrisford, P., Poli, P., Kobayashi, S., Andrae, U., Balmaseda, M.A., Balsamo, G., Bauer, D.P. and Bechtold, P., 2011. The ERA-Interim reanalysis: Configuration and performance of the data assimilation system. Q J R Meteorol Soc, 137(656), pp.553-597. https://doi.org/10.1002/qj.828

De Luis, M., Gonzalez-Hidalgo, J.C., Brunetti, M. and Longares, L.A., 2011. Precipitation concentration changes in Spain 1946-2005. Nat. Hazards Earth Syst. Sci., 11(5), 1259. https://doi.org/10.5194/nhess-11-1259-2011

Deshpande, N.R., Kothawale, D.R. and Kulkarni, A., 2016. Changes in climate extremes over major river basins of India. Int J Climatol, 36(14), pp.4548-4559. https://doi.org/10.1002/joc.4651

Deng, S., Chen, T., Yang, N., Qu, L., Li, M. and Chen, D., 2018. Spatial and temporal distribution of rainfall and drought characteristics across the Pearl River basin. Sci. Total Environ., 619, 28-41. https://doi.org/10.1016/j.scitotenv.2017.10.339

Dey, R., Gallant, A.J. and Lewis, S.C., 2020. Evidence of a continent-wide shift of episodic rainfall in Australia. Weather. Clim. Extremes, 29, p.100274. https://doi.org/10.1016/j.wace.2020.100274

Duan, Z., Liu, J., Tuo, Y., Chiogna, G. and Disse, M., 2016. Evaluation of eight high spatial resolution gridded precipitation products in Adige Basin (Italy) at multiple temporal and spatial scales. Sci. Total Environ., 573, 1536-1553. https://doi.org/10.1016/j.scitotenv.2016.08.213

Ebita, A., Kobayashi, S., Ota, Y., Moriya, M., Kumabe, R., Onogi, K., Harada, Y., Yasui, S., Miyaoka, K., Takahashi, K. and Kamahori, H., 2011. The Japanese 55-year reanalysis "JRA-55": an interim report. Sola, 7, pp.149-152. https://doi.org/10.2151/sola.2011-038

El Kenawy, A.M. and McCabe, M.F., 2016. A multi-decadal assessment of the performance of gauge-and model-based rainfall products over Saudi Arabia: climatology, anomalies and trends. Int J Climatol, 36(2), pp.656-674. https://doi.org/10.1002/joc.4374

Emori, S. and Brown, S.J., 2005. Dynamic and thermodynamic changes in mean and extreme precipitation under changed climate. Geophys. Res. Lett, 32(17). https://doi.org/10.1029/2005GL023272

Faiz, M.A., Liu, D., Fu, Q., Wrzesiński, D., Baig, F., Nabi, G., Khan, M.I., Li, T. and Cui, S., 2018a. Extreme precipitation and drought monitoring in northeastern China using general circulation models and pan evaporation-based drought indices. Clim. Res., 74, 231-250. https://doi.org/10.3354/cr01503

Faiz, M.A., Liu, D., Fu, Q., Sun, Q., Li, M., Baig, F., Li, T. and Cui, S., 2018b. How accurate are the performances of gridded precipitation data products over Northeast China?. Atmos. Res., 211, 12-20. https://doi.org/10.1016/j.atmosres.2018.05.006

Fallah, A. and Orth, R., 2020. Climate-dependent propagation of precipitation uncertainty into the water cycle. Hydrol Earth Syst Sci, 24(7), pp.3725-3735. https://doi.org/10.5194/hess-24-3725-2020

Fallah, A., Rakhshandehroo, G.R., Berg, P., O, S. and Orth, R., 2019. Evaluation of precipitation datasets against local observations in Southwestern Iran. Int J Climatol. https://doi.org/10.1002/joc.6445

Falkenmark, M. and Rockström, J., 2006. The new blue and green water paradigm: Breaking new ground for water resources planning and management. J. Water Resour. Plan. Manag. https://doi.org/10.1061/(ASCE)0733-9496(2006)132:3(129)

Fischer, E.M. and Knutti, R., 2015. Anthropogenic contribution to global occurrence of heavy-precipitation and high-temperature extremes. Nat Clim Chang, 5(6), pp.560-564. https://doi.org/10.1038/nclimate2617

Forestieri, A., Arnone, E., Blenkinsop, S., Candela, A., Fowler, H. and Noto, L.V., 2018. The impact of climate change on extreme precipitation in Sicily, Italy. Hydrol Process, 32(3), pp.332-348. https://doi.org/10.1002/hyp.11421

Funk, C., Peterson, P., Landsfeld, M., Pedreros, D., Verdin, J., Shukla, S., Husak, G., Rowland, J., Harrison, L., Hoell, A. and Michaelsen, J., 2015. The climate hazards infrared precipitation with stations—a new environmental record for monitoring extremes. Sci. Data, 2(1), pp.1-21. https://doi.org/10.1038/sdata.2015.66

Gadgil, S., 2018. The monsoon system: Land–sea breeze or the ITCZ?. J. Earth. Syst. Sci., 127(1). https://doi.org/10.1007/s12040-017-0916-x

Gelaro, R., McCarty, W., Suárez, M.J., Todling, R., Molod, A., Takacs, L., Randles, C.A., Darmenov, A., Bosilovich, M.G., Reichle, R. and Wargan, K., 2017. The modern-era retrospective analysis for research and applications, version 2 (MERRA-2). J. Clim., 30(14), pp.5419-5454. https://doi.org/10.1175/JCLI-D-16-0758.1

Gervais, M., Tremblay, L.B., Gyakum, J.R. and Atallah, E., 2014. Representing extremes in a daily gridded precipitation analysis over the United States: Impacts of station density, resolution, and gridding methods. J. Clim., 27(14), pp.5201-5218. https://doi.org/10.1175/JCLI-D-13-00319.1

Gilmont, M., Hall, J.W., Grey, D., Dadson, S.J., Abele, S. and Simpson, M., 2018. Analysis of the relationship between rainfall and economic growth in Indian states. Glob Environ Change, 49, pp.56-72. https://doi.org/10.1016/j.gloenvcha.2018.01.003

Ghodichore, N., Vinnarasi, R., Dhanya, C.T. and Roy, S.B., 2018. Reliability of reanalyses products in simulating precipitation and temperature characteristics over India. J. Earth Syst. Sci., 127(8), p.115. https://doi.org/10.1007/s12040-018-1024-2

Gleckler, P.J., Taylor, K.E. and Doutriaux, C., 2008. Performance metrics for climate models. J. Geophys. Res. Atmos., 113(D6). https://doi.org/10.1029/2007JD008972

Godbole, R.V., 1977. The composite structure of the monsoon depression. Tellus, 29(1), pp.25-40. https://doi.org/10.1111/j.2153-3490.1977.tb00706.x

Golian, S., Javadian, M. and Behrangi, A., 2019. On the use of satellite, gauge, and reanalysis precipitation products for drought studies. Environ. Res. Lett., 14(7), p.075005. https://doi.org/10.1088/1748-9326/ab2203

Goswami, B.N., Venugopal, V., Sengupta, D., Madhusoodanan, M.S. and Xavier, P.K., 2006. Increasing trend of extreme rain events over India in a warming environment. Science, 314(5804), pp.1442-1445. https://doi.org/10.1126/science.1132027

Griffith, C.G., Woodley, W.L., Grube, P.G., Martin, D.W., Stout, J. and Sikdar, D.N., 1978. Rain estimation from geosynchronous satellite imagery—Visible and infrared studies. Mon Weather Rev, 106(8), pp.1153-1171. https://doi.org/10.1175/1520-0493(1978)106%3C1153:REFGSI%3E2.0.CO;2

Guo, E., Wang, Y., Jirigala, B. and Jin, E., 2020. Spatiotemporal variations of precipitation concentration and their potential links to drought in mainland China. Journal of Cleaner Production, p.122004.

Gupta, V., Jain, M.K., Singh, P.K. and Singh, V., 2019. An assessment of global satellite-based precipitation datasets in capturing precipitation extremes: A comparison with observed precipitation dataset in India. Int J Climatol. https://doi.org/10.1002/joc.6419

Gupta, V. and Jain, M.K., 2020. Impact of ENSO, global warming, and land surface elevation on extreme precipitation in India. J Hydrol Eng, 25(1), p.05019032. https://doi.org/10.1061/(ASCE)HE.1943-5584.0001872

Herold, N., Behrangi, A. and Alexander, L.V., 2017. Large uncertainties in observed daily precipitation extremes over land. J. Geophys. Res. Atmos., 122(2), pp.668-681. https://doi.org/10.1002/2016JD025842

Hersbach, H., Bell, B., Berrisford, P., Hirahara, S., Horányi, A., Muñoz-Sabater, J., Nicolas, J., Peubey, C., Radu, R., Schepers, D. and Simmons, A., 2020. The ERA5 global reanalysis. Q J R Meteorol Soc, 146(730), pp.1999-2049. https://doi.org/10.1002/qj.3803

Hong, Y.I.N. and Ying, S.U.N., 2018. Characteristics of extreme temperature and precipitation in China in 2017 based on ETCCDI indices.Adv. Clim. Chang. Res., 9(4), pp.218-226. https://doi.org/10.1016/j.accre.2019.01.001

Hu, Z., Hu, Q., Zhang, C., Chen, X. and Li, Q., 2016. Evaluation of reanalysis, spatially interpolated and satellite remotely sensed precipitation data sets in central Asia. J. Geophys. Res.-Atmos. 121(10), 5648-5663. https://doi.org/10.1002/2016JD024781

Huang, D.Q., Zhu, J., Zhang, Y.C., Huang, Y. and Kuang, X.Y., 2016. Assessment of summer monsoon precipitation derived from five reanalysis datasets over East Asia. Q J R Meteorol Soc, 142(694), pp.108-119. https://doi.org/10.1002/qj.2634

Huang, Y., Wang, H., Xiao, Wh. et al 2019. Spatiotemporal characteristics of precipitation concentration and the possible links of precipitation to monsoons in China from 1960 to 2015. Theor Appl Climatol 138, 135–152. https://doi.org/10.1007/s00704-019-02814-y

Hunt, K.M., Turner, A.G., Inness, P.M., Parker, D.E. and Levine, R.C., 2016. On the structure and dynamics of Indian monsoon depressions. Mon Weather Rev, 144(9), pp.3391-3416. https://doi.org/10.1175/MWR-D-15-0138.1

Hunt, K.M., Turner, A.G. and Parker, D.E., 2016. The spatiotemporal structure of precipitation in Indian monsoon depressions. Q J R Meteorol Soc, 142(701), pp.3195-3210. https://doi.org/10.1002/qj.2901

Hunt, K.M., Turner, A.G. and Shaffrey, L.C., 2018. Extreme daily rainfall in Pakistan and north India: Scale interactions, mechanisms, and precursors. Mon Weather Rev, 146(4), pp.1005-1022. https://doi.org/10.1175/MWR-D-17-0258.1

Hurley, J.V. and Boos, W.R., 2015. A global climatology of monsoon low-pressure systems. Q J R Meteorol Soc, 141(689), pp.1049-1064. https://doi.org/10.1002/qj.2447

Hwang, S.O., Park, J. and Kim, H.M., 2019. Effect of hydrometeor species on very-short-range simulations of precipitation using ERA5. Atmos. Res, 218, pp.245-256. https://doi.org/10.1016/j.atmosres.2018.12.008

Iqbal, M.F. and Athar, H., 2018. Validation of satellite based precipitation over diverse topography of Pakistan. Atmos. Res, 201, pp.247-260. https://doi.org/10.1016/j.atmosres.2017.10.026

IPCC, 2013. The Physical Science Basis. Contribution of working Group I to the Fifth Assessment Report of the IPCC.

IPCC Fifth Assessment Report (AR5) (Cambridge Univ. Press, 2014)

Iskander, S.M., Rajib, M.A. and Rahman, M.M., 2014. Trending regional precipitation distribution and intensity: use of climatic indices. Atmospheric and Climate Sciences, 2014.

Jackson, D.L., Hughes, M. and Wick, G.A., 2016. Evaluation of landfalling atmospheric rivers along the US West Coast in reanalysis data sets. J. Geophys. Res.-Atmos., 121(6), 2705-2718. https://doi.org/10.1002/2015JD024412

Jena, P., Garg, S. and Azad, S., 2020. Performance Analysis of IMD High-Resolution Gridded Rainfall (0.25°× 0.25°) and Satellite Estimates for Detecting Cloudburst Events over the Northwest Himalayas. J. Hydrometeorol., 21(7), pp.1549-1569. https://doi.org/10.1175/JHM-D-19-0287.1

Ji, C., Zhang, Y., Cheng, Q., Li, Y., Jiang, T. and San Liang, X., 2019. Analyzing the variation of the precipitation of coastal areas of eastern China and its association with sea surface temperature (SST) of other seas. Atmos Res, 219, pp.114-122. https://doi.org/10.1016/j.atmosres.2018.12.027

Jiang, P., Wang, D. and Cao, Y., 2016. Spatiotemporal characteristics of precipitation concentration and their possible links to urban extent in China. Theoretical and applied climatology, 123(3-4), pp.757-768.

Kanamitsu, M., Ebisuzaki, W., Woollen, J., Yang, S.K., Hnilo, J.J., Fiorino, M. and Potter, G.L., 2002. Ncep–doe amip-ii reanalysis (r-2). Bull Am Meteorol Soc, 83(11), pp.1631-1644. https://doi.org/10.1175/BAMS-83-11-1631

Kendall, M.G., 1975. Rank correlation methods, 4th ed. Charles Griffin, London, 202

Khalili, K., Tahoudi, M.N., Mirabbasi, R. and Ahmadi, F., 2016. Investigation of spatial and temporal variability of precipitation in Iran over the last half century. Stochastic environmental research and risk assessment, 30(4), pp.1205-1221.

Kharin, V.V., Zwiers, F.W., Zhang, X. and Wehner, M., 2013. Changes in temperature and precipitation extremes in the CMIP5 ensemble. Climatic change, 119(2), pp.345-357. https://doi.org/10.1007/s10584-013-0705-8

Kidd, C., 2001. Satellite rainfall climatology: A review. Int J Climatol, 21(9), pp.1041-1066. https://doi.org/10.1002/joc.635

Kidd, C., Becker, A., Huffman, G.J., Muller, C.L., Joe, P., Skofronick-Jackson, G. and Kirschbaum, D.B., 2017. So, how much of the Earth's surface is covered by rain gauges?. Bull Am Meteorol Soc, 98(1), pp.69-78. http://dx.doi.org/10.1175/BAMS-D-14-00283.1

Kidd, C. and Levizzani, V., 2011. Status of satellite precipitation retrievals. Hydrol. Earth Syst. Sci., 15(4), 1109-1116. https://doi.org/10.5194/hess-15-1109-2011

Kim, I.W., Oh, J., Woo, S. and Kripalani, R.H., 2019. Evaluation of precipitation extremes over the Asian domain: observation and modelling studies. Clim. Dyn., 52(3-4), pp.1317-1342. https://doi.org/10.1007/s00382-018-4193-4

Kim, Y.H., Min, S.K., Zhang, X., Sillmann, J. and Sandstad, M., 2020. Evaluation of the CMIP6 multi-model ensemble for climate extreme indices. Weather. Clim. Extremes, 29, p.100269. https://doi.org/10.1016/j.wace.2020.100269

King, A.D., Alexander, L.V. and Donat, M.G., 2013. The efficacy of using gridded data to examine extreme rainfall characteristics: a case study for Australia. Int J Climatol, 33(10), pp.2376-2387. https://doi.org/10.1002/joc.3588

Kishore, P., Jyothi, S., Basha, G., Rao, S.V.B., Rajeevan, M., Velicogna, I. and Sutterley, T.C., 2016. Precipitation climatology over India: validation with observations and reanalysis datasets and spatial trends. Clim. Dyn., 46, 541–556. https://doi.org/10.1007/s00382-015-2597-y

Kobayashi, S., Ota, Y., Harada, Y., Ebita, A., Moriya, M., Onoda, H., Onogi, K., Kamahori, H., Kobayashi, C., Endo, H. and Miyaoka, K., 2015. The JRA-55 reanalysis: General specifications and basic characteristics. J. Meteorol. Soc. Japan. Ser. II, 93(1), pp.5-48. https://doi.org/10.2151/jmsj.2015-001

Kolluru, V., Kolluru, S. and Konkathi, P., 2020. Evaluation and integration of reanalysis rainfall products under contrasting climatic conditions in India. Atmos Res, 246, p.105121. https://doi.org/10.1016/j.atmosres.2020.105121

Koutsouris, A.J., Chen, D. and Lyon, S.W., 2016. Comparing global precipitation data sets in eastern Africa: A case study of Kilombero Valley, Tanzania. Int. J. Climatol., 36(4), 2000-2014. https://doi.org/10.1002/joc.4476

Krishnamurthy, C.K.B., Lall, U. and Kwon, H.H., 2009. Changing frequency and intensity of rainfall extremes over India from 1951 to 2003. J. Clim., 22(18), pp.4737-4746. https://doi.org/10.1175/2009JCLI2896.1

Kumar, V., Jain, S.K. and Singh, Y., 2010. Analysis of long-term rainfall trends in India. Hydrol. Sci. J., 55(4), 484-496. https://doi.org/10.1080/02626667.2010.481373

Kumar, P., Wiltshire, A., Mathison, C., Asharaf, S., Ahrens, B., Lucas-Picher, P., Christensen, J.H., Gobiet, A., Saeed, F., Hagemann, S. and Jacob, D., 2013. Downscaled climate change projections with uncertainty assessment over India using a high resolution multi-model approach. Sci. Total Environ., 468, S18-S30. https://doi.org/10.1016/j.scitotenv.2013.01.051

Kundu, S.K. and Mondal, T.K., 2019. Analysis of long-term rainfall trends and change point in West Bengal, India. Theor Appl Climatol 138, 1647–1666 (2019). https://doi.org/10.1007/s00704-019-02916-7

Kunkel, K.E., Karl, T.R., Brooks, H., Kossin, J., Lawrimore, J.H., Arndt, D., Bosart, L., Changnon, D., Cutter, S.L., Doesken, N. and Emanuel, K., 2013. Monitoring and understanding trends in extreme storms: State of knowledge. Bull Am Meteorol Soc, 94(4), pp.499-514. https://doi.org/10.1175/BAMS-D-11-00262.1

Kursinski, A.L. and Zeng, X., 2006. Areal estimation of intensity and frequency of summertime precipitation over a midlatitude region. Geophys. Res. Lett., 33(22). https://doi.org/10.1029/2006GL027393

Laiti, L., Mallucci, S., Piccolroaz, S., Bellin, A., Zardi, D., Fiori, A., Nikulin, G. and Majone, B., 2018. Testing the Hydrological Coherence of High-Resolution Gridded Precipitation and Temperature Data Sets. Wat. Resour. Res., 54(3), 1999-2016. https://doi.org/10.1002/2017WR021633

Li, H., Haugen, J.E. and Xu, C.Y., 2018. Precipitation pattern in the Western Himalayas revealed by four datasets. Hydrol. Earth. Syst. Sci., 22(10), pp.5097-5110. https://doi.org/10.5194/hess-22-5097-2018

Lu, Y., Jiang, S., Ren, L., Zhang, L., Wang, M., Liu, R. and Wei, L., 2019. Spatial and temporal variability in precipitation concentration over mainland China, 1961–2017. Water, 11(5), p.881.

Ma, D., Xu, Y.P., Gu, H., Zhu, Q., Sun, Z. and Xuan, W., 2019. Role of satellite and reanalysis precipitation products in streamflow and sediment modeling over a typical alpine and gorge region in Southwest China. Sci. Total Environ., 685, 934-950. https://doi.org/10.1016/j.scitotenv.2019.06.183

Madsen, H., Lawrence, D., Lang, M., Martinkova, M. and Kjeldsen, T.R., 2014. Review of trend analysis and climate change projections of extreme precipitation and floods in Europe. J. Hydrol., 519, pp.3634-3650. https://doi.org/10.1016/j.jhydrol.2014.11.003

Mahto, S.S. and Mishra, V., 2019. Does ERA-5 outperform other reanalysis products for hydrologic applications in India?. J. Geophys. Res. Atmos., 124(16), pp.9423-9441. https://doi.org/10.1029/2019JD031155

Malik, N., Bookhagen, B. and Mucha, P.J., 2016. Spatiotemporal patterns and trends of Indian monsoonal rainfall extremes. Geophys. Res. Lett, 43(4), pp.1710-1717. https://doi.org/10.1002/2016GL067841

Maidment, R.I., Allan, R.P. and Black, E., 2015. Recent observed and simulated changes in precipitation over Africa. Geophys. Res. Lett., 42(19), 8155-8164. https://doi.org/10.1002/2015GL065765

Mal S., Singh R.B., Huggel C., Grover A. (2018) Introducing Linkages Between Climate Change, Extreme Events, and Disaster Risk Reduction. In: Mal S., Singh R., Huggel C. (eds) Climate Change, Extreme Events and Disaster Risk Reduction. Sustainable Development Goals Series. Springer, Cham.

Mann, H.B., 1945. Nonparametric tests against trend. Econometrica: Journal of the Econometric Society, pp.245-259

Marengo, J.A. and Espinoza, J.C., 2016. Extreme seasonal droughts and floods in Amazonia: causes, trends and impacts. Int. J. Climatol., 36(3), 1033-1050. https://doi.org/10.1002/joc.4420

Martin-Vide, J., 2004. Spatial distribution of a daily precipitation concentration index in peninsular Spain. Int. J. Climatol., 24, 959–971. http://dx.doi.org/10.1002/joc.1030

Matthews, T., Wilby, R.L. and Murphy, C., 2019. An emerging tropical cyclone–deadly heat compound hazard. Nat Clim Chang, 9(8), pp.602-606. https://doi.org/10.1038/s41558-019-0525-6

Masunaga, H., Schröder, M., Furuzawa, F.A., Kummerow, C., Rustemeier, E. and Schneider, U., 2019. Inter-product biases in global precipitation extremes. Environ. Res. Lett., 14(12), p.125016. https://doi.org/10.1088/1748-9326/ab5da9

Mazzoleni, M., Brandimarte, L. and Amaranto, A., 2019. Evaluating precipitation datasets for large-scale distributed hydrological modelling. J. Hydrol., 578, 124076. https://doi.org/10.1016/j.jhydrol.2019.124076

Michaelides, S., Levizzani, V., Anagnostou, E., Bauer, P., Kasparis, T. and Lane, J.E., 2009. Precipitation: Measurement, remote sensing, climatology and modeling. Atmos Res, 94(4), pp.512-533. https://doi.org/10.1016/j.atmosres.2009.08.017

Molod, A., Takacs, L., Suarez, M. and Bacmeister, J., 2015. Development of the GEOS-5 atmospheric general circulation model: Evolution from MERRA to MERRA2. Geosci Model Dev, 8(5), p.1339. https://doi.org/10.5194/gmd-8-1339-2015

Mondal, A., Khare, D. and Kundu, S., 2015. Spatial and temporal analysis of rainfall and temperature trend of India. Theor. Appl. Climatol., 122(1-2), 143-158. https://doi.org/10.1007/s00704-014-1283-z

Mondal, A., Lakshmi, V. and Hashemi, H., 2018. Intercomparison of trend analysis of multisatellite monthly precipitation products and gauge measurements for river basins of India. J. Hydrol., 565, pp.779-790. https://doi.org/10.1016/j.jhydrol.2018.08.083

Mondol, M.A.H., Al-Mamun, Iqbal, M., Jang, D., 2018. Precipitation concentration in Bangladesh over different temporal periods. Adv. Meteorol., 2018, 1849050 https://doi.org/10.1155/2018/1849050.

Moriasi, D.N., Arnold, J.G., Van Liew, M.W., Bingner, R.L., Harmel, R.D. and Veith, T.L., 2007. Model evaluation guidelines for systematic quantification of accuracy in watershed simulations. Trans ASABE, 50(3), pp.885-900. doi: 10.13031/2013.23153

Mukherjee, S., Aadhar, S., Stone, D. and Mishra, V., 2018. Increase in extreme precipitation events under anthropogenic warming in India. Weather. Clim. Extremes., 20, pp.45-53. https://doi.org/10.1016/j.wace.2018.03.005

Nguyen, P., Ombadi, M., Sorooshian, S., Hsu, K., AghaKouchak, A., Braithwaite, D., Ashouri, H. and Thorstensen, A.R., 2018. The PERSIANN family of global satellite precipitation data: A review and evaluation of products. Hydrol Earth Syst Sci22(11), pp.5801-5816. https://doi.org/10.5194/hess-22-5801-2018

Nandargi, S.S. and Aman, K., 2018. Precipitation concentration changes over India during 1951 to 2015. Scientific Research and Essays, 13(3), pp.14-26.

Nogueira, M., 2020. Inter-comparison of ERA-5, ERA-interim and GPCP rainfall over the last 40 years: Process-based analysis of systematic and random differences. J. Hydrol., 583, p.124632. https://doi.org/10.1016/j.jhydrol.2020.124632

Olauson, J., 2018. ERA5: The new champion of wind power modelling?. Renew. Energ., 126, pp.322-331. https://doi.org/10.1016/j.renene.2018.03.056

Oliver, J.E., 1980. Monthly precipitation distribution: a comparative index. Prof. Geogr., 32(3), 300-309. https://doi.org/10.1111/j.0033-0124.1980.00300.x

Pai, D.S., Sridhar, L., Rajeevan, M., Sreejith, O.P., Satbhai, N.S. and Mukhopadhyay, B., 2014. Development of a new high spatial resolution (0.25× 0.25) long period (1901–2010) daily gridded rainfall data set over India and its comparison with existing data sets over the region. Mausam, 65(1), pp.1-18.

Pai, D.S., Sridhar, L. and Kumar, M.R., 2016. Active and break events of Indian summer monsoon during 1901–2014. Clim. Dyn., 46(11-12), pp.3921-3939. https://doi.org/10.1007/s00382-015-2813-9

Paik, S., Min, S.K., Zhang, X., Donat, M.G., King, A.D. and Sun, Q., 2020. Determining the anthropogenic greenhouse gas contribution to the observed intensification of extreme precipitation. Geophys. Res. Lett., 47(12), p.e2019GL086875. https://doi.org/10.1029/2019GL086875

Panda, D.K., Panigrahi, P., Mohanty, S., Mohanty, R.K. and Sethi, R.R., 2016. The 20th century transitions in basic and extreme monsoon rainfall indices in India: Comparison of the ETCCDI indices. Atmos Res, 181, pp.220-235. https://doi.org/10.1016/j.atmosres.2016.07.002

Pang, J., Zhang, H., Xu, Q., Wang, Y., Wang, Y., Zhang, O. and Hao, J., 2020. Hydrological evaluation of open-access precipitation data using SWAT at multiple temporal and spatial scales. Hydrol Earth Syst Sci, 24(7), pp.3603-3626. https://doi.org/10.5194/hess-24-3603-2020

Paredes-Trejo, F.J., Barbosa, H.A. and Kumar, T.L., 2017. Validating CHIRPS-based satellite precipitation estimates in Northeast Brazil. J. Arid Environ, 139, pp.26-40. https://doi.org/10.1016/j.jaridenv.2016.12.009

Pattanaik, D.R. and Rajeevan, M., 2010. Variability of extreme rainfall events over India during southwest monsoon season. Meteorol. Appl., 17(1), pp.88-104. https://doi.org/10.1002/met.164

Pendergrass, A.G., 2018. What precipitation is extreme?. Science, 360(6393), pp.1072-1073. http://dx.doi.org/10.1126/science.aat1871

Perkins-Kirkpatrick, S.E. and Lewis, S.C., 2020. Increasing trends in regional heatwaves. Nat. Commun., 11(1), pp.1-8. https://doi.org/10.1038/s41467-020-16970-7

Pradhan, R.K., Sharma, D., Panda, S.K., Dubey, S.K. and Sharma, A., 2019. Changes of precipitation regime and its indices over Rajasthan state of India: impact of climate change

scenarios experiments. Clim. Dyn., 52(5-6), pp.3405-3420. https://doi.org/10.1007/s00382-018-4334-9

Prakash, S., 2019. Performance assessment of CHIRPS, MSWEP, SM2RAIN-CCI, and TMPA precipitation products across India. J. Hydrol., 571, pp.50-59. https://doi.org/10.1016/j.jhydrol.2019.01.036

Prakash, S., Mitra, A.K., Momin, I.M., Rajagopal, E.N., Basu, S., Collins, M., Turner, A.G., Achuta Rao, K. and Ashok, K., 2015. Seasonal intercomparison of observational rainfall datasets over India during the southwest monsoon season. Int. J. Climatol., 35(9), 2326-2338. https://doi.org/10.1002/joc.4129

Prigent, C., 2010. Precipitation retrieval from space: An overview. Comptes Rendus Geoscience, 342(4-5), pp.380-389. https://doi.org/10.1016/j.crte.2010.01.004

Priya, P., Krishnan, R., Mujumdar, M. and Houze, R.A., 2017. Changing monsoon and midlatitude circulation interactions over the Western Himalayas and possible links to occurrences of extreme precipitation. Clim. Dyn., 49(7-8), pp.2351-2364. https://doi.org/10.1007/s00382-016-3458-z

Rai, P.K., Singh, G.P. and Dash, S.K., 2020. Projected changes in extreme precipitation events over various subdivisions of India using RegCM4. Clim. Dyn., 54(1-2), pp.247-272. https://doi.org/10.1007/s00382-019-04997-6

Ramarao, M.V.S., Sanjay, J., Krishnan, R., Mujumdar, M., Bazaz, A. and Revi, A., 2019. On observed aridity changes over the semiarid regions of India in a warming climate. Theor. Appl. Climatol., 136, 693–702. https://doi.org/10.1007/s00704-018-2513-6

Rajeevan, M., Bhate, J., Kale, J.D. and Lal, B., 2006. High resolution daily gridded rainfall data for the Indian region: Analysis of break and active. Curr. Sci., 91(3), pp.296-306.

Rajeevan, M., Bhate, J. and Jaswal, A.K., 2008. Analysis of variability and trends of extreme rainfall events over India using 104 years of gridded daily rainfall data. Geophys. Res. Lett., 35(18). https://doi.org/10.1029/2008GL035143

Rajeevan, M. and Bhate, J., 2009. A high resolution daily gridded rainfall dataset (1971–2005) for mesoscale meteorological studies. Curr. Sci., pp.558-562.

Rajeevan, M., Gadgil, S. and Bhate, J., 2010. Active and break spells of the Indian summer monsoon. J. Earth Syst. Sci., 119(3), pp.229-247. https://doi.org/10.1007/s12040-010-0019-4

Rana, S., McGregor, J. and Renwick, J., 2015. Precipitation seasonality over the Indian subcontinent: An evaluation of gauge, reanalyses, and satellite retrievals. J Hydrometeorol 16(2), pp.631-651. https://doi.org/10.1175/JHM-D-14-0106.1

Raziei, T., Daryabari, J., Bordi, I. et al. 2014. Spatial patterns and temporal trends of precipitation in Iran. Theor Appl Climatol 115, 531–540. https://doi.org/10.1007/s00704-013-0919-8

Reichle, R.H., Liu, Q., Koster, R.D., Draper, C.S., Mahanama, S.P. and Partyka, G.S., 2017. Land surface precipitation in MERRA-2. J. Clim., 30(5), pp.1643-1664. https://doi.org/10.1175/JCLI-D-16-0570.1

Revadekar, J.V., Varikoden, H., Preethi, B. and Mujumdar, M., 2016. Precipitation extremes during Indian summer monsoon: role of cyclonic disturbances. Nat Hazards, 81(3), pp.1611-1625. https://doi.org/10.1007/s11069-016-2148-9

Roxy, M.K., Ghosh, S., Pathak, A., Athulya, R., Mujumdar, M., Murtugudde, R., Terray, P. and Rajeevan, M., 2017. A threefold rise in widespread extreme rain events over central India. Nat. Commun., 8(1), pp.1-11. https://doi.org/10.1038/s41467-017-00744-9

Sabeerali, C.T., Rao, S.A., George, G., Rao, D.N., Mahapatra, S., Kulkarni, A. and Murtugudde, R., 2014. Modulation of monsoon intraseasonal oscillations in the recent warming period. J. Geophys. Res. Atmos., 119(9), pp.5185-5203. https://doi.org/10.1002/2013JD021261

Sagar, S.K., Rajeevan, M. and Rao, S.V.B., 2017. On increasing monsoon rainstorms over India. Nat Hazards, 85(3), pp.1743-1757. https://doi.org/10.1007/s11069-016-2662-9

Saha, S., Moorthi, S., Pan, H.L., Wu, X., Wang, J., Nadiga, S., Tripp, P., Kistler, R., Woollen, J., Behringer, D. and Liu, H., 2010. The NCEP climate forecast system reanalysis. Bull Am Meteorol Soc, 91(8), pp.1015-1058. https://doi.org/10.1175/2010BAMS3001.1

Salman, S.A., Shahid, S., Ismail, T., Rahman, N.B.A., Wang, X. and Chung, E.S., 2018. Unidirectional trends in daily rainfall extremes of Iraq. Theor. Appl. Climatol., 134(3-4), 1165-1177. https://doi.org/10.1007/s00704-017-2336-x

Salman, S.A., Shahid, S., Ismail, T., Al-Abadi, A.M., Wang, X.J. and Chung, E.S., 2019. Selection of gridded precipitation data for Iraq using compromise programming. Measurement, 132, pp.87-98. https://doi.org/10.1016/j.measurement.2018.09.047

Satgé, F., Defrance, D., Sultan, B., Bonnet, M.P., Seyler, F., Rouché, N., Pierron, F. and Paturel, J.E., 2020. Evaluation of 23 gridded precipitation datasets across West Africa. J. Hydrol., 581, p.124412. https://doi.org/10.1016/j.jhydrol.2019.124412

Schamm, K., Ziese, M., Becker, A., Finger, P., Meyer-Christoffer, A., Schneider, U., Schröder, M. and Stender, P., 2014. Global gridded precipitation over land: a description of the new GPCC First Guess Daily product. Earth Syst. Sci. Data, 6(1), p.49. https://doi.org/10.5194/essd-6-49-2014

Schneider, U., Becker, A., Finger, P., Meyer-Christoffer, A., Ziese, M. and Rudolf, B., 2014. GPCC's new land surface precipitation climatology based on quality-controlled in situ data and its role in quantifying the global water cycle. Theor. Appl. Climatol., 115(1-2), pp.15-40. https://doi.org/10.1007/s00704-013-0860-x

Schoof, J.T. and Robeson, S.M., 2016. Projecting changes in regional temperature and precipitation extremes in the United States. Weather. Clim. Extremes, 11, pp.28-40. https://doi.org/10.1016/j.wace.2015.09.004

Sen, P.K., 1968. Estimates of the regression coefficient based on Kendall's tau. J. Am. Stat. Assoc., 63(324), 1379-1389.

Seneviratne, S.I., Nicholls, N., Easterling, D., 2012. Changes in climate extremes and their impacts on the natural physical environment. In: Field, C.B., Barros, V., Stocker, T.F., Qin, D., Dokken, D., Ebi, K.L., Mastrandrea, M.D., Mach, K.J., Plattner, G.-K., Allez, S.K. (Eds.), Managing the Risks of Extreme Events and Disasters to Advance Climate Change Adaptation. A Special Report of Working Groups I and II of the Intergovernmental Panel on Climate Change (IPCC). Cambridge University Press, Cambridge, UK, pp. 109–230.

Singh, C., 2013. Changing pattern of the Indian summer monsoon rainfall: an objective analysis. Clim. Dyn., 41(1), pp.195-203. https://doi.org/10.1007/s00382-013-1710-3

Shah, R. and Mishra, V., 2014. Evaluation of the reanalysis products for the monsoon season droughts in India. J. Hydrometeorol., 15(4), 1575-1591.

Sharma, A. and Goyal, M.K., 2020. Assessment of the changes in precipitation and temperature in Teesta River basin in Indian Himalayan Region under climate change. Atmos Res, 231, p.104670. https://doi.org/10.1016/j.atmosres.2019.104670

Sheffield, J., Goteti, G. and Wood, E.F., 2006. Development of a 50-year high-resolution global dataset of meteorological forcings for land surface modeling. J. Clim., 19(13), pp.3088-3111. https://doi.org/10.1175/JCLI3790.1

Shepard, D., 1968, January. A two-dimensional interpolation function for irregularly-spaced data. In Proceedings of the 1968 23rd ACM national conference (pp. 517-524). https://doi.org/10.1145/800186.810616

Shrestha, S., Yao, T., Kattel, D.B. and Devkota, L.P., 2019. Precipitation characteristics of two complex mountain river basins on the southern slopes of the central Himalayas. Theor. Appl. Climatol., 138, 1159–1178. https://doi.org/10.1007/s00704-019-02897-7

Singh, C., 2013. Characteristics of monsoon breaks and intraseasonal oscillations over central India during the last half century. Atmos Res, 128, pp.120-128. https://doi.org/10.1016/j.atmosres.2013.03.003

Singh, D., Tsiang, M., Rajaratnam, B. and Diffenbaugh, N.S., 2014. Observed changes in extreme wet and dry spells during the South Asian summer monsoon season. Nat Clim Chang, 4(6), pp.456-461. https://doi.org/10.1038/nclimate2208

Singh, D., Ghosh, S., Roxy, M.K. and McDermid, S., 2019. Indian summer monsoon: Extreme events, historical changes, and role of anthropogenic forcings. Wiley Interdiscip Rev Clim Change, 10(2), p.e571. https://doi.org/10.1002/wcc.571

Singh, A.K., Tripathi, J.N., Singh, K.K., Singh, V. and Sateesh, M., 2019. Comparison of different satellite-derived rainfall products with IMD gridded data over Indian meteorological subdivisions during Indian Summer Monsoon (ISM) 2016 at weekly

temporal resolution. J. Hydrol., 575, pp.1371-1379. https://ui.adsabs.harvard.edu/link_gateway/2019JHyd..575.1371K/doi:10.1016/j.jhydrol.2019.02.016

Sorooshian, S., Gao, X., Hsu, K., Maddox, R.A., Hong, Y., Gupta, H.V. and Imam, B., 2002. Diurnal variability of tropical rainfall retrieved from combined GOES and TRMM satellite information. J. Clim., 15(9), pp.983-1001. https://doi.org/10.1175/1520-0442(2002)015%3C0983:DVOTRR%3E2.0.CO;2

Srivastava, A., Grotjahn, R. and Ullrich, P.A., 2020. Evaluation of historical CMIP6 model simulations of extreme precipitation over contiguous US regions. Weather. Clim. Extremes, 29, p.100268. https://doi.org/10.1016/j.wace.2020.100268

Sushama, L., Said, S.B., Khaliq, M.N., Kumar, D.N. and Laprise, R., 2014. Dry spell characteristics over India based on IMD and APHRODITE datasets. Clim. Dyn., 43(12), 3419-3437. https://doi.org/10.1007/s00382-014-2113-9

Sun, Q., Miao, C., Duan, Q., Ashouri, H., Sorooshian, S. and Hsu, K.L., 2018. A review of global precipitation data sets: Data sources, estimation, and intercomparisons. Rev. Geophys., 56(1), pp.79-107. https://doi.org/10.1002/2017RG000574

Sunilkumar, K., Narayana Rao, T., Saikranthi, K. and Purnachandra Rao, M., 2015. Comprehensive evaluation of multisatellite precipitation estimates over India using gridded rainfall data. J. Geophys. Res. Atmos., 120(17), pp.8987-9005. https://doi.org/10.1002/2015JD023437

Tandon, N.F., Zhang, X. and Sobel, A.H., 2018. Understanding the dynamics of future changes in extreme precipitation intensity. Geophys. Res. Lett, 45(6), pp.2870-2878. https://doi.org/10.1002/2017GL076361

Tapiador, F.J., Kidd, C., Levizzani, V. and Marzano, F.S., 2004. A neural networks–based fusion technique to estimate half-hourly rainfall estimates at 0.1 resolution from satellite passive microwave and infrared data. J Appl Meteorol Climatol, 43(4), pp.576-594. https://doi.org/10.1175/1520-0450(2004)043%3C0576:ANNFTT%3E2.0.CO;2

Tapiador, F.J., Turk, F.J., Petersen, W., Hou, A.Y., García-Ortega, E., Machado, L.A., Angelis, C.F., Salio, P., Kidd, C., Huffman, G.J. and De Castro, M., 2012. Global precipitation measurement: Methods, datasets and applications. Atmos Res, 104, pp.70-97. https://doi.org/10.1016/j.atmosres.2011.10.021

Teegavarapu, R.S., Goly, A. and Obeysekera, J., 2013. Influences of Atlantic multidecadal oscillation phases on spatial and temporal variability of regional precipitation extremes. J. Hydrol., 495, pp.74-93. https://doi.org/10.1016/j.jhydrol.2013.05.003

Thomas, J. and Prasannakumar, V., 2016. Temporal analysis of rainfall (1871–2012) and drought characteristics over a tropical monsoon-dominated State (Kerala) of India. J. Hydrol., 534, 266-280. https://doi.org/10.1016/j.jhydrol.2016.01.013

Thornton, P.K., Ericksen, P.J., Herrero, M. and Challinor, A.J., 2014. Climate variability and vulnerability to climate change: a review. Glob Chang Biol, 20(11), pp.3313-3328. https://doi.org/10.1111/gcb.12581

Timmermans, B., Wehner, M., Cooley, D., O'Brien, T. and Krishnan, H., 2019. An evaluation of the consistency of extremes in gridded precipitation data sets. Clim. Dyn., 52(11), pp.6651-6670. https://doi.org/10.1007/s00382-018-4537-0

Tolika, K., 2019. On the analysis of the temporal precipitation distribution over Greece using the Precipitation Concentration Index (PCI): annual, seasonal, monthly analysis and association with the atmospheric circulation. Theor. Appl. Climatol., 137, 2303–2319. https://doi.org/10.1007/s00704-018-2736-6

Trenberth, K.E., Dai, A., Rasmussen, R.M. and Parsons, D.B., 2003. The changing character of precipitation. Bull Am Meteorol Soc, 84(9), pp.1205-1218. https://doi.org/10.1175/BAMS-84-9-1205

Ummenhofer, C.C. and Meehl, G.A., 2017. Extreme weather and climate events with ecological relevance: a review. Philos. Trans. R. Soc. Lond., B, Biol. Sci., 372(1723), p.20160135. https://doi.org/10.1098/rstb.2016.0135

Valli M, Shanti Sree K, Murali Krishna IV (2013) Analysis of precipitation concentration index and rainfall prediction in various agro-climatic zones of Andhra Pradesh, India. Int Res J Environ Sci 2:53–61

Van de Pol, M., Jenouvrier, S., Cornelissen, J.H. and Visser, M.E., 2017. Behavioural, ecological and evolutionary responses to extreme climatic events: challenges and directions. Philos. Trans. R. Soc. Lond., B, Biol. Sci. 372: 20160134. https://doi.org/10.1098/rstb.2016.0134

Vellore, R.K., Kaplan, M.L., Krishnan, R., Lewis, J.M., Sabade, S., Deshpande, N., Singh, B.B., Madhura, R.K. and Rao, M.R., 2016. Monsoon-extratropical circulation interactions in Himalayan extreme rainfall. Clim. Dyn., 46(11-12), pp.3517-3546. https://doi.org/10.1007/s00382-015-2784-x

Viney, N.R. and Bates, B.C., 2004. It never rains on Sunday: the prevalence and implications of untagged multi-day rainfall accumulations in the Australian high quality data set. Int J Climatol, 24(9), pp.1171-1192. https://doi.org/10.1002/joc.1053

Vinnarasi, R. and Dhanya, C.T., 2016. Changing characteristics of extreme wet and dry spells of Indian monsoon rainfall. J. Geophys. Res. Atmos., 121(5), pp.2146-2160. https://doi.org/10.1002/2015JD024310

Vittal, H., Karmakar, S. and Ghosh, S., 2013. Diametric changes in trends and patterns of extreme rainfall over India from pre-1950 to post-1950. Geophys. Res. Lett, 40(12), pp.3253-3258. https://doi.org/10.1002/grl.50631

Walsh, R.P.D. and Lawler, D.M., 1981. Rainfall seasonality: description, spatial patterns and change through time. Weather., 36(7), 201-208. https://doi.org/10.1002/j.1477-8696.1981.tb05400.x

Wang, Y., Xu, Y., Lei, C., Li, G., Han, L., Song, S., Yang, L. and Deng, X., 2016. Spatio-temporal characteristics of precipitation and dryness/wetness in Yangtze River Delta, eastern China, during 1960–2012. Atmos. Res., 172, 196-205. https://doi.org/10.1016/j.atmosres.2016.01.008

Westra, S., Alexander, L.V. and Zwiers, F.W., 2013. Global increasing trends in annual maximum daily precipitation. J. Clim., 26(11), pp.3904-3918. https://doi.org/10.1175/JCLI-D-12-00502.1

Wiel, K.V.D., Kapnick, S.B., Oldenborgh, G.J.V., Whan, K., Philip, S., Vecchi, G.A., Singh, R.K., Arrighi, J. and Cullen, H., 2017. Rapid attribution of the August 2016 flood-inducing extreme precipitation in south Louisiana to climate change. Hydrol Earth Syst Sci21(2), pp.897-921. https://doi.org/10.5194/hess-21-897-2017

Xie P, Yatagai A, Chen M, Hayasaka T, Fukushima Y, Liu C. and Yang, S., 2007. A gaugebased analysis of daily precipitation over East Asia. J. Hydrometeorol., 8:607–626. https://doi.org/10.1175/JHM583.1

Xu, Z., Wu, Z., He, H., Wu, X., Zhou, J., Zhang, Y. and Guo, X., 2019. Evaluating the accuracy of MSWEP V2. 1 and its performance for drought monitoring over mainland China. Atmos. Res., 226, 17-31. https://doi.org/10.1016/j.atmosres.2019.04.008

Yang, Q., Leung, L.R., Rauscher, S.A., Ringler, T.D. and Taylor, M.A., 2014. Atmospheric moisture budget and spatial resolution dependence of precipitation extremes in aquaplanet simulations. J. Clim., 27(10), pp.3565-3581. https://doi.org/10.1175/JCLI-D-13-00468.1

Yao, J., Chen, Y., Yu, X., Zhao, Y., Guan, X. and Yang, L., 2020. Evaluation of multiple gridded precipitation datasets for the arid region of northwestern China. Atmos. Res.. 236, 104818. https://doi.org/10.1016/j.atmosres.2019.104818

Yatagai, A., Kamiguchi, K., Arakawa, O., Hamada, A., Yasutomi, N. and Kitoh, A., 2012. APHRODITE: Constructing a long-term daily gridded precipitation dataset for Asia based on a dense network of rain gauges. Bull Am Meteorol Soc, 93(9), pp.1401-1415. https://doi.org/10.1175/BAMS-D-11-00122.1

Zamani, R., Mirabbasi, R., Nazeri, M., Meshram, S.G. and Ahmadi, F., 2018. Spatio-temporal analysis of daily, seasonal and annual precipitation concentration in Jharkhand state, India. Stoch. Environ. Res. Risk. Assess., 32, 1085–1097. https://doi.org/10.1007/s00477-017-1447-3

Zhan, W., Guan, K., Sheffield, J. and Wood, E.F., 2016. Depiction of drought over sub-Saharan Africa using reanalyses precipitation data sets. J. Geophys. Res. Atmos., 121(18), pp.10-555. https://doi.org/10.1002/2016JD024858

Zhang, K., Yao, Y., Qian, X. and Wang, J., 2019. Various characteristics of precipitation concentration index and its cause analysis in China between 1960 and 2016. Int. J. Climatol., 39(12), 4648-4658. https://doi.org/10.1002/joc.6092

Zhao, N., Yue, T., Li, H., Zhang, L., Yin, X. and Liu, Y., 2018. Spatio-temporal changes in precipitation over Beijing-Tianjin-Hebei region, China. Atmos. Res., 202, 156-168. https://doi.org/10.1016/j.atmosres.2017.11.029

Zhong, Y., Wang, B., Zou, C.B., Hu, B.X., Liu, Y. and Hao, Y., 2017. On the teleconnection patterns to precipitation in the eastern Tianshan Mountains, China. Clim Dyn, 49(9-10), pp.3123-3139. https://doi.org/10.1007/s00382-016-3500-1

Zhong, R., Chen, X., Lai, C., Wang, Z., Lian, Y., Yu, H. and Wu, X., 2019. Drought monitoring utility of satellite-based precipitation products across mainland China. J. Hydrol., 568, 343-359. https://doi.org/10.1016/j.jhydrol.2018.10.072

Zhu, J., Huang, D.Q., Yan, P.W., Huang, Y. and Kuang, X.Y., 2017. Can reanalysis datasets describe the persistent temperature and precipitation extremes over China?. Theor. Appl. Climatol., 130(1-2), pp.655-671. https://doi.org/10.1007/s00704-016-1912-9